

การบ่งชี้และวินิจฉัยความผิดพร้อมด้วยการอนุมานนิรโทษชี้แบบปรับตัวได้



บทคัดย่อและแฟ้มข้อมูลฉบับเต็มของวิทยานิพนธ์ตั้งแต่ปีการศึกษา 2554 ที่ให้บริการในคลังปัญญาจุฬาฯ (CUIR)
เป็นแฟ้มข้อมูลของนิสิตเจ้าของวิทยานิพนธ์ ที่ส่งผ่านทางบัณฑิตวิทยาลัย

The abstract and full text of theses from the academic year 2011 in Chulalongkorn University Intellectual Repository (CUIR)
are the thesis authors' files submitted through the University Graduate School.

วิทยานิพนธ์นี้เป็นส่วนหนึ่งของการศึกษาตามหลักสูตรปริญญาวิศวกรรมศาสตรดุษฎีบัณฑิต

สาขาวิชาวิศวกรรมไฟฟ้า ภาควิชาวิศวกรรมไฟฟ้า

คณะวิศวกรรมศาสตร์ จุฬาลงกรณ์มหาวิทยาลัย

ปีการศึกษา 2558

ลิขสิทธิ์ของจุฬาลงกรณ์มหาวิทยาลัย

Fault Detection and Identification With Adaptive Neuro-Fuzzy Inference System

Mrs. Noramalina Abdullah



A Dissertation Submitted in Partial Fulfillment of the Requirements
for the Degree of Doctor of Philosophy Program in Electrical Engineering

Department of Electrical Engineering

Faculty of Engineering

Chulalongkorn University

Academic Year 2015

Copyright of Chulalongkorn University

5471463321 : MAJOR ELECTRICAL ENGINEERING

KEYWORDS: TRANSMISSION LINE, FAULT IDENTIFICATION, CLASSIFICATION AND LOCALIZATION, WAVELET TRANSFORM, ADAPTIVE NEURO-FUZZY INFERENCE SYSTEM, GUSTAFSON-KESSEL

NORAMALINA ABDULLAH: Fault Detection and Identification With Adaptive Neuro-Fuzzy Inference System. ADVISOR: DOCTOR CHANNARONG BANMONKOL, Ph.D., CO-ADVISOR: ASST. PROF. DR. NAEBBOON HOONCHAREON, Ph.D., PROF. DR. KUNIHICO HIDAKA, Ph.D., 96 pp.

An algorithm that is not influenced by the line parameters is an option to overcome a few drawbacks of conventional approach especially in fault identification. Such algorithm should be independence on the power network configuration to be more generalized. In artificial intelligence, artificial intelligent network seems efficient and practical when mathematical model of the system is not available. As for fuzzy logic, it possess a capability to copy the sensing, generalizing, operating, processing and learning capability of human operator.

This research implemented fuzzy system in the framework of adaptive network and then combines with discrete wavelet transform to obtain a great performance. A novel approach to implementing Gustafson-Kessel clustering algorithm have performed significant results for a better fault analysis tool using artificial intelligence. Results show that the scheme has ability on justifying the type of fault and estimate the fault distance in a small range of error. The proposed method also has very less involving of calculation and almost no affected by the fault resistance.

Department: Electrical Engineering

Field of Study: Electrical Engineering

Academic Year: 2015

Student's Signature

Advisor's Signature

Co-Advisor's

Signature

Co-Advisor's Signature

ACKNOWLEDGEMENTS

First and foremost, I am grateful to The Mighty God for enabling me to complete this Ph.D. journey. My deepest appreciation goes to my advisor, Dr Channarong Banmongkol, for his support and supervision throughout my graduate studies at Chulalongkorn University. This dissertation also would not have been possible without the enormous guidance of my co-advisor, Assistant Professor Dr Naebboon Hoonchareon and Prof. Dr Kunihiko Hidaka. I extend my gratitude to Assistant Professor Dr. Widhyakorn Asdornwised, Assistant Professor Dr. Thavatchai Tayjasanant, Assistant Professor Dr. Surachai Chaitusaney and Assistant Professor Dr. Kittiphan Techakittiroj for their insightful advice and willingness to serve as the Dissertation Advisory Committee. Also, I would like to thank Dr Wuttikorn Threevithayan for his support and all respective friends at Power System Research Laboratory (PSRL). I gratefully acknowledge the ASEAN University Network/Southeast Asia Engineering Education Development Network (AUN/SEED-Net) for their financial support. My sincere appreciation is also extended to the International School of Engineering (ISE), Chulalongkorn University for their care and help during my study.

Finally, special thanks to my beloved husband, Khairul Azman Ahmad with his encouragement and sacrifice in making this research a reality. His great patience at all time for which my sheer expression of thanks does not suffice. My deepest appreciation goes to my daughters; Nur Aina Zulaikha, Nur Amni Rahmah and Nur Ainni Raudhah for their love, patience and understanding. I will never forget the support from my family and family in law with daily prayers all the time throughout these precious years. My late mother passed away on the 2nd month of this Ph. D. journey. Her courage and advice gave me strength to carry on till the end of the path. May Allah bless her soul, Amen.

CONTENTS

| | Page |
|---|------|
| THAI ABSTRACT | iv |
| ENGLISH ABSTRACT | v |
| ACKNOWLEDGEMENTS..... | vi |
| CONTENTS..... | vii |
| List of Figures | xi |
| List of Tables | xiv |
| CHAPTER 1.0 | 1 |
| INTRODUCTION..... | 1 |
| 1.1 Motivation..... | 1 |
| 1.2 Objective..... | 3 |
| 1.3 Scope of Works | 3 |
| 1.4 Research Methodology | 4 |
| 1.5 Expected Contribution..... | 5 |
| CHAPTER 2.0 | 7 |
| CONVENTIONAL APPROACHES OF FAULT ANALYSIS IN POWER SYSTEM..... | 7 |
| 2.1 Fault Detection in Power System..... | 7 |
| 2.2 Fault Classification in Power System..... | 9 |
| 2.3 Fault Location in Power System | 9 |
| 2.4 The Trends of Fault Analys in Power System..... | 11 |
| CHAPTER 3.0 | 16 |
| ARTIFICIAL INTELLIGENCE TECHNIQUES AND FAULT ANALYSIS IN POWER SYSTEM..... | 16 |

| | Page |
|--|------|
| 3.1 Artificial Neural Networks (ANN) in Power System | 16 |
| 3.2 Fuzzy Logic in Power System..... | 17 |
| 3.3 Issues of ANN and FIS | 21 |
| 3.4 Adaptive Neuro-Fuzzy Inference System (ANFIS)..... | 22 |
| 3.5 Fault Detection in Power System..... | 26 |
| 3.6 Fault Classification in Power System..... | 27 |
| 3.6.1 Artificial Neural Networks Based Methods | 27 |
| 3.6.2 Combination of ANN and Wavelet Transform Based Method..... | 28 |
| 3.6.3 Fuzzy Logic Based Method | 29 |
| 3.6.4 Combination of ANN and Fuzzy Logic Based..... | 30 |
| 3.7 Fault Location in Power System | 30 |
| 3.7.1 Artificial Neural Network (ANN) Based Methods..... | 30 |
| 3.7.2 Combination of the ANN and Traveling Wave Method | 31 |
| 3.7.3 Combination of the ANN and Wavelet Transform Based Method..... | 31 |
| 3.7.4 Fuzzy Logic Based Method | 32 |
| 3.7.5 Combination of the ANN and Fuzzy Logic Based Method | 33 |
| CHAPTER 4.0 | 34 |
| FAULT DETECTION AND IDENTIFICATION WITH ANFIS..... | 34 |
| 4.1 Proposed Framework | 34 |
| 4.2 Fault Detection Algorithm | 35 |
| 4.3 Implementation of Wavelet Transform..... | 36 |
| 4.4 Modeling of ANFIS..... | 38 |

| | Page |
|---|------|
| 4.5 ANFIS Architecture and Layers | 39 |
| 4.5.1 Input layers | 39 |
| 4.5.2 Rule layer | 39 |
| 4.5.3 Output layers | 40 |
| 4.6 Membership Functions | 40 |
| 4.7 New Approach in Fault Identification using the Gustafson-Kessel Algorithm | 42 |
| 4.8 Fault Identification | 45 |
| 4.9 Flowchart of Fault Classification Algorithm | 48 |
| 4.10 Flowchart of Fault Location Algorithm | 49 |
| 4.11 Parameters Setting for Training Patterns | 51 |
| 4.11.1 Simulation Data | 52 |
| 4.12 Sampling Frequency and Data Reduction | 54 |
| CHAPTER 5 | 56 |
| RESULTS AND DISCUSSION | 56 |
| 5.1 Performance of Fault Detection | 56 |
| 5.2 Performance of Fault Classification | 58 |
| 5.3 Performance of Fault Location | 64 |
| 5.4 Performance on High Impedance Fault (HIF) | 73 |
| 5.5 Case Studies | 74 |
| 5.5.1 Fault Classification and Fault Location of IEEE 14 Bus System | 74 |
| 5.5.2 Fault Classification and Location of Real Data from Utility | 78 |
| 5.5.3 Comparison ANFIS-GK With ANN Approaches | 82 |

| | Page |
|---|------|
| 5.5.4 Comparison and Performance of GK with FCM Algorithms..... | 84 |
| 5.6 Graphic User Interface (GUI) | 87 |
| CHAPTER 6.0 | 90 |
| CONCLUSION AND FUTURE WORKS | 90 |
| 6.1 Conclusion | 90 |
| 6.2 Contribution | 90 |
| 6.3 Thesis Limitation | 91 |
| 6.4 Future Works | 92 |
| REFERENCES..... | 93 |
| VITA | 96 |



List of Figures

| | |
|--|----|
| Figure 2.1 Illustration of summary for fault detection in power system..... | 13 |
| Figure 2.2 Illustration of summary for fault classification in power system..... | 14 |
| Figure 2.3 Illustration of summary for fault localization in power system..... | 15 |
| Figure 3.1 An Artificial Neuron..... | 16 |
| Figure 3.2 Fuzzy inference system..... | 18 |
| Figure 3.3 Fuzzy system which membership functions adjusted by ANN..... | 23 |
| Figure 3.4 Architecture of ANFIS..... | 24 |
| Figure 3.5 Basic structure of ANN learning procedure..... | 26 |
| Figure 3.6 Basic components of a pattern recognition system..... | 27 |
| Figure 3.7 Fault Classification Scheme..... | 28 |
| Figure 3.8 General illustration based on wavelet transforms..... | 29 |
| Figure 3.9 Wavelet-ART2 proposed scheme..... | 29 |
| Figure 3.10 Functional block diagram based on frequency component and ANN..... | 31 |
| Figure 3.11 Functional block diagram of fault detector and locator..... | 31 |
| Figure 3.12 Proposed Fuzzy Inference System..... | 33 |
| Figure 3.13 Proposed distance protection scheme..... | 33 |
| Figure 4. 1 Illustration of Model in Details..... | 34 |
| Figure 4. 2 Illustration of Model in Details..... | 34 |
| Figure 4. 3 Proposed algorithm for fault detection..... | 35 |
| Figure 4. 4 Snapshot on part of fault detection algorithm..... | 36 |
| Figure 4. 5 Illustration of Nyquist's rule..... | 37 |
| Figure 4. 6 Snapshot of initialization algorithm..... | 40 |
| Figure 4. 7 Example of membership function's plotting..... | 41 |
| Figure 4. 8 Part of algorithm on membership function..... | 42 |

| | |
|---|----|
| Figure 4. 9 Part of algorithm used for membership function regressor | 42 |
| Figure 4. 10 Illustration of GK Algorithm Implementation | 44 |
| Figure 4. 11 a and b Parts of Implemented extended GK algorithm | 45 |
| Figure 4. 12 Fault Identification scheme | 46 |
| Figure 4. 13 Scheme for Fault Classifier..... | 47 |
| Figure 4. 14 Scheme for ANFIS-GK Fault Locator | 47 |
| Figure 4. 15 Flowchart of classification algorithm | 48 |
| Figure 4. 16 Flowchart of location algorithm | 49 |
| Figure 4. 17 Flow chart on tested signal | 50 |
| Figure 4. 18 Snapshot of the system in EMTP | 52 |
| Figure 4. 19 One-line diagram of the studied system | 52 |
| Figure 4. 20 Illustration of reduction process for data and sampling frequency | 55 |
| Figure 5. 1 Voltage plotting with RMS | 71 |
| Figure 5. 2 Current plotting with RMS..... | 57 |
| Figure 5. 3 Plotting of FFT fault voltage | 57 |
| Figure 5. 4 Plotting of FFT fault current | 58 |
| Figure 5. 5 Results of classification phase | 59 |
| Figure 5. 6 Confusion matrix of 3 classes | 60 |
| Figure 5. 7 ROC of single line to ground fault | 61 |
| Figure 5. 8 Snapshot of fault classification..... | 62 |
| Figure 5. 9 Results of confusion matrix | 62 |
| Figure 5. 10 ROC of double line fault | 63 |
| Figure 5. 11 Results of classification phase | 63 |
| Figure 5. 12 Results of confusion matrix | 63 |
| Figure 5. 13 ROC of double line to ground fault | 64 |

| | |
|---|----|
| Figure 5. 14 Plotting of membership function for phase A to ground $R_f=0.5\text{ohm}$ | 65 |
| Figure 5. 15 Illustration of actual and predicted value..... | 65 |
| Figure 5. 16 Plotting of membership function for phase B, $R_f= 0.5 \text{ ohm}$ | 66 |
| Figure 5. 17 Illustration of actual and predicted value..... | 67 |
| Figure 5. 18 Plotting of membership function for phase ABG, $R_f= 0.5\text{ohm}$ | 68 |
| Figure 5. 19 Illustration of Actual and Predicted Value | 68 |
| Figure 5. 20 Plotting of Membership function for phase ABG, $R_f= 0.5 \text{ ohm}$ | 69 |
| Figure 5. 21 Illustration of Actual and Predicted Value | 70 |
| Figure 5. 22 Overall Performance of the ANFIS-GK based at 5Ω fault resistance | 71 |
| Figure 5. 23 Overall Performance of the GK based at 100Ω fault resistance.... | 72 |
| Figure 5. 24 the IEEE-14 bus electrical power network | 75 |
| Figure 5. 25 Part of snapshot IEEE 14 bus system | 76 |
| Figure 5. 26 Circuit representation of Line Fault | 79 |
| Figure 5. 27 Scheme for ANN Fault Classifier | 82 |
| Figure 5. 28 Scheme for ANN Fault Location | 82 |
| Figure 5. 29 Plotting Comparison of ANFIS-GK and ANN | 83 |
| Figure 5. 30 GK vs FCM in terms of time completion with varying number of clusters..... | 85 |
| Figure 5. 31 Elapsed Time of FCM vs GK in completing clustering task | 86 |
| Figure 5. 32 a) the original data in scattered b) FCM clustering c) GK clustering | 86 |
| Figure 5. 33 Main window of ANFIS-GK GUI..... | 88 |
| Figure 5. 34 Selection of mode..... | 88 |
| Figure 5. 35 Automatic mode | 89 |
| Figure 5. 36 Window in manual mode (1)..... | 89 |
| Figure 5. 37 Window in manual mode (2)..... | 89 |

List of Tables

| | |
|--|----|
| Table 2. 1 Advantages and disadvantages of Traveling Wave and Impedance Based . | 11 |
| Table 3. 1 Comparison of ANN and FL In Power System Analysis | 21 |
| Table 4. 1 Truth table of fault type decision..... | 47 |
| Table 4. 2 Planning of simulation data | 53 |
| Table 4. 3 Example of the collected simulation data process..... | 53 |
| Table 4. 4 Number of simulation data samples for training and testing phase | 54 |
| Table 5. 1 Truth Table of proposed rule | 56 |
| Table 5. 2 Confusion using for justification of fault or no fault using proposed rules | 58 |
| Table 5. 3 Results of Estimation Error for Single Line to Ground Fault..... | 66 |
| Table 5. 4 Results of estimation Error for Double Line Fault..... | 67 |
| Table 5. 5 Results of Estimation Error for Double Line to Ground Fault | 69 |
| Table 5. 6 Results of Estimation Error for Three Phase Fault | 70 |
| Table 5. 7 Overall performance of the ANFIS-GK based at 5Ω fault resistance | 71 |
| Table 5. 8 Overall Performance of the ANFIS-GK at 100Ω fault resistance | 72 |
| Table 5. 9 Comparison based on fault resistance | 73 |
| Table 5. 10 Fault Location Error using 100Ω and 200Ω on SLG and DLG | 74 |
| Table 5. 11 Fault Classification | 76 |
| Table 5. 12 Fault Location..... | 77 |
| Table 5. 13 Percentage of real data classification | 78 |
| Table 5. 14 Results of Estimation Error for Utility Data | 79 |
| Table 5. 15 Result testing on Relay..... | 81 |
| Table 5. 16 Comparison on range of error..... | 82 |
| Table 5. 17 Comparison with ANFIS-GK and ANN..... | 83 |
| Table 5. 18 Comparison of GK and FCM..... | 84 |
| Table 5. 19 Parameter | 85 |

CHAPTER 1.0

INTRODUCTION

1.1 Motivation

Transmission lines are designed to transfer electric power from source locations to distribution networks. However, their lengths are among the highest fault incidence rate in the power system components since they are exposed to the environment. Protective relay and fault recorder systems, based on fundamental power frequency signals are installed to isolate the faulty line and provide the fault position. The crucial for reliability, increasing of physical dimensions and size of the transmission lines has motivated the researchers to investigate the effort to improve their accuracy by giving attention on fault detection, classification and location.

A fault is defined as a disturbance in voltage, current or frequency in the power signal. The balanced fault in a transmission line is three phases to ground circuits. Whereas, single line-to-ground (SLG), line-to-line (LL) and double line-to-ground (DLG) faults are unbalance in nature. When the power system is subjected to a line faults, load changes will take place and the system needs to adjust itself to the changing conditions. The system must be able to operate efficiently under faults conditions and successfully supply the desired amount of power line. The system should also be capable to compensate under numerous faults that occur in different locations along the transmission line. However, designing a system that can respond to numerous faults will involve a lot of equipment.

The deterministic conventional approach has helped greatly in fault analysis. However, the approaches have a few drawbacks. Firstly, they have a less accuracy due to wide variation in respective system and power network.

Secondly, conventional approach requires complex mathematical calculation in the algorithms. Thus, the requirement of handling by expert operator is desired for fault identification. Other than that, the dependence of line parameters such as value of system voltage, fault resistance and line length will limit the performance of such approaches.

An independent and parameter free algorithm is an option to overcome this problem. In line with the computational technologies, an artificial intelligence (A.I) approach may overwhelm the problem. In the real world, fault diagnosis in power system using AI techniques was still in research stage. The demand of larger power system architecture and increasing of fault data storage required the support of AI to accommodate the problems. As one of the well known technique in A.I, artificial intelligent network (ANN) is very useful when no mathematical model of the system is available whereas fuzzy logic has a capability to imitate the sensing, generalizing, processing, operating and learning ability of human operator [1]. The reference [2] mentioned that these two methods can be combined since they have the same basic structure of neuron except some or all of the components and parameters of fuzzy neuron should describe in fuzzy logic. A fuzzy neural network is built on fuzzy neurons or on standard neurons but dealing with fuzzy data. This hybrid intelligent system called as adaptive neuro-fuzzy inference system (ANFIS) is a connectionist model for the implementation and inference of fuzzy rules [3].

ANFIS has been used in fault detection and fault classification in power system since last two decades [4] and has helped to contribute many inventions in the research. Recently, the researchers have spent their interest on its capability for estimation of fault location in transmission line and distribution network [1], [4], [5], [6]. By using ANFIS, the strength of each method will contribute to the development of the proposed scheme for fault analysis in power transmission line. Still, the improvement in optimization techniques is being investigated for further research. The research in this thesis addresses neuro-

fuzzy systems and their applications especially in distance estimation tasks. ANN is trained from the dataset generated by performing clustering using Gustafson-Kessel (GK) algorithm. In order to use the learning capability of the neural network, it is combined with fuzzy systems. New algorithms for optimization and modeling should be applied to increase the performance of such system. It uses magnitudes of voltages and currents from one terminal line as input data of the ANFIS. In this approach, an ANFIS was trained and tested using various sets of field data, which was obtained from the simulation of faults at various fault scenarios pertinent to fault types, fault locations and fault resistance.

1.2 Objective

The specific objective is to develop a parameter free algorithm for power transmission lines. This includes:

- i. Detection of fault signal
- ii. Classify the types of fault
- iii. Estimate the location of fault

1.3 Scope of Works

1. Focus on power transmission line. This is based on the fact that, the impact of fault occurrence on power system transmission line and the time required to physically check the lines are larger than the faults in the sub-transmission and distribution systems.
2. The required input data are voltages and currents of the signal.
3. Pertinent to symmetrical fault; three phase, unsymmetrical fault; single line to ground, double line and double line to ground.
4. Detection of the occurrence of a fault, categorize types of faults, then estimate

the distance where the fault occurs.

5. Test the scheme with a few case studies for validation purposes including the comparison with other related methods.
6. Develop graphic user interface for better understanding of the system.
7. In the simulation, the loading conditions over the protected transmission line are assumed to be nearly constant.
8. Focus the capability of research methodology in fault identification related to artificial intelligence approaches.
9. The computations involved are ATP/ EMTP to obtain simulation data and Matlab for further analysis.

1.4 Research Methodology

1. Literature survey on:
 - i. Fault types, characteristics and diagnosis
 - ii. Methods and modeling approach
 - iii. Wavelet transforms and feature extraction
 - iv. Artificial neural network and Fuzzy logic systems
 - v. Development of ANFIS architecture
2. Determine the main objectives and scope of works
3. Develop the flow charts, algorithms and solution methods
4. Build and test the power system transmission line model
5. Analyzed and conclude the results

A lot of data is needed by using simulation data and real data. Simulated data are obtained from a test system for the purpose of training and testing. Modeling using fuzzy rules and membership parameters allows the system to track the given input and output. The propose schemes aimed to introduce the option of

checking the sets while training. Thus the process of training and testing will be much more accurate. By implementing the neural network, this method can provide a procedure to learn information about data sets. Trainings, testing and case studies will be done to identify the performance of development schemes.

1.5 Expected Contribution

1. The developed algorithms are possible for general application that can be deployed at any end of a transmission line without the need for communication devices between the two ends.
2. The system is able to be used for end user which has no required expert skill.
3. The system able to estimate the fault location without the consideration of the series impedance matrix per unit length which needed for conversational approach.
4. Improves the previous artificial intelligent approaches since the required data training set size is smaller to justify the existing data.

This dissertation is organized as follows:

Chapter 2 presents an introduction of fault analysis in power system. This includes the background knowledge about transmission line models and analysis on types of fault. Literature review of conventional approaches and algorithms for fault detection, classification and location in power system also briefly explained in this chapter.

Chapter 3 presents the artificial intelligence approaches in power system. This includes a brief review on artificial neural networks and fuzzy logic. Issues rise between these two techniques also discussed which leads to the invention of adaptive neuro-fuzzy inference system.

Chapter 4 describes the development of the proposed system for fault identification, classification and location which implementing ANFIS, wavelet transform, and other optimization methods. A novel integration with a powerful clustering technique called Gustafson-Kessel also explained in this chapter.

Chapter 5 presents the results on the simulation design which used to train the developed system and observation on its performance.

Finally, chapter 6 emphasizes the conclusions and contribution throughout the dissertation. Explanations on thesis limitation and improvement for future works are presented.



CHAPTER 2.0

CONVENTIONAL APPROACHES OF FAULT ANALYSIS IN POWER SYSTEM

This chapter explains the conventional approach of fault analysis and its trends in the past few decades. In power transmission line protection, faulty phase detection required to be addressed in a reliable and accurate manner to confirm the occurrence of fault or vice versa. The tripping action depends on the voltage and current waveform during the fault. In this condition, signal processing tools play an important role in the digital distance protection schemes. Parallel transmission lines are being concerned due to their economic and environmental benefits. The robustness and reliability of double circuit/ parallel line are important since the faults commonly happen in this type of system voltage.

2.1 Fault Detection in Power System

The conventional approach to detect fault is pertinent to the fundamental frequency and transient signals. In fundamental frequency, it can be categorized into three detail methods. The first method is identifying with the harmonic current comparison. The inductive reactance will increase and the capacitive reactance will decrease. In this situation, the harmonic order is also increasing. Taking consideration to the zero sequence current, equation 2.1 describes the flowing in the Petersen-coil when the power system capacitive currents operate in the normal feeder is more than the inductive current flowing;

$$\sum_{i,i \neq j}^n I_{0iM} \gg I_{0IM} \quad (2.1)$$

Harmonic inductive current produced by the Peterson-coil can be omitted. The current of the M th harmonic component in the faulted feeder is basically the sum of the current in sound feeders. Instead, the M th harmonic component

direction in the faulted feeder is differing to the one in the sound feeders. By using the M th harmonic component, the faulted feeder can thus be recognized. The feeder with M th harmonic current component larger than other feeders and direction opposite to other feeders is the faulted feeder. Usually, the 5th harmonic component has been chosen as M since it is related to fault arc and resistance. Different type faults have different 5th harmonic and different characteristics.

The other method is based on signal current that is injected to the grounding fault phase of faulted feeder conveyed by the bus voltage transformer. The signal frequency is between n and $n + 1$ times the power fundamental frequency 50Hz:

$$n \cdot 50 < f_0 < (n + 1) \cdot 50 \quad (2.2)$$

The injected signal is recognized based on a specific detector that is fixed at each feed. During the normal condition, the signal magnitude in each feeder is in direct proportion to its capacitance to earth. Whereas, during the grounding fault conditions, the signal is flowing to the fault point from the signal source. The signal magnitude in each normal feeder is close to zero. Then, the faulted feeder is possible to be identified by measuring injected signal magnitude. Somehow, this method couldn't identify the high impedance grounding fault since the signal is too small to be detected in the faulted feeder. The third method is detection using phase current difference. Changing currents occurred due to grounding faults in three-phase-symmetry systems. In sound feeder, the difference between three phase changing current is almost zero.

In the fundamental transient signal method, wavelets transform is being used which capable to investigate the transient signals generated. The short fourier transform is used to identify conditions of fault or healthy by generation of the frequency contour. This approach explained in which fault condition contours are produced at high frequency and healthy condition produced at lower frequency. The reference [7] has presented an algorithm that is based on time

domain analysis. Their work is dependent on short fourier transform for generating frequency contours.

2.2 Fault Classification in Power System

The distance relays detect the faulty line and type of fault whenever a fault occurs in an electrical transmission line. The impedance estimated by a digital distance relay decrease in line with the increasing of speed. Due to this condition, an impedance relay with a definite range setting couldn't operate at a high speed [8]. An algorithm that is based on the measurement of phase angles between the positive and negative sequence components of the current phasors is proposed in the reference [9]. This algorithm also measured the relative magnitudes of the zero and negative sequences quantities present in the current waveforms. The aim is to classify between grounded and ungrounded faults. Due to the changes in the power system, the reference [10] has proposed a method using rms voltage measurements to characterize it. Discrete measurements of the time interval between 2 sequential rms values in one cycle will be considered. The features of the value are then used for classification purposes.

2.3 Fault Location in Power System

Basic algorithms used in fault locators are intended to make the distance to fault calculation as accurate as possible. The fault locator is mainly associated with protection relays. Distance relays for transmission-line protection provide some hint of the possible area where a fault occurred. However, they are not aiming to determine the location. Moreover, line protection and fault location are fulfilled by processing the same currents and voltage signal which attained from the instrument transformers and recorded at the substation. Features of estimated fault location are a required in any protection scheme.

General conventional method of fault location in a power system is impedance-based. In this method, the voltage and current data at several points

are measured using per unit length of the impedance along the transmission line. Reliant on the readiness of the fault locator input signals, these methods can be classified as one-end algorithms [11] and two-end algorithms [12] [13, 14]. One-end algorithm estimate a distance to fault by using voltages and currents acquired at a particular end of the line. This method is simpler since there is no necessity of communication with the remote end [5, 15]. When the line impedance per unit length has been calculated then, the fault distance is able to be identified. For grounded fault, value of fault resistance will be high, thus will affect the result of fault location. On the other side, if the fault is ungrounded, the value of fault resistance will be low and does not affect the accuracy of the fault location. Two-end algorithm [12-14] considered signals from both terminals of the line and great amount of information is utilized. In general, performance of the two-end algorithm is much better. Different input signals are used for two-end fault locators as, for example, complete currents and voltages from the line terminals [12-14] or quantities from impedance relays at the line terminals [16, 17].

Another conventional method is based on traveling wave. In this method, an electrical pulse initiating from the fault propagates along the transmission line on both sides away from the fault point. The time required by pulse return describes the length to the fault point. This method is appropriate for a long and standardized line. However, it has the disadvantage which is that propagation can be expressively influenced by system parameters and system configuration. Other than that, it is also hard to locate faults close to the bus or faults that occurred near zero voltage inception angle. With the advances in data procurement, global positioning system (GPS) time synchronization, and communication systems, traveling wave methods could be improved [18].

Table 2. 1 Advantages and disadvantages of Traveling Wave and Impedance Based

| | Traveling Wave | Impedance Based |
|---------------|---|---|
| Advantages | <ul style="list-style-type: none"> - Possible to perform accurate fault location - The error does not depend on the distance from the fault | <ul style="list-style-type: none"> - Simpler since there is no necessity of communication with the remote end - Easy to install and operate |
| Disadvantages | <ul style="list-style-type: none"> - Need to be handled by skilled operator - Require a high speed communications channel for accurate time measurement - Accuracy is highly dependent on the sampling rate, estimation of line length and time-stamping | <ul style="list-style-type: none"> - Need to be handled by skilled operator - Affected by mutual coupling to nearby circuits, load flow and fault resistance. |

Other methods are based on wavelet transform, artificial intelligence, independent component analysis, time frequency analysis and sinusoidal steady state analysis [19] but limited if single usage in fault location purposes. Table 2.1 summarizes the advantages and disadvantages of traveling wave and impedance based approaches.

2.4 The Trends of Fault Analys in Power System

In 1960's, the digital computer for relaying to collect information has been installed. Thus, the relay engineer is possible to handle the reach characteristics of a distance relay in line with the implementation and fault location algorithms [20]. the computation of voltage and current phasors at the line faulty terminals contributes to the reactance's calculation of fault locators [14, 21]. However, some assumptions are required for the fault distance calculation in the fault location

methods for better accuracy. The one-terminal method is easier to be implemented [22-24]. The most contradict is that two-end algorithms require signals from both terminals of the line [25].

In 1970's, "ultra high speed protection" method based on the travelling wave is being explored. After the fault existed, a few early cycles comprise high frequency transient waveforms. The transient state signals of the fault location can be calculated within a few milliseconds. The traveling wave based in distance protection with various algorithms proposed in the reference [26-28]. The transit times that contain higher frequency is used on fault generated transients to justify the faulted line section [29]. However, this method does not perform greatly for faults that near to the relaying point and for faults contain small value of fault inception angle. One of the reasons is this method needs a very high sampling rate. Other than that, the implementation is quite expensive. Due to the increasing size of the power network, a real time power system changes at the transmission line protection is needed. The solution must able to operate at higher speeds to certify on the stability of transients. The references [8, 11, 12, 14] have reported regarding the real time power system changes and accurate, fast faulty phase selection and fault location.

In 1980's, real time protection implemented synchronized measurement technology. Digital measurement at a diverse line terminals can be executed synchronously by using GPS [29, 30]. The accuracy is better than distance relaying algorithms. The factors of inadequate modeling of transmission lines and parameters ambiguity have no effect on the performance. For power system applications, the Phasor Measurements Units (PMU) implement synchronized measurement devices widely. The references [14, 29, 30] have reported that the accuracy of GPS clock and PMU-based fault locators are better than the unsynchronized phasors. However, the unsynchronized approaches are cheaper because GPS is not required. It also immune to the errors pertinent to the different sampling rates or recording devices and transducers' phase shifts. The

impedance based fault location methods have been presented in the references [13, 16, 31] which have neglected the fault location error. The accuracy of power system protection has been supported by using GPS, PMU, digital communication technologies and high precision signal transducers. However, it is depending on the performance of software in security and communication.

In recent years, combination of mathematics and signal processing approaches for the fault detection, classification and location have been investigated by developing relay and protection devices. Such measuring algorithms that possible to adapt dynamically to the system operating conditions are required. The conditions are pertinent to the changes in the system configuration, fault resistance and source impedances. Thus, intelligent techniques such as Artificial Neural Network (ANN), Fuzzy Logic (FL), Fuzzy-Neuro and Fuzzy Logic-Wavelet based systems are considered under investigation to increase accuracy, reliability and speed of existing digital relays. A summary of most methods in power systems for fault detection, classification and location are illustrated in figure 2.1, 2.2 and 2.3.

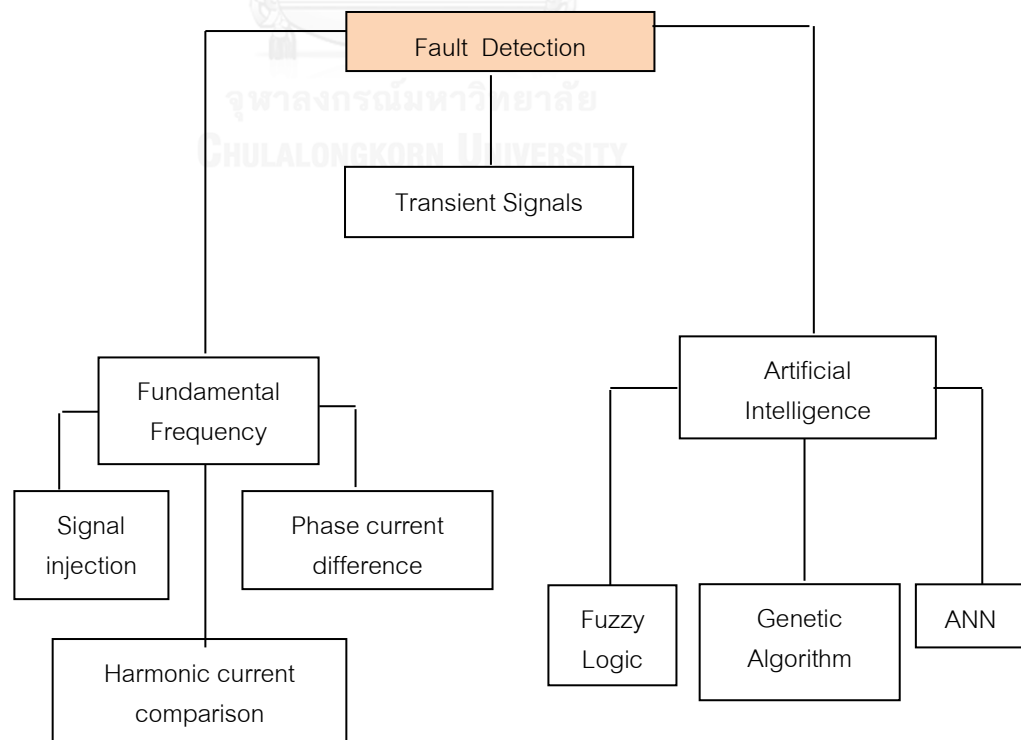


Figure 2.1 Illustration of summary for fault detection in power system

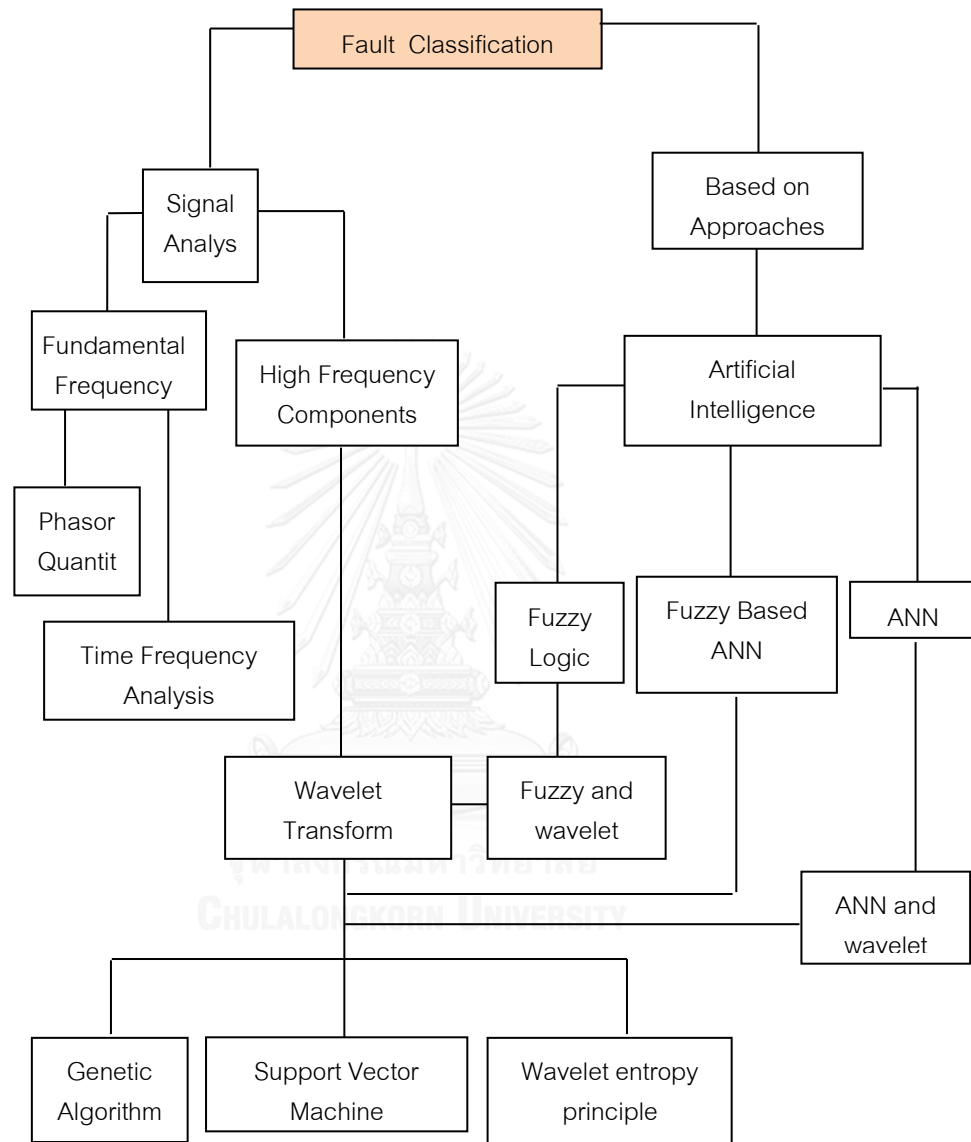


Figure 2.2 Illustration of summary for fault classification in power system

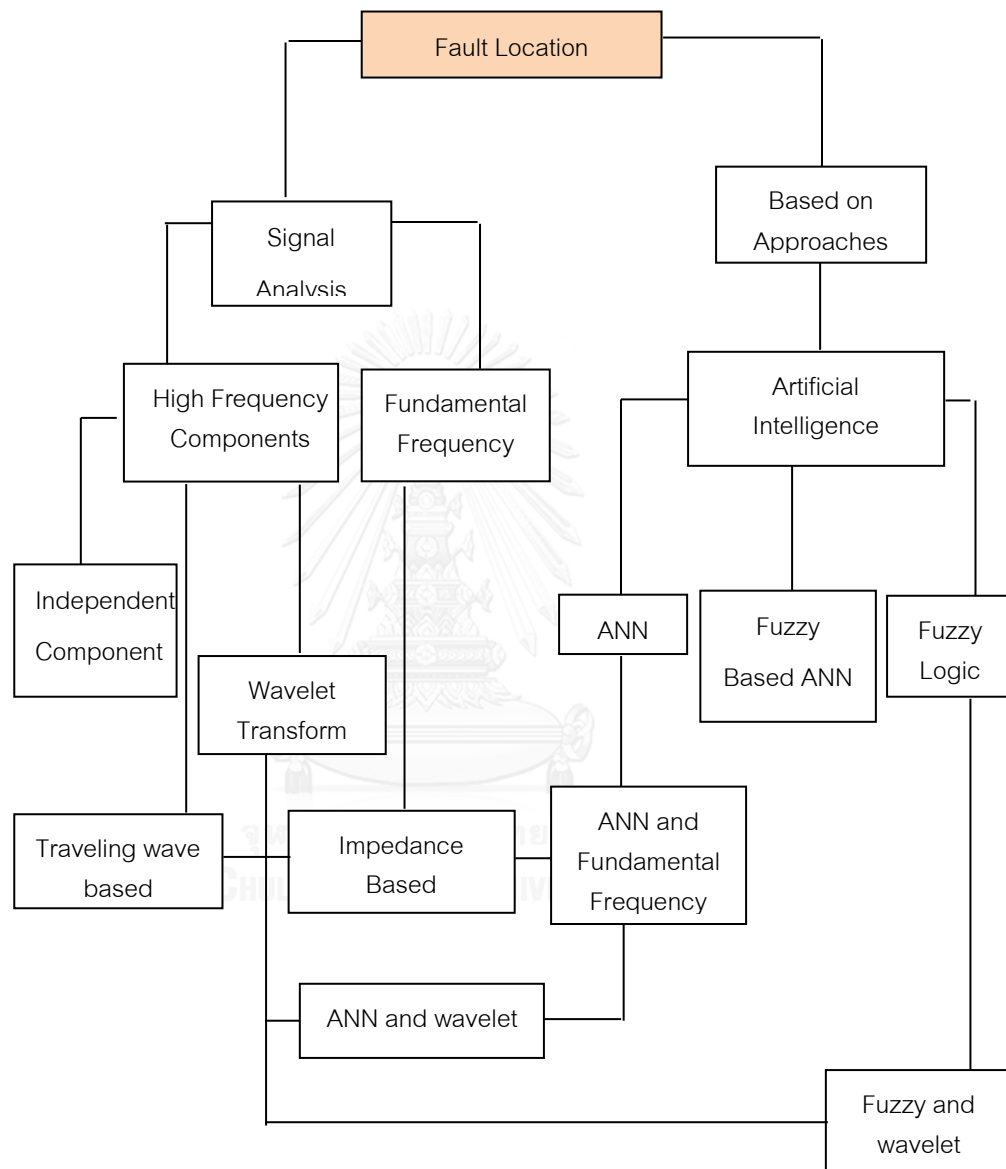


Figure 2.3 Illustration of summary for fault localization in power system

CHAPTER 3.0

ARTIFICIAL INTELLIGENCE TECHNIQUES AND FAULT ANALYSIS IN POWER SYSTEM

3.1 Artificial Neural Networks (ANN) in Power System

Neural networks can be illustrated as a biological neural networks in cooperatively performing their functions and organized in several layers. The weight was related to synaptic efficiency in biological neurons. Weights are the prime feature of the long term memory in ANNs. Usually, the initial weights of the network are set in a random number. Then, the weights will be modified accordingly depends on the set of training examples. Each weight assigned to respective signals from the input links to form as an information-processing unit. A processing element generally has many inputs and a single output as shown in figure 3.1.

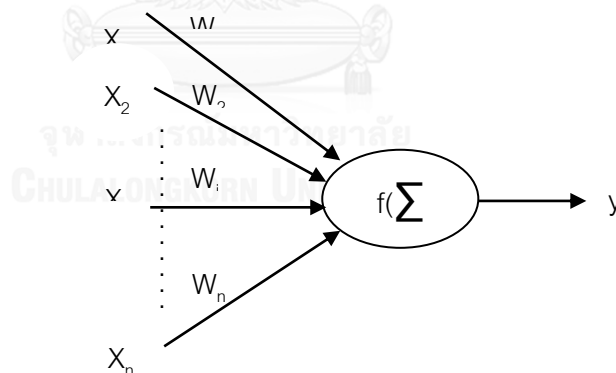


Figure 3.1 An Artificial Neuron

A set of input signals x_1, x_2, \dots, x_n (vector X) that sent to the neuron are usually the output signals of other neurons. Each input signal is multiplied by the respective connection weight, w , analogue of the synapse's efficiency. The NN is formed from the sum of neurons, connected with each other and the environment. During the process, the input vector is transformed into output one. The connections, solve the problems on computation power networks. Connections

associate the inputs of one neuron to the output of others. The weight coefficients provide the strength of the connection. Training with the network needs to be repeated until the network produces an acceptable result. In the process, learning law and related programs must be reevaluated. These are the steps involved in the training process of supervised back propagation [13]:

1. Input/output parameter selection for training.
2. Data for training is generated.
3. Training data get through the normalization
4. Provide the unknown set of data for testing purposes

The neural network has the flexibility with noisy data and corporate with a backpropagation training algorithm to learn the significant signature of disturbance. This approach is able to implement in power system which the information is very useful. In actual condition, the operator may be stunned by the unnecessary number of simultaneously operating alarms. This condition will require certain time to identify the source. The protection devices play the role in identifying the occurrence of a fault. The following action is sending the trip signals to circuit breakers (CBs) for isolation purposes.

The ANN classifiers technique has the capability to learn and adapt themselves to different statistical distribution. It is possible to slightly estimate the character of the sensor measurements. ANN is able to keep information about a fault existence in a power system to the memory [32, 33]. Overall, the prime benefit of using ANN technique is the capability on learning.

3.2 Fuzzy Logic in Power System

Fuzzy logic is based on the extension of multi valued logic systems invented by Zadeh Lotfi in 1965 [34]. It is responsible in utilizing the membership linguistic value to develop great human reasoning model. Whereas, a “fuzzy set”

is a simple extension of the typical set contained any values between 0 and 1 [35].

Equation 3.1 elaborated an example:

$$A = \{(x, \mu_A(x)) | x \in X\} \quad (3.1)$$

where $(x) A \mu$ is known as membership function for the fuzzy set A . Every x is mapped to a membership grade between 0 and 1. A fuzzy if-then rule contained of fuzzy rule which can be expressed as; **If** x is A **then** y is B . The A and B values defined by fuzzy sets. “ x is A ” which also known as “antecedent”, and “ y is B ” which also known as “consequence”.

Figure 3.2 shows the illustration of the fuzzy inference system (FIS) that contain of fuzzification, fuzzy inference engine and defuzzification stages. In fuzzification, crisp inputs are transformed into degrees of match with linguistic values. The knowledge base provides MFs and fuzzy rules required for the process. The numerical crisp variables are the input of the system that passed through a fuzzification stage. Now, the input is called fuzzy input for the fuzzy inference engine which then will be fuzzy output.

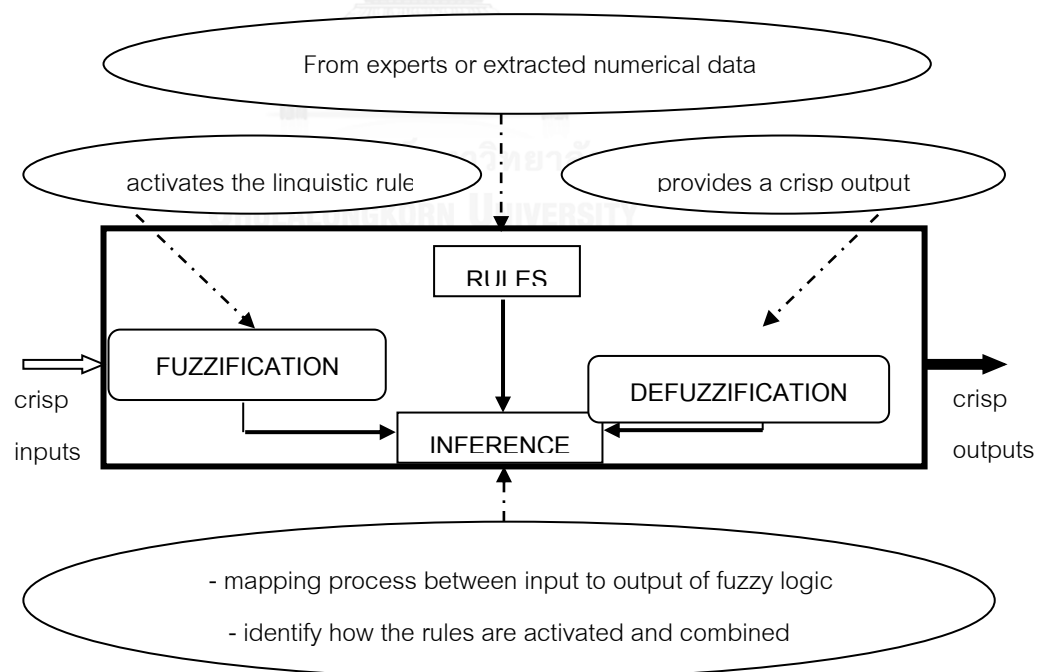


Figure 3.2 Fuzzy inference system

The linguistic results are then transformed into numerical values to become the output. Takagi-Sugeno (TS) is one of the models in FIS is proposed by Takagi and Sugeno in 1985 [36]. The fuzzy rules are in the form of; If x is A and y is B then $z = f(x,y)$. A and B are the fuzzy input membership functions, and $z = f(x,y)$ is the crisp output. Usually, the output is a polynomial expression of x and y . The order of the polynomial defines the order of the model. The output is calculated as the weighted average for the rules.

Clustering techniques are methods in a FIS that can be used to classify data into certain groups according to the data and not rely on estimation in conventional statistical methods. Therefore, they are most benefit in condition where less prior knowledge presents [37]. In the filed of pattern recognition, classification, modeling, image processing, and identification, a suitable clustering algorithm is able to be implemented. The success of such clustering algorithm depends on the execution. Theoretically, no algorithm able to prove that it has the best performance in every related characteristic. It is merely depends on the problem to be solved and the structure of the data to be clustered. Three types of fuzzy clustering algorithm are explained in following paragraphs;

Fuzzy C-Means (FCM) is dependent to the measurement of distance between samples. The Euclidean distance is used which each feature has similar importance. FCM provides a good approximation to the final solution using a few iteration steps. This algorithm normally implemented in a spherical shape. The drawback of FCM is it tends to locate the centroid in the neighborhood of the larger cluster [38].

Adaptive Fuzzy Clustering (AFC) is able to recognize elliptic or circular clusters. It is almost not affected to the number of clusters being searched. This algorithm is normally implemented in a linear clusters. The drawback of AFC is the eigenvalues have to be computed to update the prototypes. Thus, any changes are barely noticeable [39].

Gustafson-Kessel (GK) is faster than AFC. It has ability to predict the local covariance and to manage data into subsets. This characteristic is well fitted with linear sub-models and useful for identification of TS models [36, 40]. GK is a comprehended version of the standard fuzzy c-means algorithm. This algorithm employ an adaptive distance norm to detect clusters of different geometrical shapes in one data set [49]. Each cluster has a definite norm-inducing matrix A_i used as optimization variables. A_i allow each cluster to familiarize the distance norm to local topological structure of the data.

Applications of fuzzy logic in the power system network possible for a problem which due to the constantly changeable power system parameters [40, 41] The aspects to utilize fuzzy logic applications are;

1. The useful knowledge of the problem is available.
2. The solution is difficult to be expressed in terms of mathematical form.
3. The expression of mathematical forms require various assumptions.
4. The problem comprises of ambiguity and/or multiple conflicting objectives.

Fuzzy logic control presents a possibility to address the control problem. The fault presents an abrupt unknown change in the system dynamics to be the information of a controller. The fuzzy logic controller can regularly estimate any real continuous mapping to arbitrary accuracy. Thus, the fuzzy logic approach capable to implement linguistic explanations of control rules to the model systems [41]. Fuzzy logic systems made judgements on inputs in the form of linguistic variables consequent from membership functions (MFs). The fuzzy set and the degree are used by MFs to match with the specific linguistic IF-THEN rules obtained through fuzzy implication. The response of every rule is weighted based on the impedance or membership degree of its inputs. Whereas, the centroid is calculated to form the appropriate output [2, 36].

Fuzzy set based expert systems is faster compared to the traditional rule-based expert systems. Almost all rules are substituted by the calculation of the membership functions of the appropriate rules. The inference engine [5] use only

parts of rules. A drawback on implementing fuzzy logic is that the control of some systems cannot be easily specified in terms of an IF/THEN rule base. In a practical transmission line, the fault detector detects the fault and feed into the FIS. The system is used to gain the crisp output of fault diagnosis. ANN can be used to improve the performance of the line by the advantage of adjusting with the values of line parameters. Table 3.1 shows the comparison of ANN and FL in power system analysis.

Table 3. 1 Comparison of ANN and FL In Power System Analysis

| Feature | Approach | |
|--------------------------------------|---|--|
| | ANN | FL |
| Knowledge used | A training set of cases provide the extraction of information | Protection criteria provide the expert knowledge |
| Troubleshooting and refining a relay | Hard to interpret the internal signals | The internal signals are simpler to understand |
| Self-learning | Natural | Probable |
| Handling un-clear task | Natural | Natural |
| Robustness | Difficult to certify | Possible to certify |
| Setting a relay | Need large number of simulation data | Used knowledge and simulation |
| Computations | Dedicated hardware | Possible |

3.3 Issues of ANN and FIS

ANN algorithm needs to be retrained whenever there are changes in the system. It is difficult to ensure the stability of ANN and ability on learning new data sets of input/output data [42]. ANN often require a huge number of iterations for training and not guarantee to find the correct answers. Most researchers agree that the starting point vector is as important as the other aspects of the network [6]. One of the solutions for the problems is to modify the structure of ANN composing the polynomial equation based on weights to fit the stability constraints

before the training step [2]. Unfortunately, the modification is rather complex. Another option is by using adaptive neuro-fuzzy inference system [43] where the ANN is ensured to be trained on the complete I/O data space of a fuzzy logic system. Unclear information is able to be performed by using fuzzy sets [41].

Fuzzy neural network (FNN) is the combination of fuzzy rule based system to increase the learning capabilities. In [43], ANN and FIS has combined due to the advantages of both techniques to create a hybrid intelligent system that ensured ANN to be trained on the complete I/O data space of a fuzzy logic system. Another problem in implementing ANN is the possibility on occurrence of overfitting during training phase. The network has learned the training examples, but it has not educate to adapt to new situations [44]. Fortunately, the integration of ANN, FIS and optimization algorithm is possible to overcome the problem of overfitting in ANN [6].

3.4 Adaptive Neuro-Fuzzy Inference System (ANFIS)

ANFIS is basically similar to fuzzy inference system [2]. The targets are one output from several given inputs that employed using the information of membership function. The weighted values via the product were used to justify the curve of respective parameters. Then, a calculation must be done between the individual and overall weighted values. The information of adjusted membership function via learning process also being considered. The ANFIS then estimates the output based on the overall gained value. Back-propagation and least-square estimation technique are the foremost algorithms in developing ANFIS . Assuming a certain shape and finding the beginning and end points for the fuzzy values in a fuzzy set is a neural network optimization problem [43]. Figure 3.3 is a diagram of such a system.

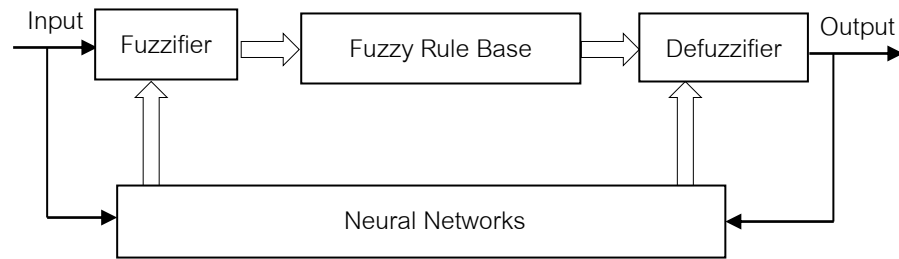


Figure 3.3 Fuzzy system which membership functions adjusted by ANN

ANFIS normally used TS type fuzzy inference system which the weighted average's rule is define as below:

$$R_i: \text{If } x \text{ is } A_i \text{ then } y_i = f_i(x), i = 1, 2, \dots, K \quad (3.2)$$

The fuzzy value of y_i required an extension principle for the calculation. The functions f_i are in the same structure. However, the parameters in each rule are divergent. Perhaps, f_i is a vector-valued function. Significantly, a scalar f_i is then will be notified. A useful parameterization is defined as below:

$$R_i: \text{If } x \text{ is } A_i \text{ then } y_i = \mathbf{a}_i^T \mathbf{x} + b_i \quad i = 1, 2, \dots, K \quad (3.3)$$

where \mathbf{a}_i is a parameter vector and b_i is a scalar offset. This is called an affine (linear in parameters) TS model. If $\mathbf{a}_i = 0$ for each i , the singleton model is obtained. TS model can be considered as a linear system with input-based parameters).

$$\gamma_i(x) = \beta_i(x) / \sum_{j=1}^K \beta_j(x) \quad (3.4)$$

$\beta_i(x)$ obviously known as a function x to acknowledged that the TS model is a quasi-linear model of the following form:

$$\mathbf{y} = \left(\sum_{i=1}^K \gamma_i(x) \mathbf{a}_i^T \right) \mathbf{x} + \sum_{i=1}^K \gamma_i(x) b_i = \mathbf{a}^T(x) \mathbf{x} + b(x) \quad (3.5)$$

The 'parameters' $\mathbf{a}(x)$, $b(x)$ are convex linear combinations of the subsequent parameters \mathbf{a}_i and b_i , i.e:

$$\mathbf{a}(x) = \sum_{i=1}^K \gamma_i(x) \mathbf{a}_i, \quad b(x) = \sum_{i=1}^K \gamma_i(x) b_i \quad (3.6)$$

TS type of fuzzy modeling required two main stages in solving the problems: 1. Structure identification and 2. Parameter optimization [43]. Structure identification is referred on identifying the input output space partition and number

of rules. Parameter optimization is referred on searching the ideal values in the system based on the parameters. Most of the literatures [36, 40, 45] related to TS type of fuzzy systems modeling considered on a trial and error method. It tends to find the optimum number of rules. ANFIS is basically similar to fuzzy inference systems [46] where a TS system mapped into a neural network. There are five-layers in the architecture of ANFIS as shown in Figure 3.4. The fuzzy inference system has two inputs x and y , one output f , and two fuzzy if-then rules of which referred to TS's type [36]:

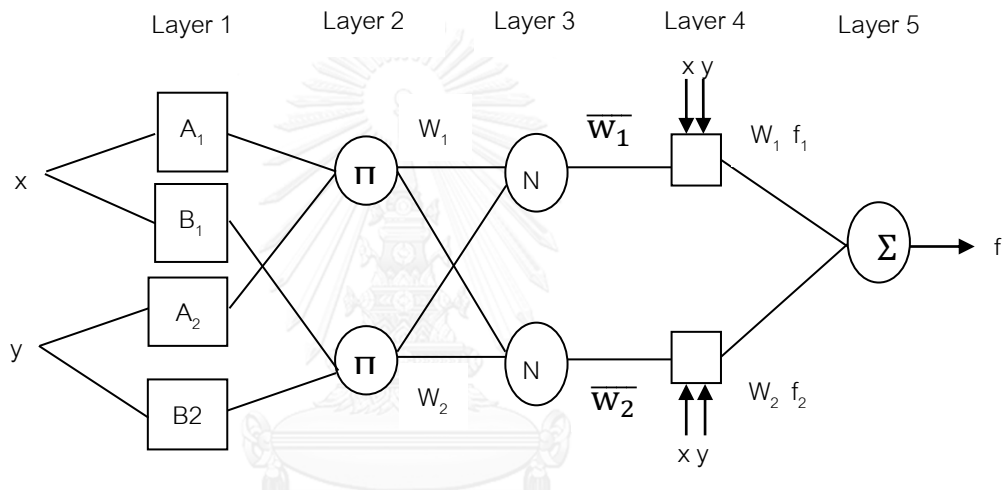


Figure 3.4 Architecture of ANFIS

The first layer is recognized as a fuzzification layer that defines the membership.

$$O_{1,i} = \mu_{A_i}(x) \quad \text{for } i = 1,2$$

$$O_{1,i} = \mu_{B_{i-2}}(y) \quad \text{for } i = 3,4$$

$$\mu_{A_i}(x) = \frac{1}{1 + \left| \frac{x - c_i}{a_i} \right|^{2b_i}} \quad (3.7)$$

$$\mu_{B_i}(y) = \frac{1}{1 + \left| \frac{y - c_i}{a_i} \right|^{2b_i}} \quad (3.8)$$

Second layer is output nodes pertinent to the firing capability of the rule as the product of the membership. Every node is a fixed node labeled T-norm operator.

$$O_{2,i} = w_i = \mu_{A_i}(x)\mu_{B_i}(y), \quad i = 1,2 \quad (3.9)$$

The third layer is recognized as the 'normalized firing strengths'. The ratio of the i th rule's firing strength to the sum of all rules' firing strength become the output of the i th nodes;

$$O = \prod_{j=1}^n \mu(x_j) = \mu(x_1) \cdot \mu(x_2) \cdot \dots \cdot \mu(x_j) \cdot \dots \cdot \mu(x_n) \quad O_{3,i} = \bar{w}_i = \frac{w_i}{w_1 + w_2} \quad (3.10)$$

In layer 4, it provides the consequent parameters which prepare towards the defuzzification process. Each node in this layer is an adaptive node with a function;

$$O_{4,i} = \bar{w}_i f_i = \bar{w}_i (p_i x + q_i y + r_i) \quad (3.11)$$

In layer 5, the single node is a static node that calculates the total output to be the received signals called defuzzification.

$$O_{5,i} = F = \sum_i \bar{w}_i f_i = \frac{\sum_i w_i f_i}{\sum_i w_i} \quad (3.12)$$

A typical rule set with two fuzzy if-then rules for a first-order Sugeno fuzzy model explained as below [18]:

Rule 1: If x_1 is A_1 and x_2 is B_1 , then $y_1 = p_1 x_1 + q_1 x_2 + r_1$,

Rule 2: If x_1 is A_2 and x_2 is B_2 , then $y_2 = p_2 x_1 + q_2 x_2 + r_2$,

Where;

$[A_1, A_2, B_1, B_2]$ are called the premise parameters.

$[p_i, q_i, r_i]$ are called the consequent parameters, $i = 1, 2$

ANFIS has a single output which attained by a defuzzification process of weighted average. The proposed rule generation algorithm is applied to the training set. This method is capable to initialize the neuro-fuzzy model on learning process and decrease the complex design. The number of rules or membership functions plays the prime role in the identification of structure. Usually, the trial and error method is implemented. However, this method may give a problem to confirm its capability. A suitable fuzzy clustering algorithm can eliminate this problem. Section 3.2 has explained about the fuzzy clustering algorithm.

3.5 Fault Detection in Power System

In detection phase, the type of structure in ANN implements multilayer perceptron and then using the backpropagation algorithm for training [47]. The weights are informed based on the error produced through the evaluation of neural output and the target output. After the training process, information on weight and bias will be used to detect the fault signal. The basic structure of ANN learning process is presented in figure 3.5.

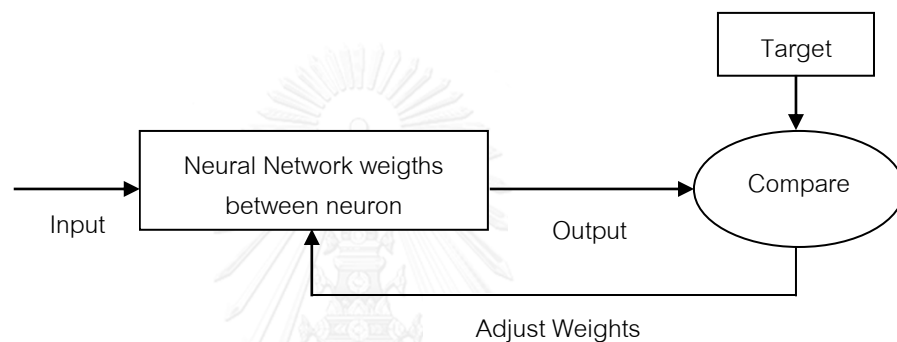


Figure 3.5 Basic structure of ANN learning procedure

The principle of fuzzy logic is possible for fault detection, which the output is either fault (1) or no fault (0). [47] have used fuzzy information fusion calculation for faulty decision making. They convert the fuzzy reliability degree into the output judgement (either fault or no fault) by using the equation; $Y = \sum_{i=1}^n K_i \mu_i$. When $Y \geq 0.5$, the fault is occur and when $Y < 0.5$, no fault occur.

Following literatures are pertinent to identification process which related to fault classification and fault location. Implementation of pattern recognition is greatly important for a good identification process. Pattern recognition aims to offer a reasonable judgement for all possible inputs and to perform the most similar match of the inputs. Figure 3.6 shows the basic modules of a pattern recognition system.

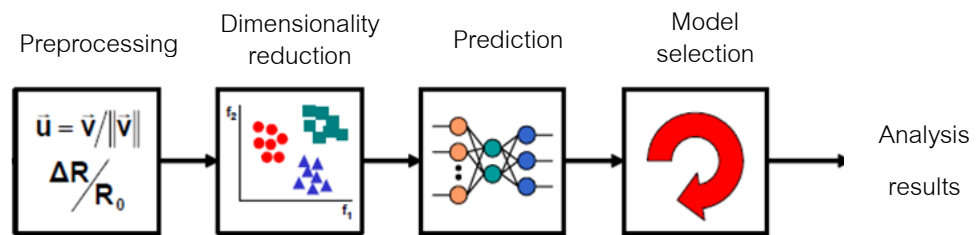


Figure 3.6 Basic modules of a pattern recognition system

3.6 Fault Classification in Power System

3.6.1 Artificial Neural Networks Based Methods

ANN has advantage as an excellent pattern recognition, and classification. Due to this benefit, many algorithms based on ANN for fault classification have been discovered [47]. ANN needs no information on impedance as basic information, has the capability to learn from examples during the training phase, capability to generalize, immune to the noise, and less affected by changes in system parameters.

By using the idea of captured waveform information, a fault classification scheme based on ANN namely feed forward network (FFNN) and time delay network (TDNN) have been proposed in [8]. This idea capable to encode the temporal relationship found in input data. Figure 3.7 describes the mentioned scheme. A recent system focusing on detection and classification in double circuit transmission line has been proposed in [3]. The steps involve in the scheme begin with preparation of appropriate training data set considering all possible criteria that ANN need to learn. Then, a suitable structure is selected to train the data. Finally, the evaluation of the trained ANN using several test patterns to justify the performance of the scheme. An implementation of an optimization algorithm, Marquardt Levenberg with FFNN is investigated in [36]. In this scheme, communication devices between the two ends are not required and the fundamental components of current and voltage are employed at relay location

which are time varying signals are used. Conventional ANNs are good at static patterns but are not suitable for patterns which change with time.

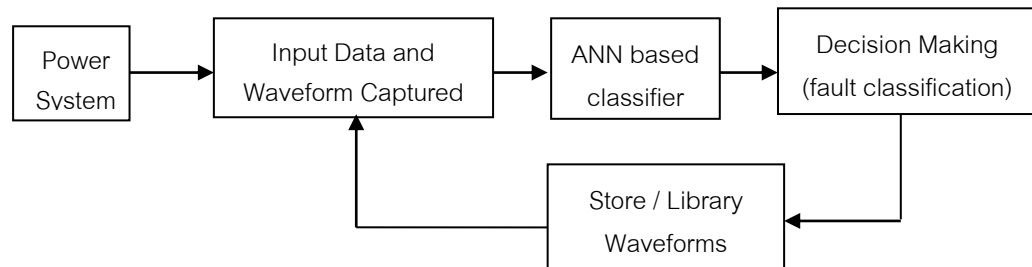


Figure 3.7 Fault Classification Scheme

3.6.2 Combination of ANN and Wavelet Transform Based Method

The wavelet transform gives the information about the frequency components exist in the signal at which time they are present [48]. It has received great attention due to its advantage on analysis of transient waveform better than other types of transform approach [49]. A novel approach of fault classification using wavelet transform to analyze power system transients is proposed in [50]. The scheme incorporated Probabilistic Neural Network (PNN) to identify types of fault after decomposing the fault signal to obtain the detail coefficients. PNN is used to justify the detail coefficients for each fault then classify them. It has received great attention due to its advantage on analysis of transient waveform better than other types of transform approach. In most of the reference research papers [33, 51, 52] wavelet coefficients are used for data input to the neural network.

A proper method integrating wavelet transform and ANN is proposed in [53] is suitable for high-voltage transmission line can detect the fault and classify using the basis of frequency found in the transients. Figure 3.8 shows the mentioned illustration. Discrete wavelet transform has combined with a method called adaptive resonance theory (ART2) to extract the features to classify the type of fault. This proposed idea explained in [52] and illustrated in figure 3.9.

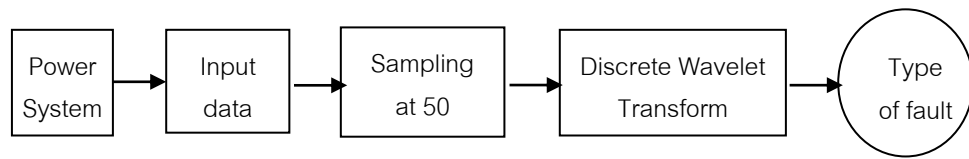


Figure 3.8 General illustration based on wavelet transforms

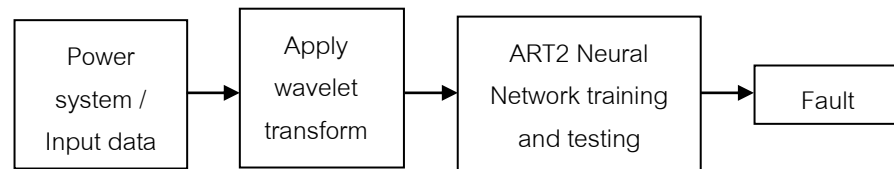


Figure 3.9 Wavelet-ART2 proposed scheme

3.6.3 Fuzzy Logic Based Method

Fuzzy logic referred to a simple, rule-based IF X AND Y THEN Z approach to solve respective problem. Since it has no need on training, it is computationally require less time compared to ANN methods. Fuzzy logic is combined with the discrete fourier transform (DFT) to detect and classify the type of faults. This approach, which discussed in [41] has used a full cycle and a separate sequence of symmetrical components of fundamental frequency. After this process, the angular differences between the sequence components during a fault current in each phase and their magnitudes fed into the fuzzy classifier. Fuzzy logic based has criteria of membership functions that possible to defeat overlap's problem. This advantage has encouraged the researchers in [54] to propose a new scheme of classification in electrical power system.

Knowledge of fuzzy expert system has combined with fourier linear combiner and explained in [55]. By using this algorithm, the peak amplitude of the voltage signal is normalized and the rate of change were able to be estimated. The fuzzy expert system is able to be used for several types of disturbance signals such as normal and sag. An adaptive resonance theory (ART) has combined with fuzzy K-NN decision rule is described in [56]. The scheme is capable to detect and classify the types of faults. Discrete wavelet transform has also potential in combining with fuzzy logic system as describe in [57]. They

investigate this algorithm to categorize the faults for series compensated transmission line.

3.6.4 Combination of ANN and Fuzzy Logic Based

A method which measured phase angles between positive and negative sequence components of the current phasors is explained in the reference [41]. It measured the relative magnitudes of the zero and negative sequence quantities to identified either grounded or ungrounded faults. A method to characterize changes in the power system using rms voltage measurements is described in [58]. Discrete measurement of rms voltage is taken into consideration for the time interval between two consecutive rms values in one cycle. Finally, rms of signatures and features is used for classification. A new algorithm which combined wavelet transform and ANFIS is proposed in [4] which involved these steps;

- i. Time frequency analysis by the wavelet transform component
- ii. ANFIS for the pattern recognition component to classify the type of faults.

3.7 Fault Location in Power System

3.7.1 Artificial Neural Network (ANN) Based Methods

By using the fundamental frequency components of the voltage and current at pre fault and post fault in one of the transmission line's end, various set of data is taken. Data is trained using the proposed neural fault locator as explained in [52]. Figure 3.10 shows the illustration of proposed scheme. The hidden layer and output layer were needed for the fault classifier and location. Similarly, [59] has used a feedforward neural network which utilized the back propagation learning algorithm for fault locators. Detail of the scheme is illustrated in figure 3.11.

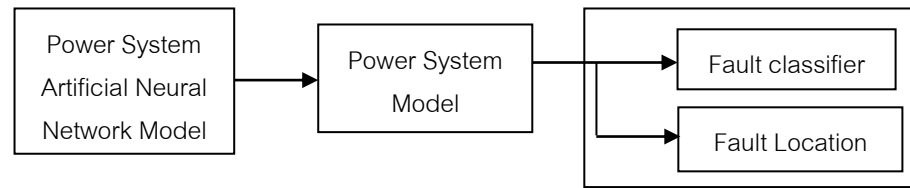


Figure 3.10 Functional block diagram based on frequency component and ANN

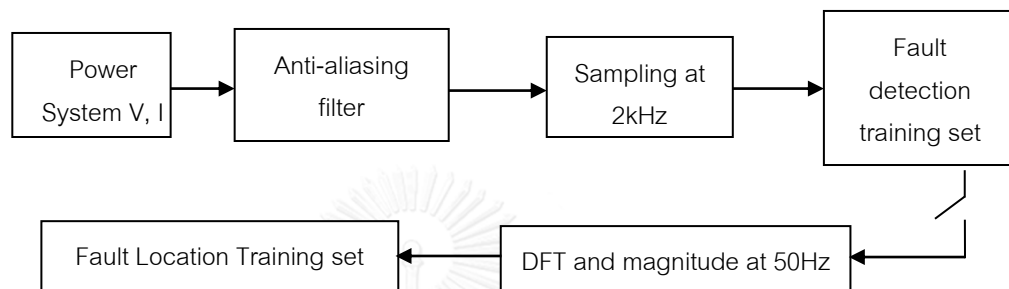


Figure 3.11 Functional block diagram of fault detector and locator

3.7.2 Combination of the ANN and Traveling Wave Method

The traveling wave principle is used in [60] to find location in high voltage DC transmission lines. This method can support the new dual-ended, principles, and single ended in traveling wave at the same time. Traveling wave theory has combined with fundamental frequencies at the beginning of fault identification. With this input data, ANN has utilized for fault location purposes. The ANN structure has been chosen by using a tool called ANN Automatic Selection System (SARENEUR) used to gain a neural network structure that shows better results in fault location within a two-terminal transmission line [5].

3.7.3 Combination of the ANN and Wavelet Transform Based Method

Combination of traveling wave theory and wavelet transform is proposed in [61]. The support vector machine helped this algorithm to estimate the fault location. The continuous wavelet transform has significant criteria that can contribute to identify fault location. This idea is investigated by constructing the mother wavelet directly from the recorded fault containing originate voltage

transient signal. The extraction of high frequency components of fault occurrence was able to contribute the knowledge for fault location. The study in [62] mentioned that the extraction is done by using the wavelet transform for underground cable fault based on the current and voltage traveling wave.

Similar to this scheme, [63] give improvement by monitoring the travel waves initiated by respective fault until the received end of transmission line. The instantaneous data is then used to justify the location of fault by implementation of discrete wavelet transform (DWT) to the modal components of the fault signal. Back-propagation neural network (BPNN) combined with DWT in [64] to identify the fault location on single transmission lines. The algorithm depends on the fault current waveforms attained from the simulation. After the implementation of DWT, feature extraction is applied and fault location estimation is justified using BPNN. DWT can provide useful information by analyzing the signals in the time-scale range then use it to estimate the fault location by using Elman recurrent networks.

3.7.4 Fuzzy Logic Based Method

Till now, FL systems have no definite contributions on fault location. The main factor is the constrain in adjusting the constructed FL network parameters. However, if FL combine with certain training methods for optimizing the parameters, the situation would be changed. Combination of wavelet transform with fuzzy logic has been proposed in [5]. The principal of their proposed algorithm is obtaining features extraction from fault signal using wavelet transforms. The information is then applied to fuzzy logic to decide the fault location. Similarly, the reference [36] has used the similar idea which decision made by the user's understanding on the variables. The output variables are taken from the fault distance from the source end, as shown in Figure 3.12. This system is able to demonstrate the main features from wavelet multi-resolution analysis (MRA) coefficients [37].

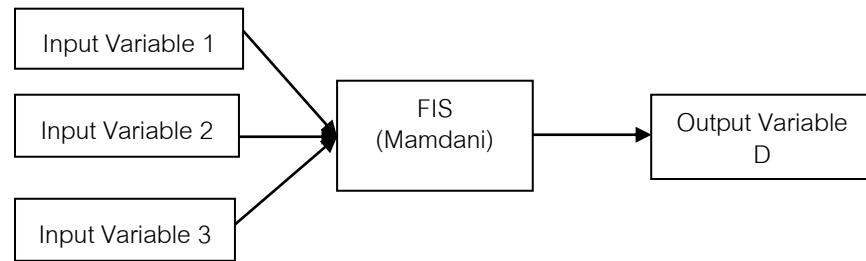


Figure 3.12 Proposed Fuzzy Inference System

3.7.5 Combination of the ANN and Fuzzy Logic Based Method

Combination of ANN and FL will produce an integrated system that is expected to overcome their drawbacks [4, 6, 36]. Generally, a neural network structure is used as a viewpoint for training purposes whereas fuzzy is used as a viewpoint to obtain insight of the system. The network is trained using back propagation algorithm. Figure 3.13 shows the proposed distance protection scheme used in [6].

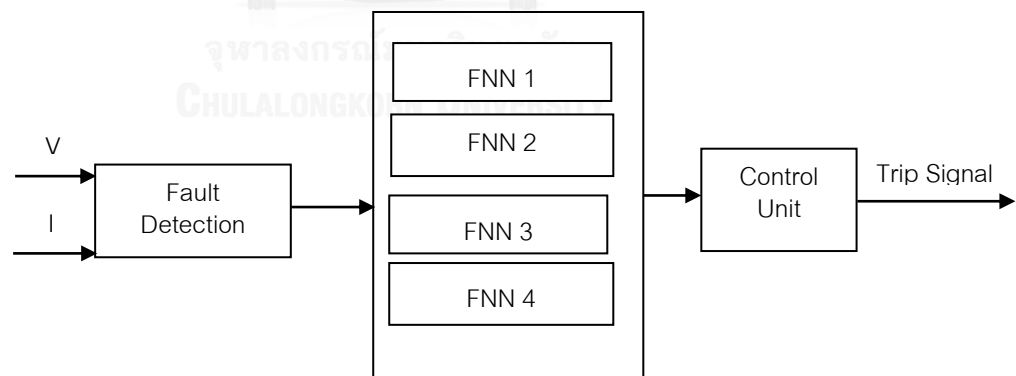


Figure 3.13 Proposed distance protection scheme

CHAPTER 4.0

FAULT DETECTION AND IDENTIFICATION WITH ANFIS

4.1 Proposed Framework

The proposed scheme and related algorithms were expected to be general enough which the implementation is not affected by the system voltage and other line parameters. Figure 4.1 illustrated the proposed framework. The required input is voltages and currents from raw signals during the fault duration. The first stage is 'detection' which aim to justify either the signal is faulty or healthy. After the signal is confirmed as faulty, it will be extracted using wavelet transform to obtain the detail coefficient. The next procedure is to identify the type of fault and the estimation of fault location.

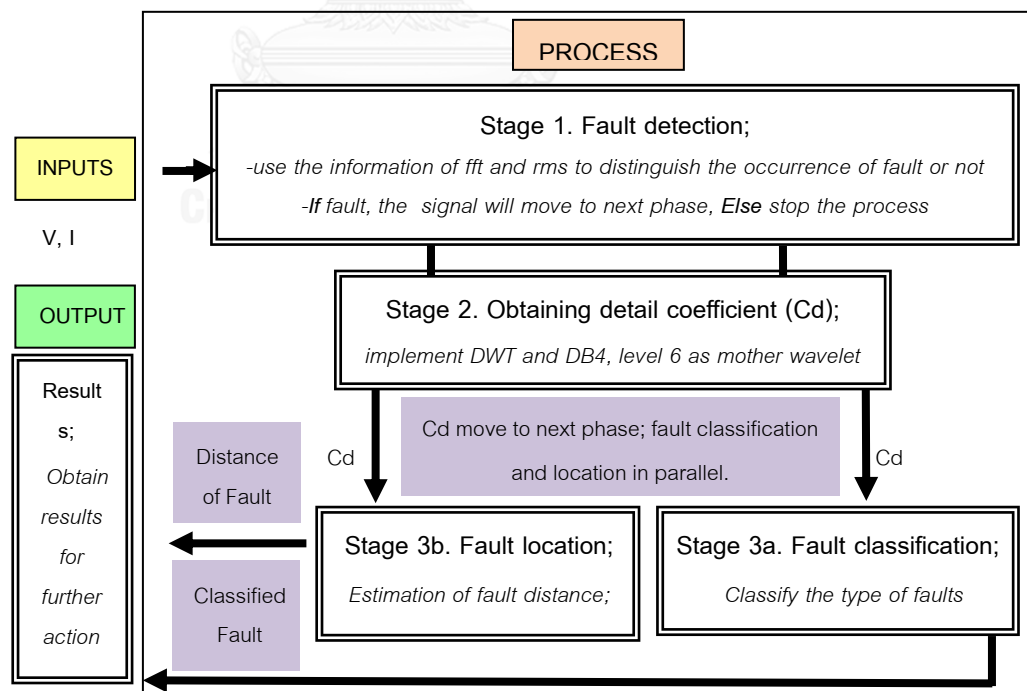


Figure 4. 2 Illustration of Model in Details

4.2 Fault Detection Algorithm

The fault detection algorithm is illustrated in figure 4.2. As the signal is discrete, the equation for RMS value of the signal, $s(n)$ (where $s(n)$ can be voltage or current) having n discrete samples $\{x_1, x_2, x_3, \dots, x_n\}$. For no fault waveforms, the RMS values are almost constant. For the fault waveforms, RMS value varies as the amplitude of the waveform varies. If the signal is fault, the rms value of the voltage of the phase in fault decreases while corresponding current rms value increases.

FFT is a tool which effectively analyzes different frequency components present in a signal. It is a fast method to compute Discrete Fourier Transform (DFT) of the signal. DFT converts a signal from time domain into the frequency domain. For no fault waveforms-have a strong peak at 50 Hz for all 3 phases with almost same amplitude. For fault condition, the magnitude of peak at 50 Hz of FFT for the voltage in fault will decrease significantly compared with FFT peak at 50 Hz of voltage not in fault. Conversely, FFT peak value at 50 Hz of the current during fault will be significantly higher than FFT peak value at 50 Hz of current in no fault. Figure 4.3 shows the snapshot of the algorithm in the program.

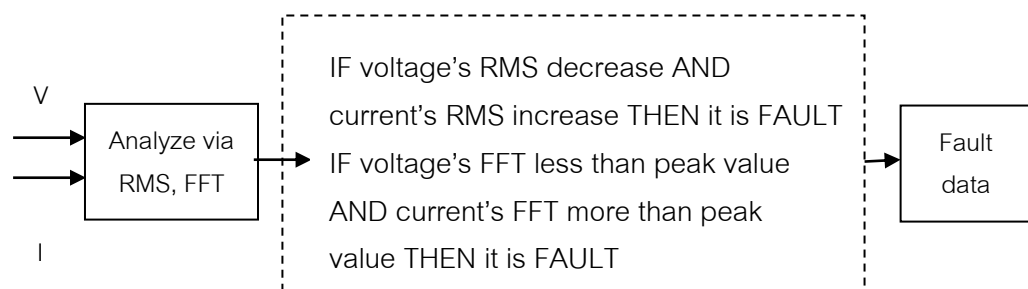


Figure 4. 3 Proposed algorithm for fault detection

```

samplingTime = diff(time(1200:1201));
sample_freq = 1/samplingTime;
SignalFrequency = 50;

% RMS values of Va, Vb, Vc, Ia, Ib, Ic
rmsVa = calcRMS(Va, samplingTime, SignalFrequency);
rmsVb = calcRMS(Vb, samplingTime, SignalFrequency);
rmsVc = calcRMS(Vc, samplingTime, SignalFrequency);
rmsIa = calcRMS(Ia, samplingTime, SignalFrequency);
rmsIb = calcRMS(Ib, samplingTime, SignalFrequency);
rmsIc = calcRMS(Ic, samplingTime, SignalFrequency);

% FFT of Va, Vb, Vc, Ia, Ib, Ic
[freq1, FFTVa] = calcFFT(Va, 500, samplingTime, time(1), time(end));
[freq2, FFTVb] = calcFFT(Vb, 500, samplingTime, time(1), time(end));
[freq3, FFTVc] = calcFFT(Vc, 500, samplingTime, time(1), time(end));
[freq4, FFTIa] = calcFFT(Ia, 500, samplingTime, time(1), time(end));
[freq5, FFTIb] = calcFFT(Ib, 500, samplingTime, time(1), time(end));
[freq6, FFTIc] = calcFFT(Ic, 500, samplingTime, time(1), time(end));

length1 = size(rmsVa);
rmsTime = time(1:length1(2));

```

Figure 4. 4 Snapshot on part of fault detection algorithm

4.3 Implementation of Wavelet Transform

Wavelet has the capability to compress a signal without appreciable degradation. In DWT, the digital filtering technique is required to obtain a time-scale representation of a digital signal. In order to identify high frequencies, the signal is conveyed through a series of high pass filters. Then, to analyze the lower frequencies, it passes through a series of low pass filters. The highest scale and low-frequency is the approximation component of the signal. Whereas, the low-scale and high-frequency components is the detail component.

By using high pass and low pass filtering of the time domain signal, the signal is decomposed into different frequency bands. The signal now has the highest frequency of $p/2$ radians instead of p radians passing the signal through a half band low pass filter. Therefore, half of the samples can be abolished. This action is pertinent to the Nyquist's rule which stated that; sampling frequency should twice or higher than the maximum frequency present in the signal. Figure 4.4 illustrate the Nyquist's rule. Daubechies (DB4) wavelet has been chosen as the mother wavelet because it's fast decay and compactly supported structure. A half band low pass filter eliminates all frequencies that are above half of the highest frequency in the signal. For example, if a signal has a maximum of 2000

Hz component, then half band low pass filtering removes all the frequencies above 1000 Hz.

Another factor for the choice of DB4 as its shape is close to the original and it provides perfect reconstruction. The 6 level DWT on Va, Vb, Vc, Ia, Ib and Ic signals is applied in this calculation code of detail coefficients. In DWT theory, a sharp spike occurs which related to the fault detection. The spike represents the highest frequency of the fault signal. However, the theory couldn't be implemented in identifying a fault based on this spike only. Such spikes will appear when there is a sudden change in the cable current signal. Thus, it is hard to justify. The level 6 detailed coefficients show the nature of side band along with the dominant spike. The changes can be observed to significantly to identify the fault types and locations. The maximum detailed energy has been used as features of the fault classification and location scheme.

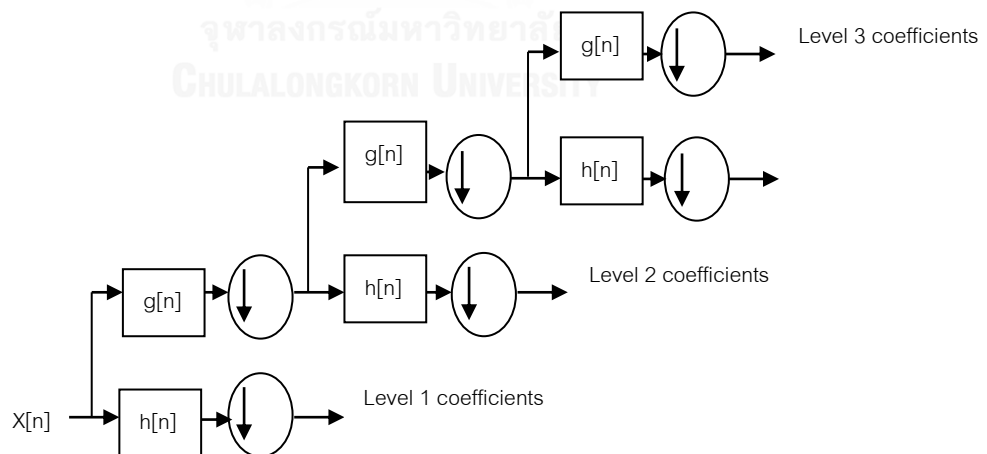


Figure 4. 5 Illustration of Nyquist's rule

4.4 Modeling of ANFIS

Modeling of ANFIS is based on pattern recognition, which explained in the previous chapter. ANFIS is equivalent to fuzzy inference systems. Thus, we have proposed a model that combines the steps on fuzzy clustering and identification [48]. The steps on fuzzy clustering consist in the following steps:

1. Used the system variables to justify the suitable model structure.
2. Attain the data using definite system variables.
3. Choose a clustering algorithm and the numbers of the relevant parameters.
4. Choose the number of clusters.
5. Clustering the data.
6. Attain the membership functions using projection technique.
7. Attain the fuzzy rule based on the membership functions.
8. Confirm the performance of model.

The steps of identification purposes contain of structure identification and parameter estimation. Structure identification can be executed in three steps [57]:

1. Selection of input and output variables,
2. Demonstration of the system's dynamics,
3. Selection of the fuzzy model's granularity.

The input and output variable selection referred to the model's objective, on the prior knowledge of process dynamics and on other variables that may contribute to the system's nonlinearity. Several models with different variables can be compared in order to assess the best model [21]. Having defined the model's structure, it follows parameter estimation, where the antecedent fuzzy sets A_i , the number of rules K , and the consequent parameters a_i and b_i for $i = 1, \dots, K$ is identified.

In the learning process of ANFIS model, the data will be categorized as training data and testing data. It is aimed for minimum estimation error from the training procedure. In order to reduce the error, variable membership function and

epoch parameters could be adjusted. The good prediction is obtained from effective input data. Table 4.3 shows the detail number of simulations.

4.5 ANFIS Architecture and Layers

The condition of ANFIS architecture required to be remained in specified intervals. The activation function for the nodes of layered structure is the sigmoidal logistic function with the similar variable gain factor in the previous layer. This gain factor should be adjusted appropriately, given the size of the weight boundary. The output layer performs a modified center of gravity defuzzification.

4.5.1 Input layers

The input variables are the ANFIS input layer that is fed to the condition element layer. It is known as fuzzification. The analysis is accomplished with the minimum and maximum points attached to adjacent centers. In confirming that some rules will be given the possibility to project for all points in the input space, the membership degrees will constantly sum up to 1 [8].

ANFIS has the advantage of more efficient with less arbitrary limitations [9]. The weights from the input to element layers of neurons can take values in $[0,1]$ since the data are assumed to be normalized. The normalization is a part of pre-processing procedure in the ANFIS. The membership functions are spaced equally over the weight space. The algorithm of initialization is shown in figure 4.5 (taking example of single line to ground fault). Some restrictions are engaged on adaptation to maintain the semantic meaningfulness of the memberships.

4.5.2 Rule layer

As the network in the system adapts, the rule layer demonstrates a single fuzzy rule that can be added to represent more rules. The activation function is the sigmoidal logistic function with a variable gain coefficient. The semantic meaning of the activation of a node is the input data that match to the antecedent

component of the associated fuzzy rule. Nevertheless, during interpretation of , such rules, the synergistic nature of rules in a fuzzy-neural architecture must be recognized. The connection weights from the element layer to the rule layer contributed to the degrees of importance. The weight limitation would certify that inputs into the rules remain within $[-1,1]$. The gain factor will let the rules to output values in $[0.1,0.9]$.

```

load AG;load BG;load CG; % loading data files

[nSamples nFeatures] = size(AGVector); % nSamples : Number of Samples (250) in AGVector, nFeatures : Number of Features in AGVector(6)
nCls = 3 ; % three classes i.e. AGW,BGW and CGW
AGVector=[ones(nSamples,1) AGVector]; % adding column of values 1 for indicating AGW
BGVector=[2*ones(nSamples,1) BGVector]; % adding column of values 2 for indicating BGW
CGVector=[3*ones(nSamples,1) CGVector]; % adding column of values 3 for indicating CGW

cLabels = 1 ; % column 1 contains class labels such that, if value in column 1 is 1 then the fault is AGW, if it is 2 then the fault is
cInputs = 2:nFeatures ; % contains columns of Inputs/features (wavelet coefficients) (goes from 2 to 7)
cOutputs = nFeatures+1; % contains column of output values (fault distances) (column 8)

```

Figure 4. 6 Snapshot of initialization algorithm

4.5.3 Output layers

The output layer represents a fuzzy label from the fuzzy quantization space. The current data used to recall the ANFIS supported the activation of the node. The connections from the rule layer to the action element layer represent justify the corresponding rules. The parameter involved in Layer 4 are predicted by using the least squares method of the forward pass. Here, the equation for the individual output is considered as the function of input. Layer 1 parameters estimate the back propagation and the gradient descent. The parameters are used for membership functions.

4.6 Membership Functions

The ANFIS technique determines the rules of membership functions from giving information to determine the full fuzzy sets using a Gaussian approach.

Neuro-adaptive learning technique has the advantage in learning information about a data set. By using input/output data, the membership function parameters can be calculated. Input membership functions and associated parameters can be interpreted using neural network type structure can. The parameters are then tuned or estimated to fit the data at hand.

The values related to the membership functions are assured to adjust during the learning process. The parameters will be computed as per the input parameter based on the value of the gradient vector to identify the value of fuzzy inference systems. When the gradient vector is computed, some of the optimization routines can be applied to adjust the parameters. This action can reduce some error measure based on the value of the performance index. The error measured usually defined by the total the squared difference between actual and desired outputs.

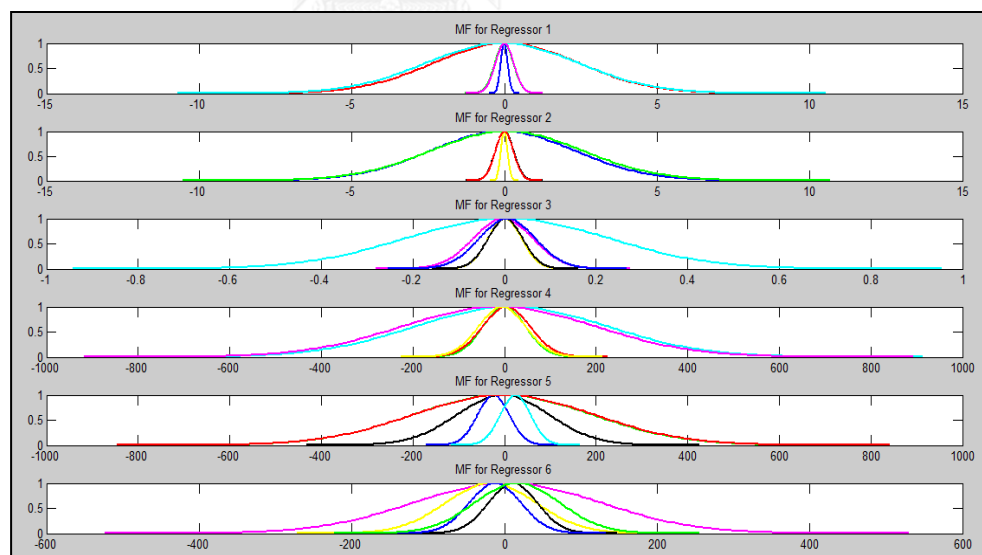


Figure 4. 7 Example of membership function's plotting

In the learning algorithm 'gbell' curved shape has been selected in the learning process since it can provide a precise and high performance on prediction. Back-propagation algorithm plays the role to vary the MF parameter in

the input side of the model. the least square estimation considered on the output side as a linear line. The minimum error percentage is a known as a small difference between target and prediction values. This is used as the indicator to observe the performance of the training process. Example of membership function's plotting is in figure 4.6. Part of the algorithm on membership function is shown in figure 4.7. The algorithm used for plotting the membership function regressor is shown in figure 4.8.

```

##### Projecting Membership on to individual regressors to create 1D antecedent fuzzy membership functions
[mu, sig]=createAntecedentMF (UTrain,XTrain);
plotmf(mu,sig);

%creating memberships of regression in projected mfs
UTrain=membership(XTrain,mu,sig,'prod');
UTest=membership(XTest,mu,sig,'prod');
disp(' ')
disp('...WAIT...')
%creating extended regressor for training and test data
XpTrain=createXp(XTrain,UTrain);
XpTest=createXp(XTest,UTest);

```

Figure 4. 8 Part of algorithm on membership function

```

function plotmf(mu,sig)
[c,r]=size(mu);
h=figure;set(h,'Name','Membership functions AG_0.5R');
N=200;
col=['b','g','r','c','m','y','k'];
ind= repmat(1:length(col),1,ceil(r*c/length(col)));
t=0;
for j=1:r
    subplot(r,1,j)
    for i=1:c
        mumf=mu(i,j);
        sigmf=sig(i,j);
        X=linspace(mumf-3*sigmf,mumf+3*sigmf,N);
        t=t+1;
        plot(X,exp(-((X-mumf)./ sigmf).^2),'LineWidth',2,'color',col(ind(t))); hold on;
    end
    title(['MF for Regressor ' num2str(j)]);
end
end

```

Figure 4. 9 Part of algorithm used for membership function regressor

4.7 New Approach in Fault Identification using the Gustafson-Kessel Algorithm

Fault data samples could be presented in a variety of features, especially for fault distance (different distance will present different features). With correspond to this understanding, this research giving attention to the fuzzy clustering that possible to perform and adapt even though using a small data set,

GK clustering algorithm has been chosen [37, 65, 66]. It is a great clustering technique that has been implemented in the area of image processing, classification and system identification [43, 45, 67]. It has the ability to predict local covariance and then partition the data into well fitted subset with linear sub-models [66, 68]. GK algorithm is able to reduce the possibility of overfitting when the amount of training samples is less compared to the number of clusters. This is attained by including a scaled unity matrix to computed covariance matrix. GK improved the standard fuzzy c-means algorithm since it employed an adaptive distance norm to justify the clusters in one data set [65]. Norm-inducing matrix A_i is vary for each cluster. The iterative optimization of the c-means type that implemented by the GK algorithm is described as below:

$$J(Z;U, V, \{A_i\}) = \sum_{i=1}^K \sum_{k=1}^N (\mu_{ik})^m D_{ikA}^2 \quad (4.1)$$

Here, $[\mu_{ik}] \in [0, 1]^{K \times N}$ is a fuzzy partition matrix of the data, $U = Z \in \mathbb{R}^{n \times N}$, $V = [v_1, v_2, \dots, v_k]$, $v_i \in \mathbb{R}^n$ is a K – tuple of cluster prototypes and $m \in [1, \infty]$ is a scalar parameter which used to justify the result's fuzziness. The distance norm D_{ikA} is able to identify the clusters of different geometrical shapes in one data set:

$$D_{ikA}^2 (Z_k - v_i)^T A_i (Z_k - v_i) \quad (4.2)$$

Figure 4.9 shows the steps on integration with GK algorithm that implemented in classification and location phase. Figure 4.10a and 4.10b illustrated parts of GK algorithm. A special modified GK algorithm [41] has been implemented as explained in the steps below;

Step 1: Identify the cluster prototypes (means)

$$V_i^{(1)} = \frac{\sum_{k=1}^N (\mu_{ik}^{(1-1)})^m Z_k}{\sum_{k=1}^N (\mu_{ik}^{(1-1)})^m}, \quad 1 \leq i \leq K \quad (4.3)$$

Step 2: Identify the cluster covariance matrices

$$F_i = \frac{\sum_{k=1}^N (\mu_{ik}^{(1-1)})^m (z_k - V_i^{(1)})(z_k - V_i^{(1)})^T}{\sum_{k=1}^N (\mu_{ik}^{(1-1)})^m}, \quad 1 \leq i \leq K. \quad (4.4)$$

$$\text{Include a scaled identity matrix: } F_i = (1 - \gamma)F_i + \gamma \det(F_0)^{\frac{1}{n}} I, \quad (4.5)$$

Extract eigenvalues λ_{ij} and eigenvectors ϕ_{ij} from F_i .

Find $\lambda_{i \max} = \max_j \lambda_{ij}$ and set:

$$\lambda_{ij} = \lambda_{i \max} / \beta \quad \forall j \text{ for which } \lambda_{i \max} / \lambda_{ij} > \beta \quad (4.6)$$

Reconstruct F_i by :

$$F_i = [\phi_{i1} \dots \phi_{in}] \text{diag}(\lambda_{i1}, \dots, \lambda_{in}) [\phi_{i1} \dots \phi_{in}]^{-1} \quad (4.7)$$

Step 3: Identify the distances

$$D_{ikA_i}^2 = (z_k - V_i^{(l)})^T [\rho_i \det(F_i)^{\frac{1}{n}} F_i^{-1}] (z_k - V_i^{(l)}), 1 \leq i \leq K, 1 \leq k \leq N \quad (4.8)$$

Step 4: Check the partition matrix

for $1 \leq k \leq N$, if $D_{ikA_i} > 0$ for $1 \leq i \leq K$,

$$\mu_{ik}^{(l)} = \frac{1}{\sum_{j=1}^K (D_{ikA_i} / D_{jkA_i})^{2/(m-1)}}, \quad \text{otherwise} \quad (4.9)$$

$$\mu_{ik}^{(l)} = 0 \text{ if } D_{ikA_i} > 0, \text{ and } \mu_{ik}^{(l)} \in [0, 1] \quad (4.10)$$

with $\sum_{i=1}^K \mu_{ik}^{(l)} = 1$ otherwise. until $\|U^{(l)} - U^{(l-1)}\| < \epsilon$

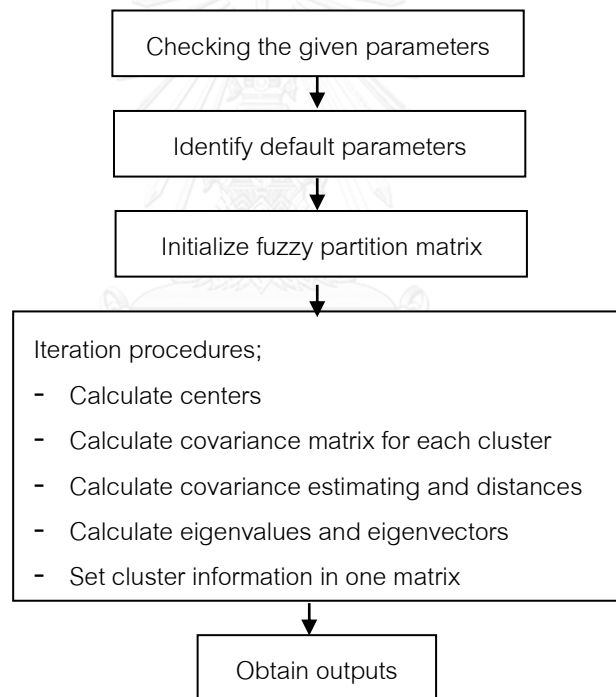


Figure 4. 10 Illustration of GK Algorithm Implementation

Given parameters:

X = regressor , y = regressend

c = number of local models/cluster prototypes

r = dimension of regressor / number of inputs

N = size of input

Default parameters:

M= fuzziness of clustering

Ro = termination tolerance

a)

```

% Initialize fuzzy partition matrix

if max(Nf0,nf0) == 1,      % only number of cluster given
    c = f0;
    mm = mean(X);
    aa = max(abs(X - ones(N,1)*mm));
    v = 2*(ones(c,1)*aa).*(rand(c,n)-0.5) + ones(c,1)*mm;
    for j = 1 : c,
        xv = X - X1*v(j,:);
        d(:,j) = sum((xv.^2),2);
    end;
    d = (d+1e-10).^(-1/(m-1));
    f0 = (d ./ (sum(d,2)*ones(1,c)));
else %if the partition matrix was given
    c = size(f0,2);
    fm = f0.^m; sumf = sum(fm);
    v = (fm'*X)./(sumf'*ones(1,n));
end;

f = zeros(N,c);          % partition matrix
iter = 0;                % iteration counter
A0 = eye(n)*det(cov(X)).^(1/n); % "identity" matr.

```

b)

```

% Iterate
while max(max(f0-f)) > e
    iter = iter + 1;
    f = f0;
    % Calculate centers
    fm = f.^m; sumf = sum(fm);
    v = (fm'*X)./(sumf'*ones(1,n));
    for j = 1 : c,
        xv = X - X1*v(j,:);
        % Calculate covariance matrix for each clusters
        A = ones(n,1)*fm(:,j)'.*xv'*xv/sumf(j);
        %Covariance estimating for the GK algorithm
        A = (1-gamma)*A+gamma*(A0.^(1/n));
        if cond(A) > beta;
            [ev,ed]=eig(A); edmax = max(diag(ed));
            ed(beta*ed < edmax) = edmax/beta;
            A = ev*diag(diag(ed))*inv(ev);
        end;
        %Calculate distances
        M = (1/det(pinv(A))/rho(j)).^(1/n)*pinv(A);
        %M(:,j) = (det(A)/rho(j)).^(1/n)*pinv(A);
        d(:,j) = sum((xv*M.*xv),2);
    end
end

```

Figure 4. 11 a and b Parts of Implemented extended GK algorithm

4.8 Fault Identification

Fault identification is separated into two schemes; fault type classification and fault distance estimation. ANFIS-GK is implemented in fault identification which the general explanation has been explained in the previous sections. The extracted data is fed to the fault identification as shown in figure 4.11. In GK, the

distance to all existing cluster towards incoming data points is calculated. If the distance is less than or equal to the radius of the nearest cluster, then the data point is assigned to the cluster. For a given data point, the higher the number of surrounding neighbors, the higher its potential values.

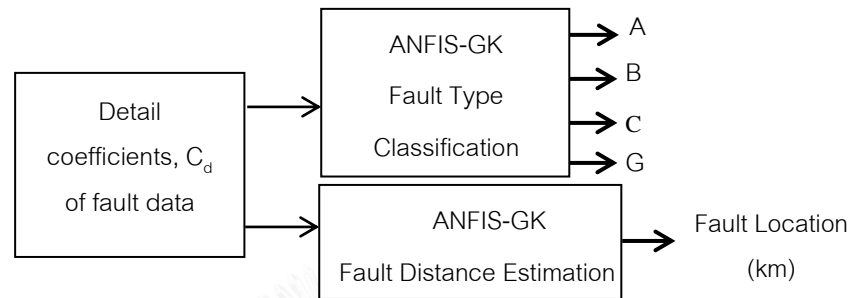


Figure 4. 12 Fault Identification scheme

The proposed scheme of ANFIS-GK approach for fault classification and location in transmission lines were independent. Thus, the result of fault classification will not affect the result of fault location. This is one of the benefits of the proposed scheme. In fault classification scheme, the structure of ANFIS-GK is performed as shown in figure 4.12. It is based on the features of each type of fault. For this scheme, GK is implemented to categorize the data to respective clusters. ANN helps to train the algorithm. The structure of an ANFIS used an acceptable and simple criterion after the training procedures. The maximum energy of detail coefficient for all three phases are selected as inputs. Table 4.1 describes about the decision of fault type. There are 4 outputs, namely 'A', 'B', 'C', 'G'. The number of rules has increased from 1 during the training process till the satisfactory network is achieved. The obtained structures are 6 inputs, 4 rules, 23 fuzzification neurons and 4 outputs. The number of rules and fuzzification however possible to be tuned based on the problems in hand.

Table 4. 1 Truth table of fault type decision

| Fault type | A | B | C | G |
|------------|---|---|---|---|
| No fault | 0 | 0 | 0 | 0 |
| AG | 1 | 0 | 0 | 1 |
| ABG | 1 | 1 | 0 | 1 |
| AB | 1 | 1 | 0 | 0 |
| ABC | 1 | 1 | 1 | 0 |

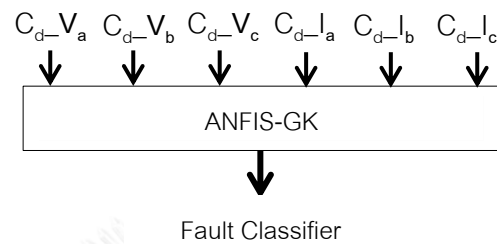


Figure 4. 13 Scheme for Fault Classifier

In fault location scheme, the structure of ANFIS-GK is performed with the structure in figure 4.13. For this scheme, GK couldn't work on its own for clustering purposes since the aim is to estimate the exact fault distance. Thus, system identification is required which has been explained in section 4.4. The inputs for the scheme are same as those in the classification. The output is the fault distance from the sending end in km. During the training procedure, the algorithm was taught to learn on patterns of signal for respective distance. When a fault data is tested, the general procedures were implemented until obtaining the detail coefficients. To estimate the fault location, concept of least square error estimation and neighboring hood were implemented based on training process.

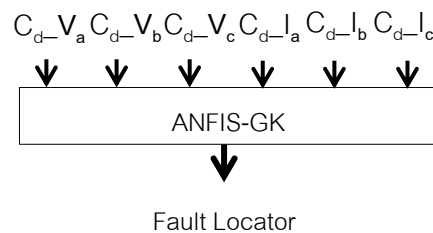


Figure 4. 14 Scheme for ANFIS-GK Fault Locator

4.9 Flowchart of Fault Classification Algorithm

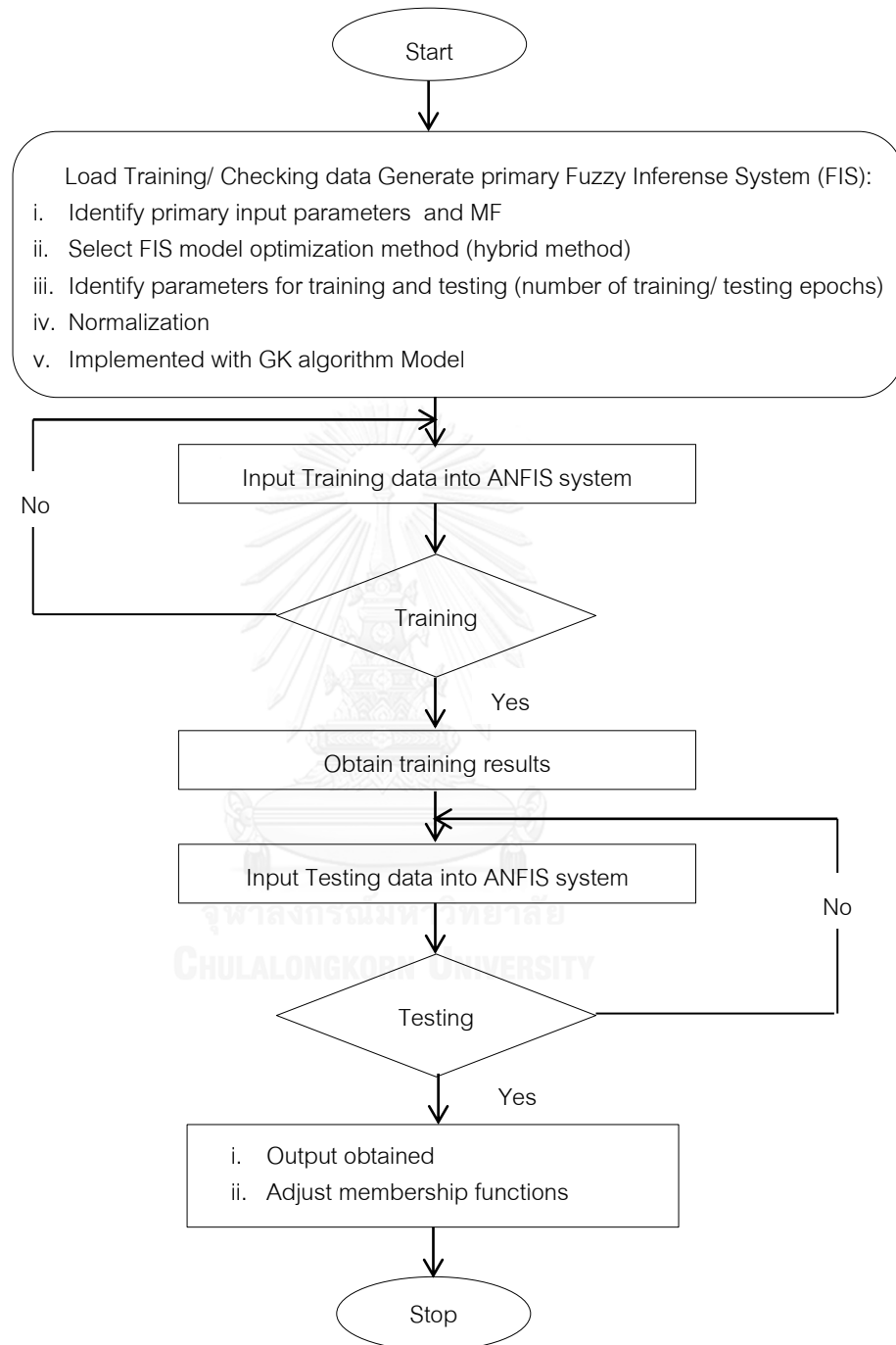


Figure 4. 15 Flowchart of classification algorithm

4.10 Flowchart of Fault Location Algorithm

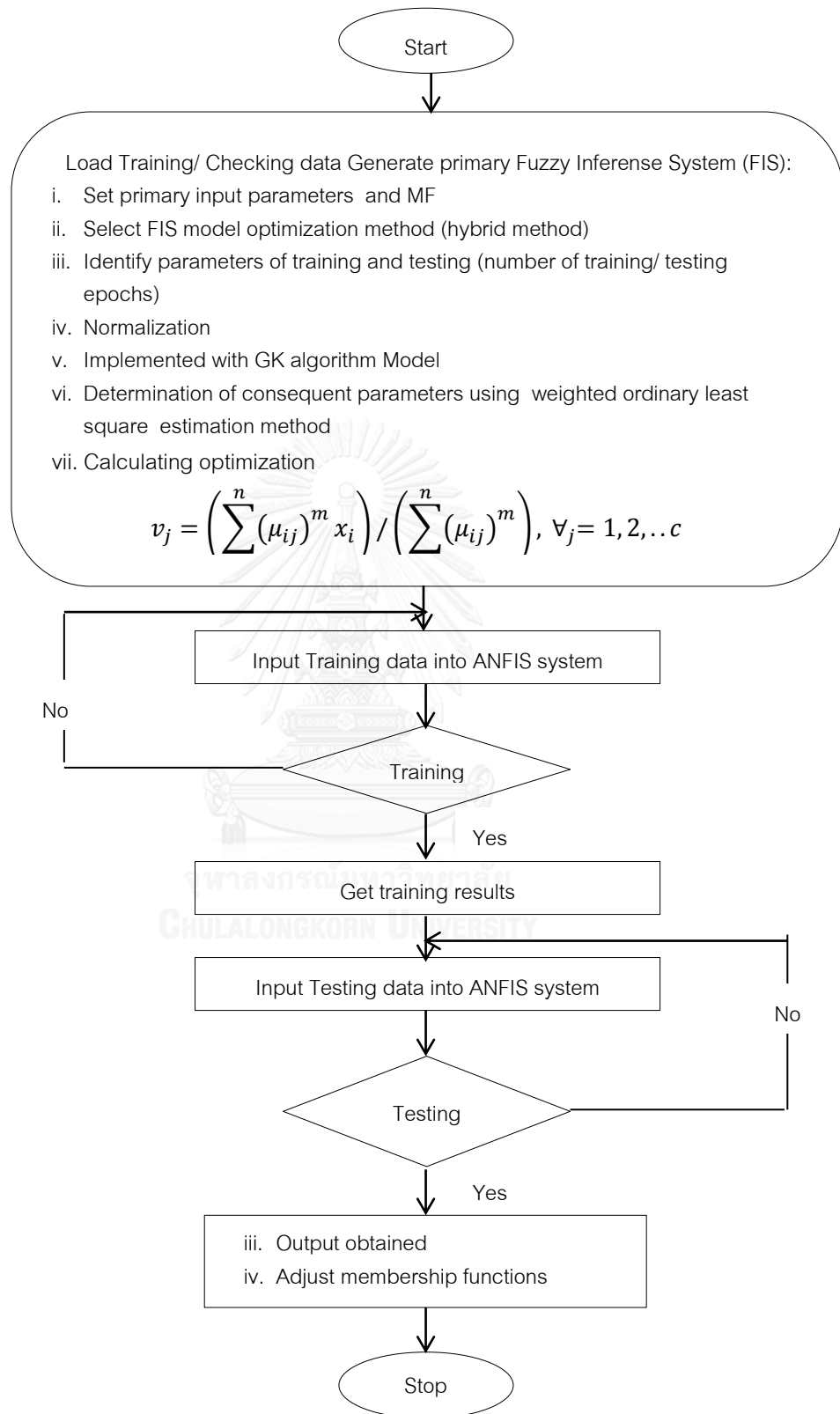


Figure 4. 16 Flowchart of location algorithm

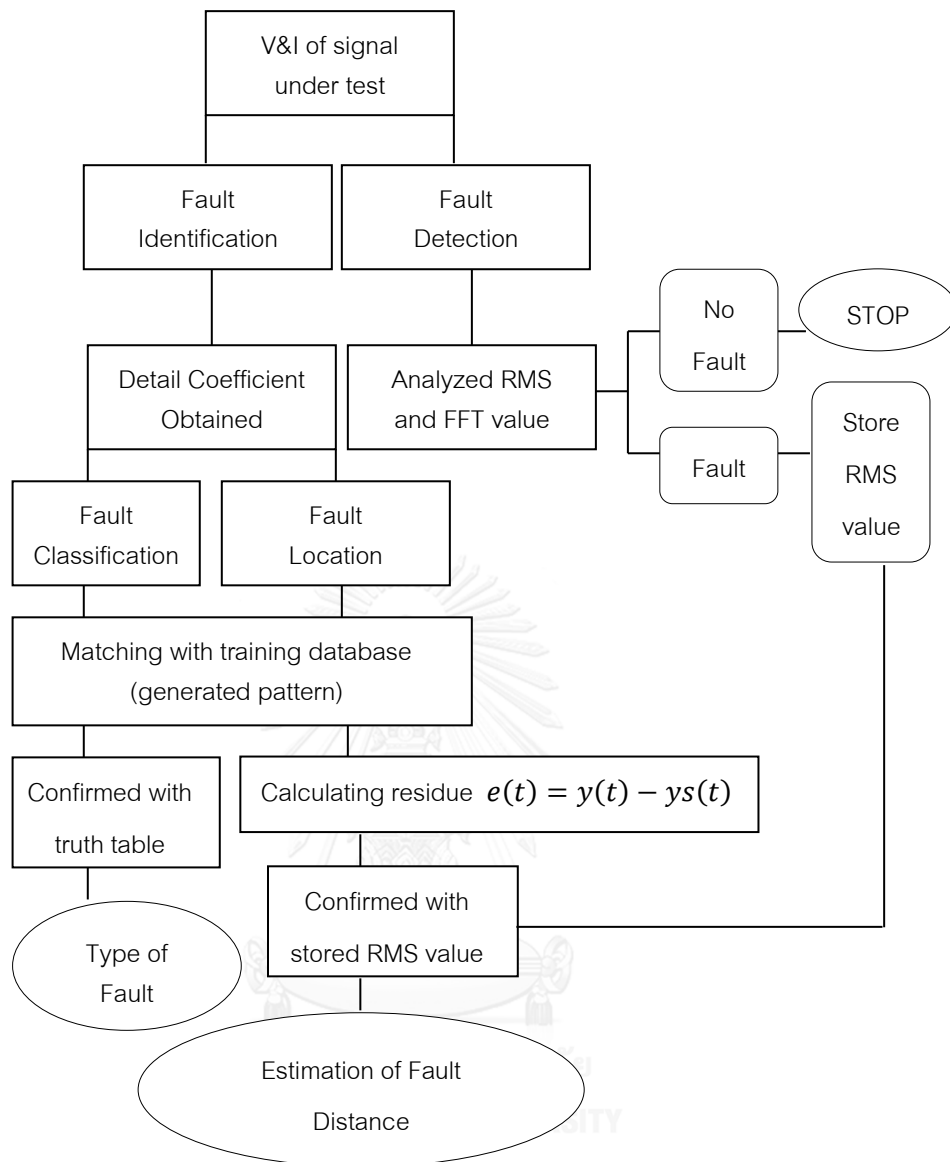


Figure 4. 17 Flow chart on tested signal

Details of equations in figure 4.16 and 4.17:

n = number of data points

v_j = the j^{th} cluster center

m = fuzziness index $m \in [1, \infty]$

c = number of cluster center

μ_{ij} = membership of i^{th} data to j^{th} cluster center

calculating residue $e(t) = y(t) - ys(t)$

where $y(t) = x(t + 1)$ and $ys(t) = xs(t + 1)$ (model output from fuzzy)

The proposed scheme needs to be tested using an amount of data. When sufficient data have been obtained, they will divide into training and testing set of data. Basically, the amount of data was 70% for training and 30% for testing purposes. Performance features in neural network via Matlab have been used to justify that the amount of data is sufficient for the requirement of the algorithm. Input for the fault identification scheme is the detail coefficients. Thus, the set of detail coefficient of training is different than testing set. The selection was done by using back-propagation neural network that implemented in the Matlab codes.

4.11 Parameters Setting for Training Patterns

Since the practical amount of fault data is inadequate, it is required to generate training/ testing data using simulation. Alternate Transients Program (ATP) / Electromagnetic Transient Program (EMTP) is implemented to simulate the typical transmission system overhead cable model to obtain currents and voltage data at various fault locations with different types of faults. The simulation data is used to test the fault detection algorithm and fault identification.

The power system model in figure 4.16 is a double circuit transmission line developed by imitating the actual circumstance of real transmission line. The ATP-EMTP software packaging has been used to simulate faults on 115kV, 50MVA, p.f 0.95 transmission network. The robustness and reliability of double circuit/ parallel line are important since the faults are commonly happening at this type of system voltage. The distributed parameters have been used in the model that able to accurately describe a very long transmission line. The voltage and current samples at one-end are measured by using the three phase V-I measurement block. The transmission line (line 1 and line 2 together) is 100 km long. The three-phase fault simulator is used to simulate various types of faults at varying locations along the transmission line. A few numbers of fault resistances are considered during the measurement. The fault data is in terms of voltages and currents. Figure 4.17 shows the one-line diagram of the test system.

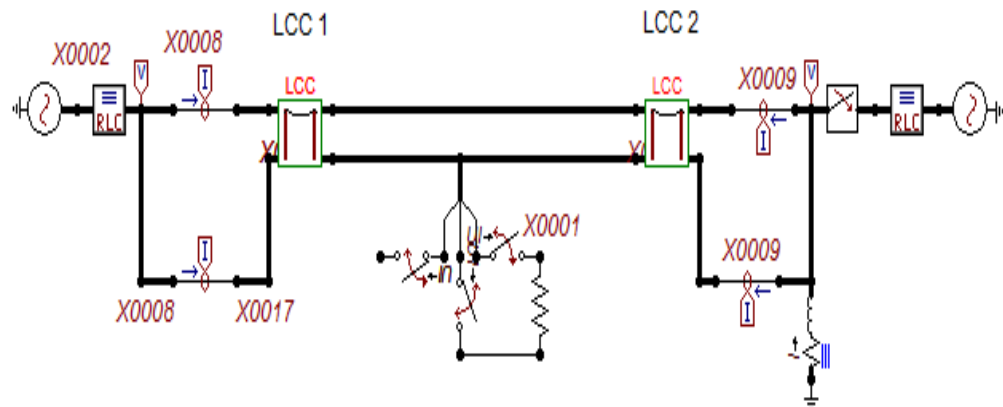


Figure 4. 18 Snapshot of the system in EMTF

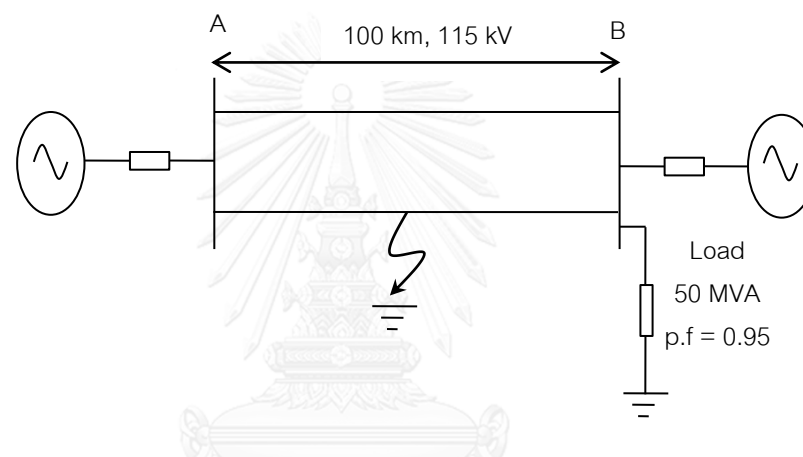


Figure 4. 19 One-line diagram of the studied system

4.11.1 Simulation Data

The simulated data obtained from EMTF/ ATP are then transferred to Matlab 2012a ® for further analysis. Overall obtained simulation data is 2600 including single line to ground fault (AG, BG, CG), double line fault (AB, BC, AC), double line to ground fault (ABG, BCG, ACG) and three phase fault (ABC). For healthy or no fault data, it is taken at every km along 100 km with no considering of fault resistance value. Table 4.1 shows the planning of data attained while doing the simulation.

Table 4. 2 Planning of simulation data

| No. | Type | No. of cases | Fault Location | Fault resistance |
|-----|----------|--------------|---------------------------------|---|
| 1 | No fault | 100 | Every 2km along the line length | 0.5 Ω , 5 Ω , 25 Ω , 100 Ω , 200 Ω |
| 2 | A G | 250 | | |
| 3 | B G | 250 | | |
| 4 | C G | 250 | | |
| 5 | A B G | 250 | | |
| 6 | C A G | 250 | | |
| 7 | B C G | 250 | | |
| 8 | A B C | 250 | | |
| 9 | A B | 250 | | |
| 10 | C A | 250 | | |
| 11 | B C | 250 | | |

Table 4. 3 Example of the collected simulation data process

| Type | Distance (km) | Fault resistance (Ω) |
|---------------------------------------|---------------|-------------------------------|
| Single line to ground (AG, BG, CG) | 2 | 0.5 |
| | | 5 |
| | | 25 |
| | | 100 |
| | | 200 |

Table 4.1 shows the planning simulation data for training purposes. Large training set contributes for a better model/ hypothesis, whereas a large testing set helps for better estimation of unseen/ general cases. The simulation data which have different features according to types and distance are preserved as the prime reference and database in implementing the algorithms. Table 4.2 shows the example of collected simulation data process pertinent to single line to ground. The total number of simulation data samples is illustrated in table 4.3.

Table 4. 4 Number of simulation data samples for training and testing phase

| Fault data | Data samples in term of detail coefficient | |
|-----------------------|--|---------|
| | Training | Testing |
| Single line to ground | 1645 | 705 |
| Double line | 1645 | 705 |
| Double line to ground | 1645 | 705 |
| Three phase | 1645 | 705 |
| Total | 6580 | 2820 |

4.12 Sampling Frequency and Data Reduction

When the simulation data have been obtained, wavelet transform is implemented for the purpose of data reduction. Other than that, the main interest is to extract the features to obtain the detail coefficient. The brief description has been explained in section 4.3. For the simulated data set, the signal of voltage (Va) contains total of 150000 data points. At the initial decomposition level, the signal conveys over the high pass and low pass filters, the signals have to be sub-sampling of 2.

The output of the high pass filter has 75000 data points. For further decomposition, this signal passed through the same low pass and high pass filters. The output of second low pass filter followed by sub sampling has 37500 data points. The output of second high pass filter followed by sub sampling has 37500 data points. At every step, the result of high pass filter (Cd) contains the high frequency components of the signal whereas low pass filter contains a coarse approximation. The process is continued and stopped at level 6 since the signal started to lose its shape which the basic frequency component (health data) started to get filtered. Finally, we will obtain Cd which is the coefficient that contains information about the fault occurrence. In the fault analysis, Cd vector is considered as input that will reduce the computation and efficient data reduction.

The signal data has been reduced from 15000 to 2350. Consequently, with this method, the sampling frequency will reduce with the reduction of signal data. Three phase voltages and three phase current input signals were sampled at a sampling frequency of 15 kHz. One full cycle DWT, Daubechies type, at level 6 is used to calculate the detail coefficients of voltages and currents. The input signals were first needs to be normalized. Level 6 is chosen based on the condition during the simulation process. However, the decision of level may vary between level 4 to 6 according to the coming inputs.

After decomposition process, the sampling frequency reduced from 1MHz to about 16kHz. The sampling frequency at DFR being used at EGAT and other power utilities is between 3kHz to 25 kHz (vary according to the type of DFR). Figure 4.18 describes the mentioned process.

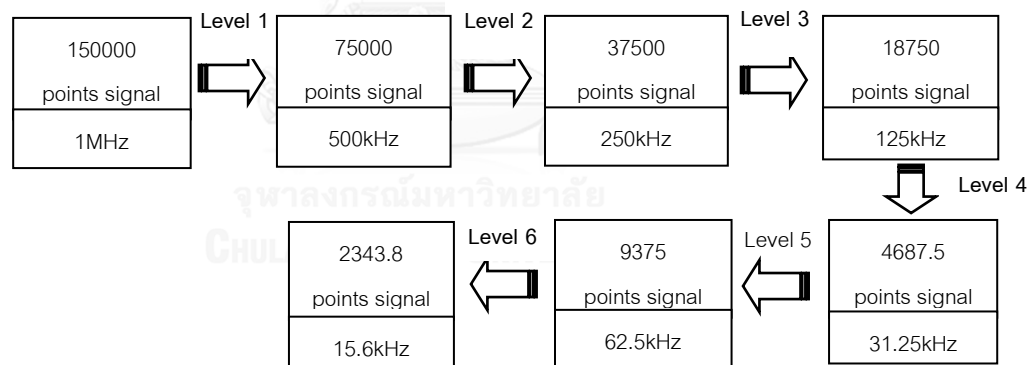


Figure 4. 20 Illustration of reduction process for data and sampling frequency

CHAPTER 5

RESULTS AND DISCUSSION

5.1 Performance of Fault Detection

The phase on fault detection used to justify either the signal/ input is 'fault' or 'no fault' by using the information of RMS and FFT. Table 5.1 shows the description of the proposed 'OR' rules that determines by RMS (RULE 1) and FFT (RULE 2).

Table 5. 1 Truth Table of proposed rule

| RMS | FFT | Decision |
|-----|-----|----------|
| 0 | 0 | 0 |
| 0 | 1 | 1 |
| 1 | 0 | 1 |
| 1 | 1 | 1 |

In figure 5.1 and 5.2 respectively, for no fault waveforms, the RMS values are almost constant. For the fault waveforms, RMS value varies as the amplitude of the waveform varies. Reduced RMS amplitude can help to identify fault. For no fault waveforms, it has a strong peak at 50 Hz for all 3 phases with almost same amplitude. Whereas, for fault condition, the magnitude of peak at 50 Hz of FFT for the voltage in fault will decrease significantly compared with FFT peak at 50 Hz of voltage not in fault. The conditions are shown in figure 5.3 and 5.4. RMS value of current and voltage are represented by dashed lines. The RMS values vary during fault conditions. Table 5.2 shows the confusion matrix used for justification of fault or no fault using proposed rules.

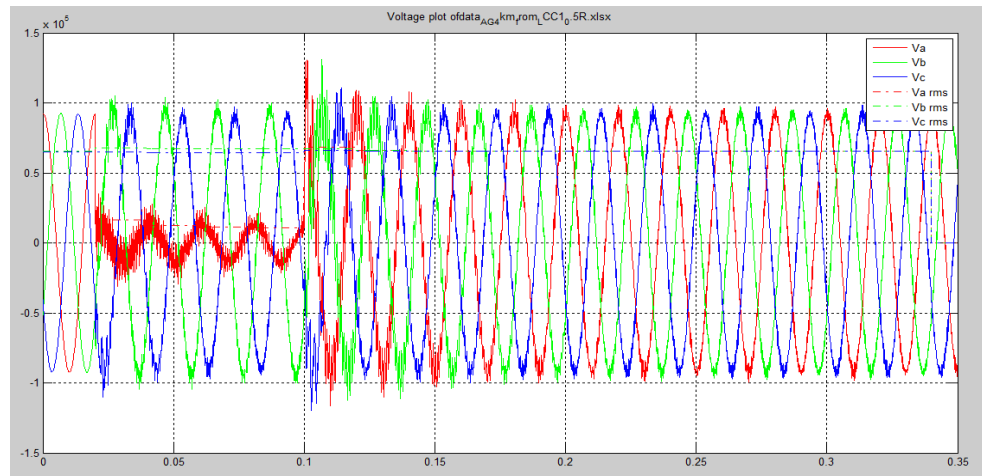


Figure 5. 1 Voltage plotting with RMS

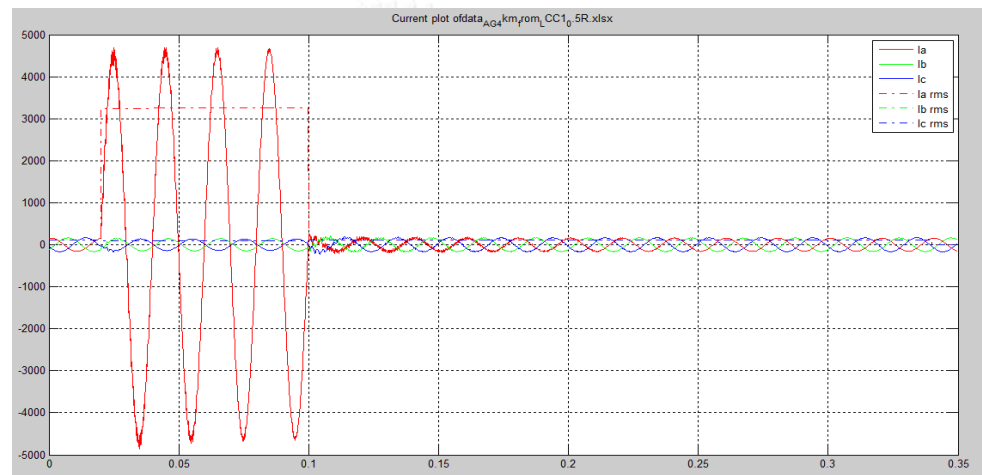


Figure 5. 2 Current plotting with RMS

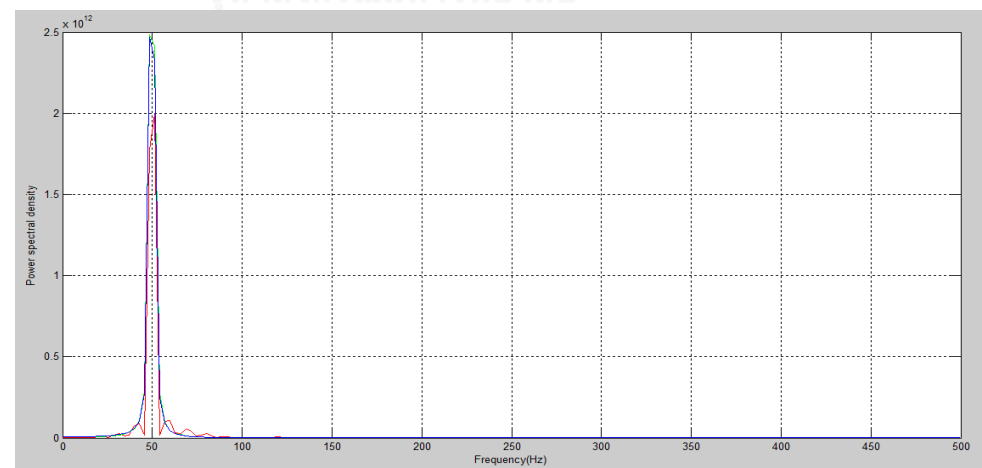


Figure 5. 3 Plotting of FFT fault voltage

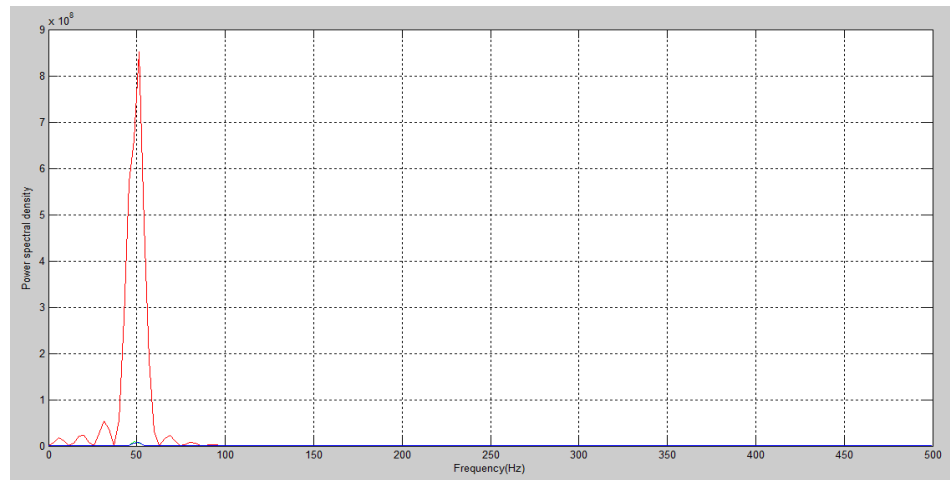


Figure 5. 4 Plotting of FFT fault current

Table 5. 2 Confusion using for justification of fault or no fault using proposed rules

| Type of fault | Samples | Confusion matrix | | | | | | | | | | | Accuracy(%) |
|---------------|---------|------------------|----|----|-----|-----|-----|----|----|----|-----|----------|-------------|
| | | AG | BG | CG | ABG | ACG | BCG | AB | AC | BC | ABC | No fault | |
| A-G | 20 | 20 | 0 | 0 | 0 | 0 | 0 | 0 | 0 | 0 | 0 | 0 | 100 |
| B-G | 20 | 0 | 20 | 0 | 0 | 0 | 0 | 0 | 0 | 0 | 0 | 0 | 100 |
| C-G | 20 | 0 | 0 | 20 | 0 | 0 | 0 | 0 | 0 | 0 | 0 | 0 | 100 |
| AB-G | 20 | 0 | 0 | 0 | 20 | 0 | 0 | 0 | 0 | 0 | 0 | 0 | 100 |
| AC-G | 20 | 0 | 0 | 0 | 0 | 20 | 0 | 0 | 0 | 0 | 0 | 0 | 100 |
| BC-G | 20 | 0 | 0 | 0 | 0 | 0 | 20 | 0 | 0 | 0 | 0 | 0 | 100 |
| AB | 20 | 0 | 0 | 0 | 0 | 0 | 0 | 20 | 0 | 0 | 0 | 0 | 100 |
| AC | 20 | 0 | 0 | 0 | 0 | 0 | 0 | 0 | 20 | 0 | 0 | 0 | 100 |
| BC | 20 | 0 | 0 | 0 | 0 | 0 | 0 | 0 | 0 | 20 | 0 | 0 | 100 |
| ABC | 20 | 0 | 0 | 0 | 0 | 0 | 0 | 0 | 0 | 0 | 20 | 0 | 100 |
| No fault | 20 | 0 | 0 | 0 | 0 | 0 | 0 | 0 | 0 | 0 | 0 | 20 | 100 |

5.2 Performance of Fault Classification

Phase of fault classification will justify the type of fault either single line to ground, double line, double line to ground or three phase. The proposed scheme is based on ANFIS modeling with implemented of GK algorithm. Classification of

full simulation data which contain 2600 cases, including 100 no fault data has obtained approximately 95%. From 2600 cases, a total of 25850 data samples has been collected in terms of feature extraction which extracted from wavelet transform. 70% of data samples are used for training set and 15% is set of validation and testing purposes. Further analysis is deliberated by separate types of fault for better performance. The training procedure will concern on the type of fault in a form of cluster.

i. **Single line to ground fault.**

3 sets of fault data considered as the input; phase A to ground, phase B to ground and phase C to ground contributed to 750 cases. Each set has 2350 data samples which total of 7050 data samples is getting through the algorithm in scattered form. As a result, the algorithm has successfully classified the data with the percentage of 32% - 34%. Figure 5.5 shows the snapshot of fault classification result from the proposed algorithm. The calculation below illustrated the understanding of this percentage;

$$\frac{2350}{7050} \times 100\% = 33.333\%$$

```
>> fault_classification1
Model Target
Fault is AGW
Percentage of above mentioned fault successfully classified: 32.5 %

Model Target
Fault is BGW
Percentage of above mentioned fault successfully classified: 34.3 %

Model Target
Fault is CGW
Percentage of above mentioned fault successfully classified: 34.0 %

Total percentage of classified:100.0 %
```

Figure 5. 5 Results of classification phase

Results confirmed that the algorithm was capable to classify the sets of fault data accordingly with high accuracy of the percentage. To verify the results, 'Neural Network Start' from Neural Network Toolbox has been used. 'Pattern Recognition and Classification (nprtool)' is used for overall performance. In nprtool, input or samples were divided into 3 sets; training, validation and testing. The percentages of samples were chosen by default which is 70% for training, 15% for validation and 15% for testing. The selection of layers' architectures in was also done by default. The first analysis is using confusion matrix. It is a specific layout of table that shows a visualization of the performance of a typically a supervised learning. Each column of the matrix represents the instances in a predicted class. Each row represents the instances in the actual class. The green square indicates the highest number of correct responses. The red square indicates the low number of incorrect responses. The sum of accuracies was indicated by the lower right blue squares. Figure 5.6 shows the confusion matrix which class 1 stands for AG, class 2 for BG and class 3 for CG.

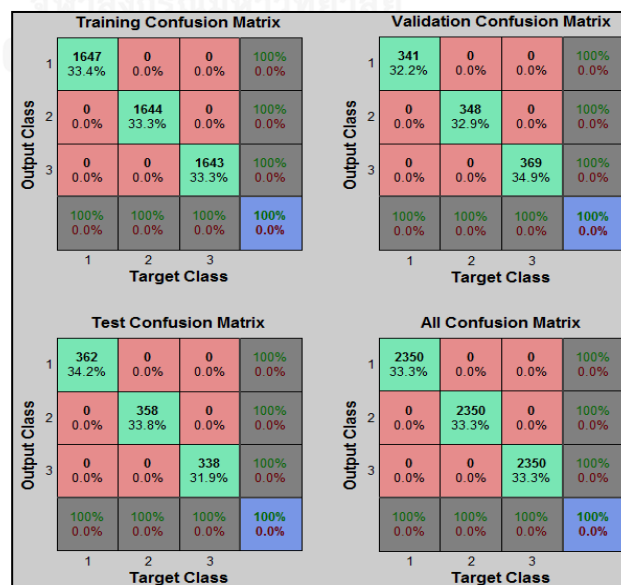


Figure 5. 6 Confusion matrix of 3 classes

A second analysis is pertinent to the *receiver operating characteristic* (ROC) that used to check the quality of classifiers. The ROC curve is the sensitivity as a function of fall-out. Each point in the ROC space was the result of the prediction of the confusion matrix. The upper left corner of the ROC space indicated the best prediction. No false negative is represented by 100% sensitivity and no false positives is represented by 100% specificity. Figure 5.7 shows the obtained result.

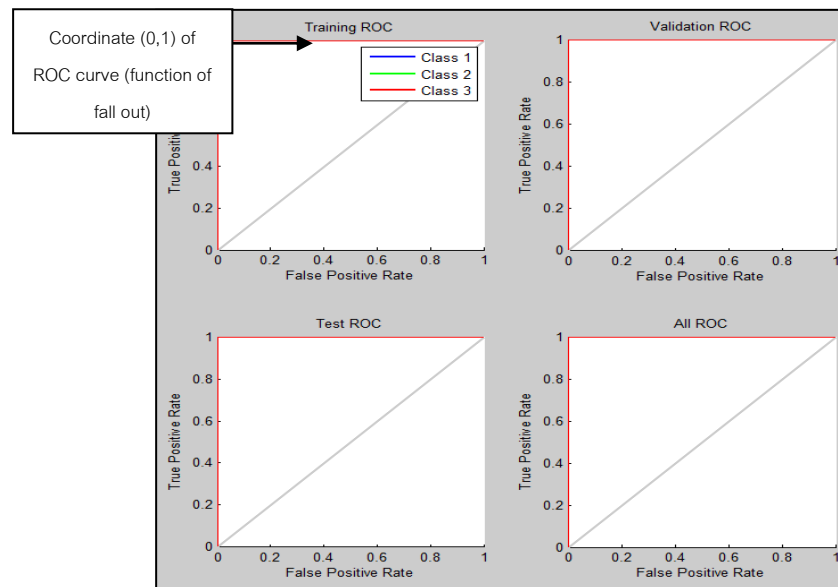


Figure 5. 7 ROC of single line to ground fault

i. Double line fault.

Figure 5.8 shows the snapshot of fault classification result from the proposed algorithm. Confusion matrix and ROC were presented for analysis of performance in figure 5.9 and 5.10 respectively.

```

>> fault_classification1
Model Target

Fault is ABW
Percentage of above mentioned fault successfully classified: 32.8 %

Model Target

Fault is BCW
Percentage of above mentioned fault successfully classified: 34.2 %

Model Target

Fault is CAW
Percentage of above mentioned fault successfully classified: 33.0 %

Total percentage of classified:100.0 %

```

Figure 5. 8 Snapshot of fault classification

| | | Training Confusion Matrix | | | | Validation Confusion Matrix | | | |
|--------------|---------------|---------------------------|---------------|--------------|--------------|-----------------------------|--------------|--------------|--------------|
| Output Class | | Target Class | | | 100% 0.0% | Target Class | | | 100% 0.0% |
| | | 1 | 2 | 3 | | 1 | 2 | 3 | |
| 1 | 1654 33.5% | 0 0.0% | 0 0.0% | 100% 0.0% | 361 34.1% | 0 0.0% | 0 0.0% | 100% 0.0% | |
| 2 | 0 0.0% | 1610 32.6% | 0 0.0% | 100% 0.0% | 0 0.0% | 356 33.6% | 0 0.0% | 100% 0.0% | |
| 3 | 0 0.0% | 0 0.0% | 1670 33.8% | 100% 0.0% | 0 0.0% | 0 0.0% | 341 32.2% | 100% 0.0% | |
| | 100% 0.0% | 100% 0.0% | 100% 0.0% | 100% 0.0% | 100% 0.0% | 100% 0.0% | 100% 0.0% | 100% 0.0% | |

| | | Test Confusion Matrix | | | | All Confusion Matrix | | | |
|--------------|--------------|-----------------------|--------------|--------------|---------------|----------------------|---------------|--------------|--------------|
| Output Class | | Target Class | | | 100% 0.0% | Target Class | | | 100% 0.0% |
| | | 1 | 2 | 3 | | 1 | 2 | 3 | |
| 1 | 335 31.7% | 0 0.0% | 0 0.0% | 100% 0.0% | 2350 33.3% | 0 0.0% | 0 0.0% | 100% 0.0% | |
| 2 | 0 0.0% | 384 36.3% | 0 0.0% | 100% 0.0% | 0 0.0% | 2350 33.3% | 0 0.0% | 100% 0.0% | |
| 3 | 0 0.0% | 0 0.0% | 339 32.0% | 100% 0.0% | 0 0.0% | 0 0.0% | 2350 33.3% | 100% 0.0% | |
| | 100% 0.0% | 100% 0.0% | 100% 0.0% | 100% 0.0% | 100% 0.0% | 100% 0.0% | 100% 0.0% | 100% 0.0% | |

Figure 5. 9 Results of confusion matrix

ii. Double line to ground fault.

Figure 5.11 shows the snapshot of fault classification result. Confusion matrix and ROC were presented for analysis of performance in figure 5.12 and 5.13 respectively.

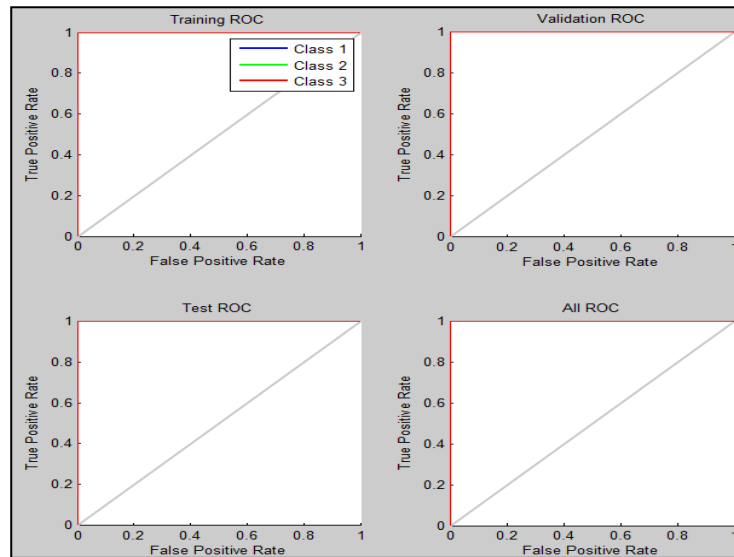


Figure 5. 10 ROC of double line fault

```
>> fault_classification1
Model Target

Fault is ABGW
Percentage of above mentioned fault successfully classified: 31.0 %

Model Target

Fault is BCGW
Percentage of above mentioned fault successfully classified: 30.6 %

Model Target

Fault is CAGW
Percentage of above mentioned fault successfully classified: 39.0 %

Total percentage of classified:100.0 %
```

Figure 5. 11 Results of classification phase

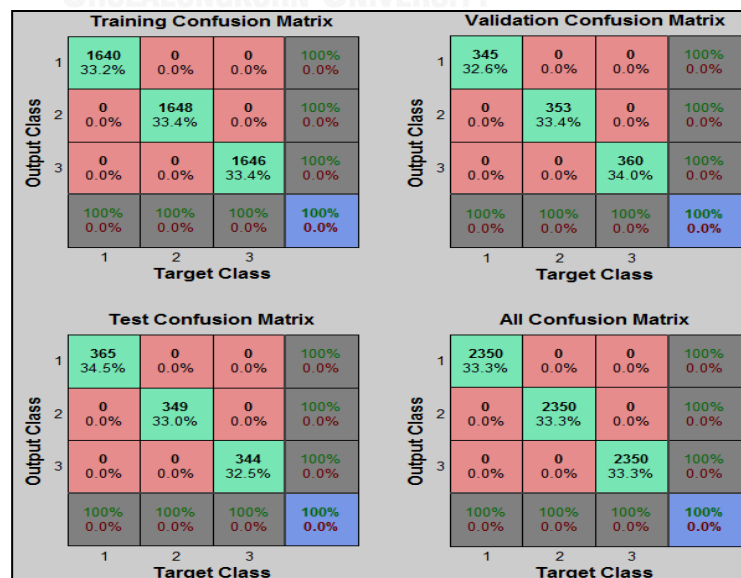


Figure 5. 12 Results of confusion matrix

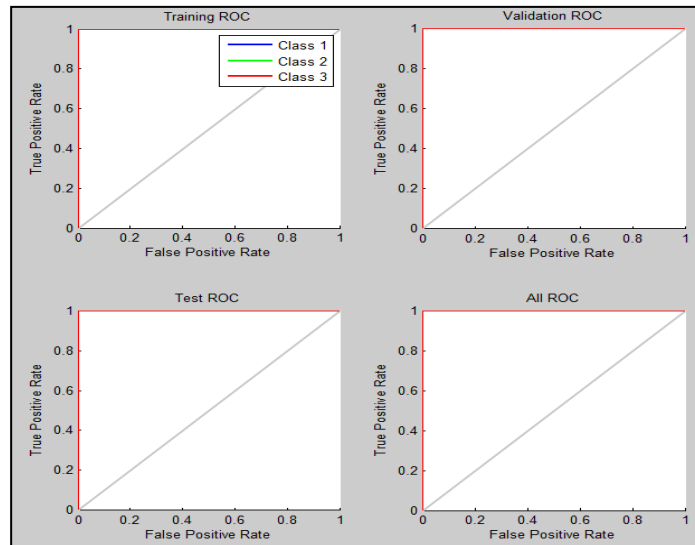


Figure 5.13 ROC of double line to ground fault

5.3 Performance of Fault Location

The training process supposed to be trained repeatedly to attain the best plotting. During the process of training, data is separated into few cases, according to distance and value of fault resistance. For results of prediction using T-S Fuzzy modeling, sample data is divided into training and testing set with percentage of 70% and 30% respectively.

i. Single line to ground fault

This is one of the results pertinent to phase A to ground for 0.5Ω fault resistance. The projected mfs is created from membership of regression. It can be seen in figure 5.14 that the gaussian curve of membership functions (mfs) performed smooth and equally to indicate that the performance is good. Figure 5.15 shows the results of training and testing data set for actual and predicted distance value. The plotting data of actual and predicted value are almost 100% overlap to show that the results are almost accurate. The results are found in the workspace after run the respective codes.

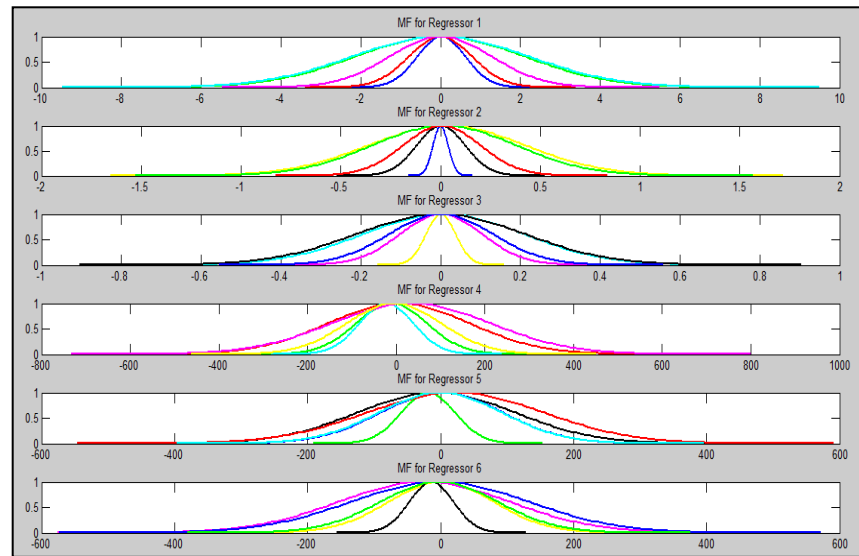


Figure 5. 14 Plotting of membership function for phase A to ground $R_f=0.5\text{ohm}$

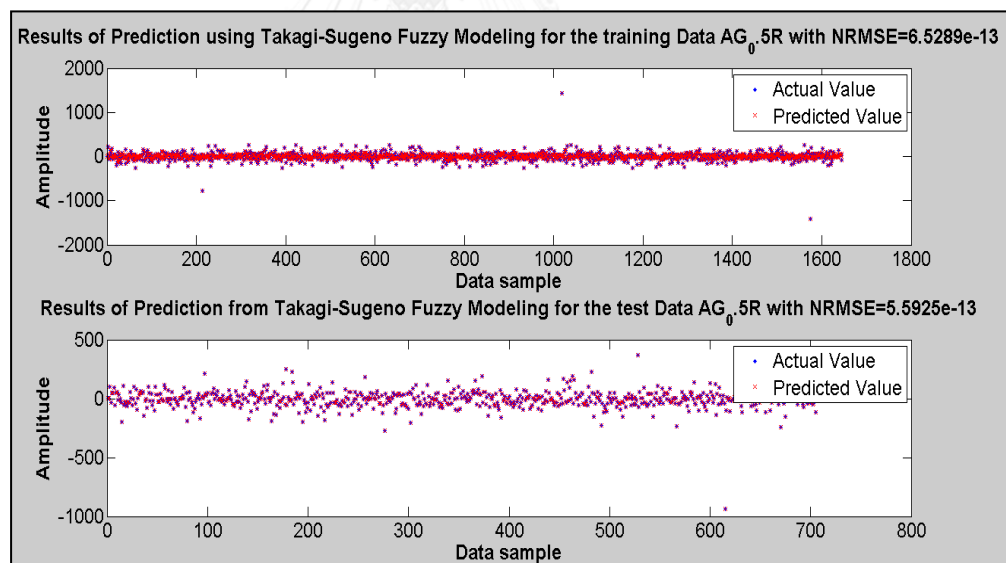


Figure 5. 15 Illustration of actual and predicted value

Table 5.3 shows part of the results on the fault distance estimation recorded for phase A, B and C to ground with R_f of 0.5Ω , 5Ω , 25Ω , 100Ω and 200Ω respectively.

Table 5. 3 Results of Estimation Error for Single Line to Ground Fault

| Fault Distance Estimation For Single Line to Ground | | | | | |
|---|---------------------------------------|-----------|------------|-------------|-------------|
| Actual distance (km) | Estimation Error (Actual – Predicted) | | | | |
| | $R_F = 0.5$ | $R_F = 5$ | $R_F = 25$ | $R_F = 100$ | $R_F = 200$ |
| 2.0 | 0.220 | 0.200 | -0.296 | -0.500 | -0.532 |
| 10.0 | 0.242 | 0.296 | -0.267 | -0.309 | -0.260 |
| 20.0 | 0.299 | 0.264 | -0.384 | 0.203 | -0.222 |
| 30.0 | 0.379 | 0.561 | 0.984 | -0.253 | -0.340 |
| 40.0 | -0.274 | -0.255 | 0.551 | 0.204 | 0.256 |
| 50.0 | 0.222 | 0.294 | -0.462 | 0.580 | -0.235 |
| 60.0 | 0.232 | 0.298 | -0.235 | 0.270 | -0.327 |
| 70.0 | -0.511 | -0.266 | 0.224 | 0.211 | -0.222 |
| 80.0 | -0.246 | -0.273 | -0.221 | 0.290 | 0.321 |
| 90.0 | 0.545 | 0.233 | 0.397 | 0.281 | 0.228 |
| 100.0 | -0.221 | 0.544 | 0.220 | 0.224 | 0.431 |

ii. Double line fault

This is one of the results pertinent to phase AB for 0.5 Ω fault resistance.

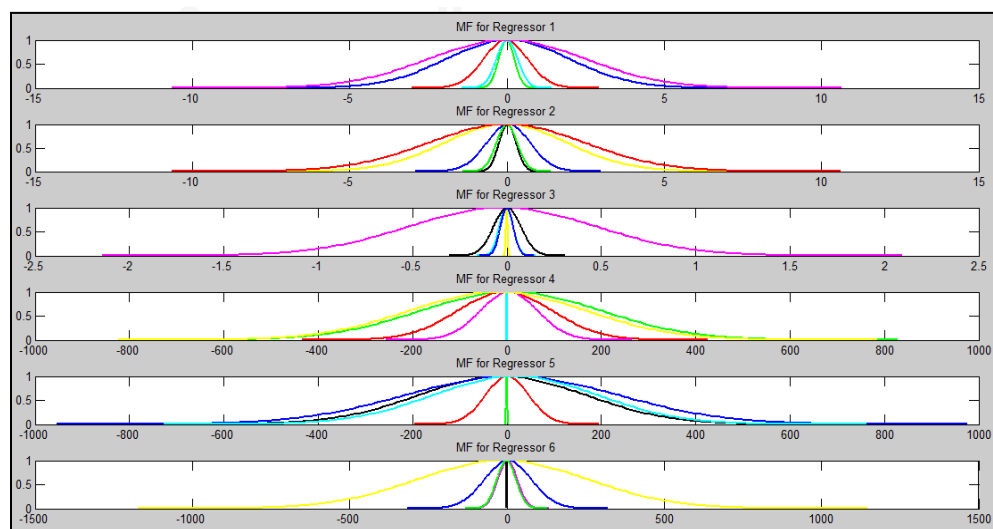


Figure 5. 16 Plotting of membership function for phase B, $R_f = 0.5$ ohm

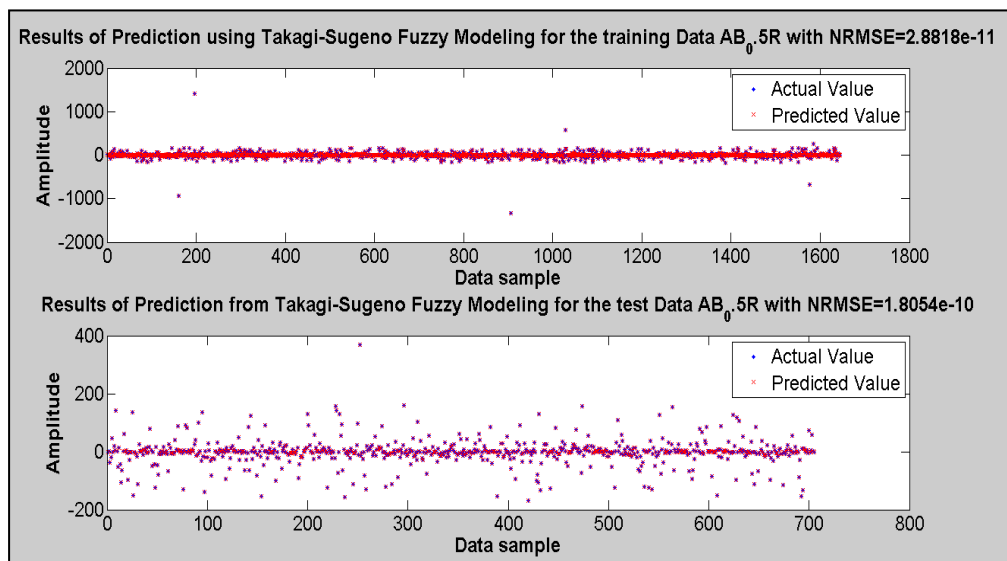


Figure 5. 17 Illustration of actual and predicted value

Table 5. 4 Results of estimation Error for Double Line Fault

| Fault Distance Estimation For Double Line | | | | | |
|---|---------------------------------------|-----------|------------|-------------|-------------|
| Actual distance (km) | Estimation Error (Actual – Predicted) | | | | |
| | $R_f = 0.5$ | $R_f = 5$ | $R_f = 25$ | $R_f = 100$ | $R_f = 200$ |
| 2.0 | 0.279 | 0.424 | -0.396 | -0.235 | -0.261 |
| 10.0 | 0.420 | -0.267 | 0.632 | 0.895 | -0.536 |
| 20.0 | 0.222 | 0.557 | -0.254 | 0.220 | 0.260 |
| 30.0 | -0.297 | -0.256 | 0.245 | -0.208 | -0.670 |
| 40.0 | 0.597 | -0.289 | 0.261 | -0.348 | 0.446 |
| 50.0 | -0.224 | 0.235 | -0.233 | -0.624 | -0.253 |
| 60.0 | 0.282 | -0.265 | -0.294 | -0.406 | 0.296 |
| 70.0 | -0.231 | -0.205 | -0.209 | 0.228 | 0.430 |
| 80.0 | -0.216 | -0.247 | -0.257 | 0.207 | 0.247 |
| 90.0 | -0.216 | -0.247 | -0.557 | 0.256 | 0.238 |
| 100.0 | -0.398 | -0.225 | 0.236 | 0.412 | 0.362 |

Table 5.4 shows part of the results on fault distance estimation recorded for phase AB, BC and CA with R_f of 0.5Ω , 5Ω , 25Ω , 100Ω and 200Ω respectively.

ii. Double line to ground fault

This is one of the results pertinent to phase ABG for 0.5Ω fault resistance.

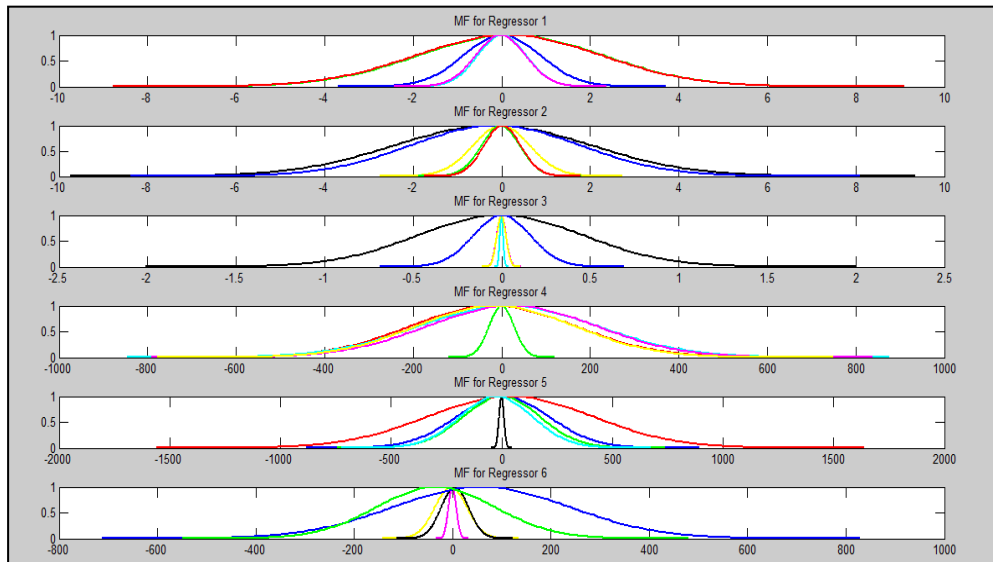


Figure 5.18 Plotting of membership function for phase ABG, $R_f = 0.5\text{ohm}$

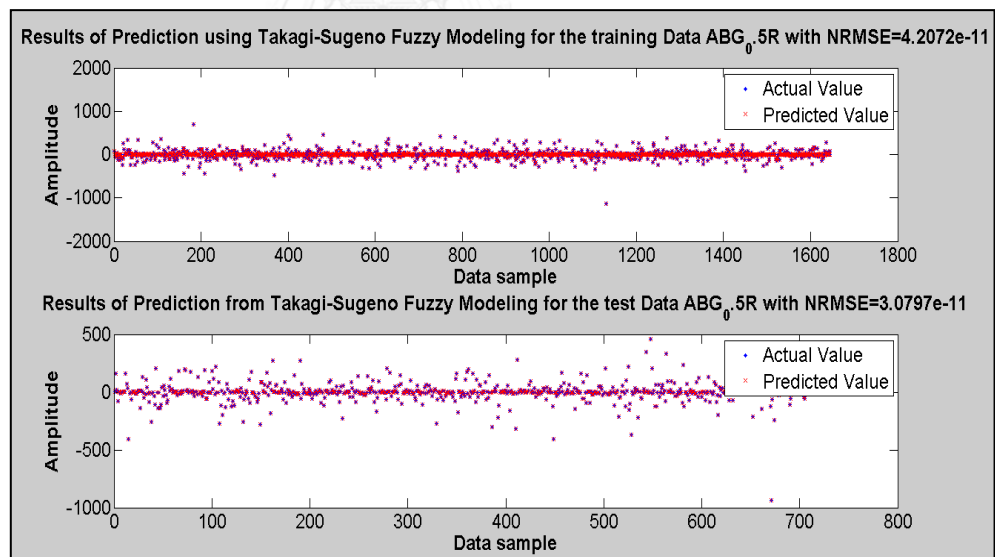


Figure 5.19 Illustration of Actual and Predicted Value

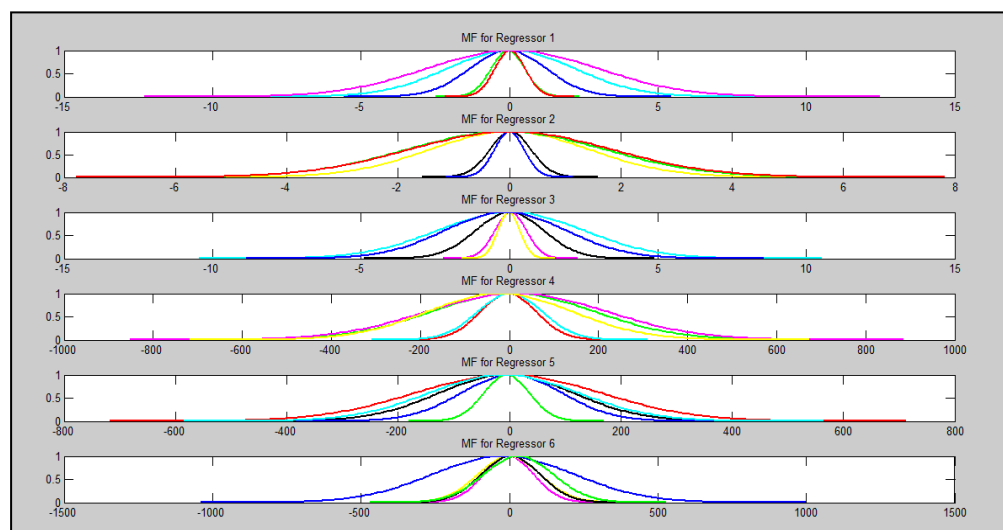
Table 5.5 shows part of the results on fault distance estimation recorded for phase ABG, BCG and CAG with R_f of 0.5Ω , 5Ω , 25Ω , 100Ω and 200Ω respectively.

Table 5. 5 Results of Estimation Error for Double Line to Ground Fault

| Fault Distance Estimation For Double Line to Ground | | | | | |
|---|---------------------------------------|-----------|------------|-------------|-------------|
| Actual distance (km) | Estimation Error (Actual – Predicted) | | | | |
| | $R_F = 0.5$ | $R_F = 5$ | $R_F = 25$ | $R_F = 100$ | $R_F = 200$ |
| 2.0 | 0.265 | 0.221 | 0.596 | -0.437 | 0.385 |
| 10.0 | 0.794 | 0.232 | 0.561 | 0.940 | -0.244 |
| 20.0 | 0.469 | 0.242 | 0.688 | -0.539 | 0.258 |
| 30.0 | 0.227 | 0.220 | 0.358 | 0.204 | 0.202 |
| 40.0 | -0.209 | -0.310 | -0.221 | 0.253 | 0.215 |
| 50.0 | 0.901 | -0.277 | 0.264 | 0.225 | -0.871 |
| 60.0 | 0.475 | -0.201 | 0.850 | -0.275 | 0.536 |
| 70.0 | -0.584 | 0.200 | 0.287 | -0.277 | -0.275 |
| 80.0 | -0.611 | 0.200 | 0.205 | -0.270 | 0.392 |
| 90.0 | 0.269 | 0.401 | 0.256 | 0.256 | 0.239 |
| 100.0 | 0.774 | 0.232 | 0.948 | -0.240 | 0.362 |

iii. Three phase fault

This is one of the results pertinent to three phase fault for 0.5Ω fault resistance.

Figure 5. 20 Plotting of Membership function for phase ABG, $R_f = 0.5$ ohm

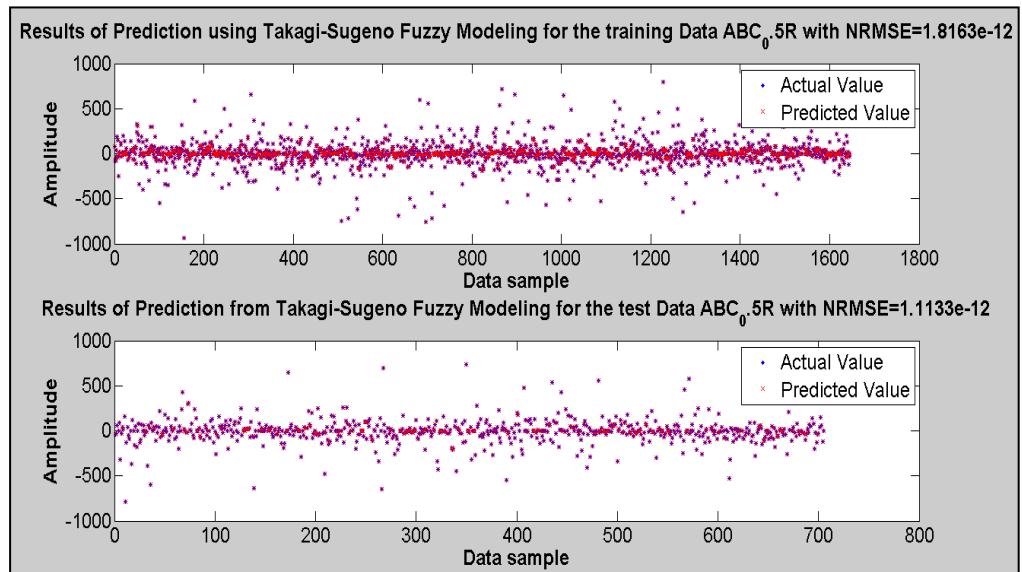


Figure 5. 21 Illustration of Actual and Predicted Value

Table 5.6 shows part of the results on fault distance estimation recorded for phase ABC with R_F of 0.5Ω , 5Ω , 25Ω , 100Ω and 200Ω respectively.

Table 5. 6 Results of Estimation Error for Three Phase Fault

| Fault Distance Estimation For Three Phase | | | | | |
|---|---------------------------------------|-----------|------------|-------------|-------------|
| Actual distance (Km) | Estimation Error (Actual – Predicted) | | | | |
| | $R_F = 0.5$ | $R_F = 5$ | $R_F = 25$ | $R_F = 100$ | $R_F = 200$ |
| 2.0 | 0.629 | 0.328 | -0.400 | -0.369 | 0.202 |
| 10.0 | -0.283 | 0.203 | -0.242 | -0.203 | -0.291 |
| 20.0 | -0.795 | 0.319 | -0.503 | -0.233 | 0.366 |
| 30.0 | 0.272 | -0.228 | -0.773 | -0.831 | 0.304 |
| 40.0 | 0.374 | 0.453 | -0.235 | -0.246 | -0.259 |
| 50.0 | 0.869 | 0.284 | 0.388 | -0.232 | -0.382 |
| 60.0 | 0.544 | 0.345 | 0.810 | -0.208 | 0.479 |
| 70.0 | 0.204 | 0.276 | -0.245 | 0.207 | 0.238 |
| 80.0 | 0.570 | 0.260 | -0.239 | 0.424 | -0.720 |
| 90.0 | 0.871 | 0.421 | 0.252 | -0.553 | 0.924 |
| 100.0 | -0.228 | 0.201 | -0.244 | 0.694 | 0.396 |

Table 5. 7 Overall performance of the ANFIS-GK based at 5Ω fault resistance

| Fault Type | Actual (km) | ANFIS-GK (km) | Error (km) | Error (%) |
|-----------------------------|-------------|---------------|-------------|-----------|
| Single Line to Ground (SLG) | 20 | 20.264 | 0.264 | 0.264 |
| | 40 | 39.745 | 0.255 | -0.255 |
| | 60 | 60.298 | 0.298 | 0.298 |
| | 80 | 79.727 | 0.273 | -0.273 |
| | 100 | 100.544 | 0.544 | 0.544 |
| Double Line to Ground (DLG) | 20 | 20.242 | 0.242 | 0.242 |
| | 40 | 39.690 | 0.310 | -0.310 |
| | 60 | 59.799 | 0.201 | -0.201 |
| | 80 | 80.200 | 0.200 | 0.200 |
| | 100 | 100.232 | 0.232 | 0.232 |
| Line to Line (LL) | 20 | 20.557 | 0.557 | 0.557 |
| | 40 | 39.711 | 0.289 | -0.289 |
| | 60 | 59.735 | 0.265 | -0.265 |
| | 80 | 79.753 | 0.247 | -0.247 |
| | 100 | 99.775 | 0.225 | -0.225 |
| Three Phase (3ϕ) | 20 | 20.319 | 0.319 | 0.319 |
| | 40 | 40.453 | 0.453 | 0.453 |
| | 60 | 60.345 | 0.345 | 0.345 |
| | 80 | 80.260 | 0.260 | 0.260 |
| | 100 | 100.201 | 0.201 | 0.201 |

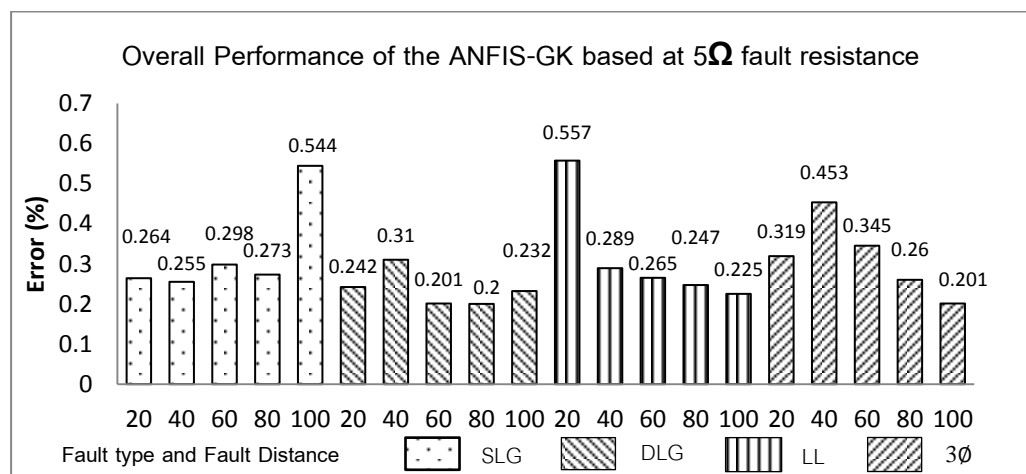
Figure 5. 22 Overall Performance of the ANFIS-GK based at 5Ω fault resistance

Table 5. 8 Overall Performance of the ANFIS-GK at 100 Ω fault resistance

| Fault Type | Actual (km) | ANFIS-GK (km) | Error (km) | Error (%) |
|-----------------------------|-------------|---------------|-------------|-----------|
| Single Line to Ground (SLG) | 20 | 20.203 | 0.203 | 0.203 |
| | 40 | 40.204 | 0.204 | 0.204 |
| | 60 | 60.270 | 0.270 | 0.270 |
| | 80 | 80.290 | 0.290 | 0.290 |
| | 100 | 100.224 | 0.224 | 0.224 |
| Double Line to Ground (DLG) | 20 | 19.461 | 0.539 | -0.539 |
| | 40 | 40.253 | 0.253 | 0.253 |
| | 60 | 59.725 | 0.275 | -0.275 |
| | 80 | 79.73 | 0.270 | -0.270 |
| | 100 | 99.76 | 0.240 | -0.240 |
| Line to Line (LL) | 20 | 20.220 | 0.220 | 0.220 |
| | 40 | 39.652 | 0.348 | -0.348 |
| | 60 | 59.594 | 0.406 | -0.406 |
| | 80 | 80.207 | 0.207 | 0.207 |
| | 100 | 100.412 | 0.412 | 0.412 |
| Three Phase (3 ϕ) | 20 | 19.767 | 0.233 | -0.233 |
| | 40 | 39.754 | 0.246 | -0.246 |
| | 60 | 59.792 | 0.208 | -0.208 |
| | 80 | 80.424 | 0.424 | 0.424 |
| | 100 | 100.694 | 0.694 | 0.694 |

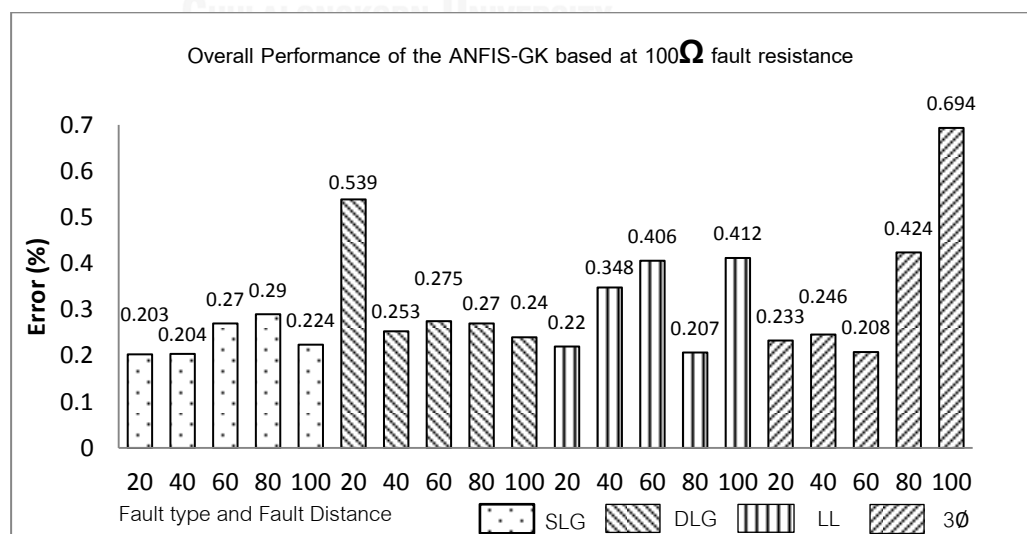
Figure 5. 23 Overall Performance of the GK based at 100 Ω fault resistance

Table 5.7 and 5.8 presented the analysis for overall training performance of the ANFIS-GK based at 5Ω and 100Ω fault resistance respectively. 5Ω was selected as generally small value and 100Ω for high value of fault resistance. The distance involved were 20km, 40km, 60km, 80km and 100km. The difference between actual and estimate were recorded as an error and percentage of error using the equation;

$$\% \text{ Error} = \frac{|\text{Actual fault location} - \text{Predicted fault location}|}{\text{total line length}} \times 100 \quad (5.1)$$

Data from the table then recorded in the form of bar chart; figure 5.23 and 5.24 respectively. Table 5.9 shows the observation pertinent to figure 5.23 and 5.24. It can be concluded that regardless the value of fault resistance, the proposed algorithm is able to perform the estimation of fault distance within a similar range of error. Thus, fault resistance has no effect to the ANFIS-GK scheme. After completing the training procedure, the proposed algorithm is ready to be verified using relevant case studies.

Table 5. 9 Comparison based on fault resistance

| Item | Error | | Average error |
|--|-------|-------|---------------|
| | Min | Max | |
| ANFIS-GK fault distance based at 5Ω | 0.20 | 0.557 | 0.299 |
| ANFIS-GK fault distance based at 100Ω | 0.203 | 0.694 | 0.308 |

5.4 Performance on High Impedance Fault (HIF)

High-impedance faults (HIF) are those with a high resistance in the fault pathway. The value of the fault resistance for a fault defined as a HIF depends on interpretation and circumstances. HIFs are ground faults that produce fault currents below the traditional ground overcurrent element pickup level. A very high nonlinear performance contributed to a difficult phenomenon. The most typical characteristics are nonlinearity, accumulation, shoulder, and asymmetry. In this research, the system voltage that being used in experimental studies is 115kV. A general study on HIFs is pertinent to fault resistance of 100Ω and 200Ω of the single line to ground fault and double line to ground fault respectively. Table

5.10 summarized the performance of fault location estimation using ANFIS-GK pertinent to fault resistance of 100Ω and 200Ω of the single line to ground fault and double line to ground fault. Based on the results, ANFIS-GK is possible for the detection of HIF.

Table 5. 10 Fault Location Error using 100Ω and 200Ω on SLG and DLG

| Actual distance (Km) | Error of fault distance (km) | | | |
|-------------------------|------------------------------|-------------|-----------------------|-------------|
| | Single line to ground | | Double line to ground | |
| | $R_F = 100$ | $R_F = 200$ | $R_F = 100$ | $R_F = 200$ |
| 2.0 | -0.500 | -0.532 | -0.437 | 0.385 |
| 10.0 | -0.309 | -0.260 | 0.940 | -0.244 |
| 20.0 | 0.203 | -0.222 | -0.539 | 0.258 |
| 30.0 | -0.253 | -0.340 | 0.204 | 0.202 |
| 40.0 | 0.204 | 0.256 | 0.253 | 0.215 |
| 50.0 | 0.580 | -0.235 | 0.225 | -0.871 |
| 60.0 | 0.270 | -0.327 | -0.275 | 0.536 |
| 70.0 | 0.211 | -0.222 | -0.277 | -0.275 |
| 80.0 | 0.290 | 0.321 | -0.270 | 0.392 |
| 90.0 | 0.281 | 0.228 | 0.256 | 0.239 |
| 100.0 | 0.224 | 0.431 | -0.240 | 0.362 |

5.5 Case Studies

The case studies in the following section were done to verify the capability of the proposed algorithm for respective purposes. For some results of case studies, the fault type that highly put into consideration is single line to ground as this type occurs most frequently (74%), followed by double line (13%), double line to ground (9%) and finally three-phase (4%).

5.5.1 Fault Classification and Fault Location of IEEE 14 Bus System

A well known IEEE 14-bus standard system was developed using MATLAB/SIMULINK software as shown in Figure 5.24. It comprises of five synchronous machines with IEEE type-1 exciters; 3 of which are synchronous condensers and 2 synchronous generators. There are 11 loads, 14 buses and 20

power lines in the system totaling 259MW and 81.3 Mvar. For an easy analysis of the system, it contains the prime features of a power grid. For example, given the IEEE 14 bus system, if line 1 couldn't operate, consequently all the power generated that connected to bus 1 has to be delivered to the network through line 2. Every line has a set of lines linked to it with certain degrees. The sets tend to be more important than another set of lines. The corresponding data for this bus can be referred in Appendix A.

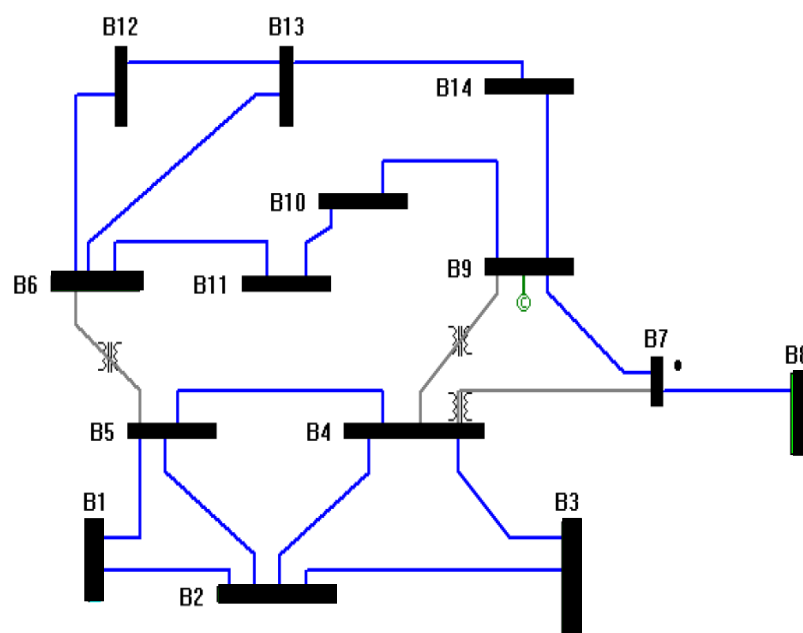


Figure 5. 24 the IEEE-14 bus electrical power network

The algorithm has been tested on the IEEE 14-bus system. The simulations in this case study will be conducted based on faults in the transmission line between a few connections. Fault resistance and fault distance were adjusted accordingly. After all parameters were confirmed, the model needs to be run and obtain the fault data produced by the adjusting of parameters. The procedures were continued for a few values of fault resistance and fault distance. Fault data are obtained from scope 2 of 'system_15_bus.mdl'. Part of the developed IEEE 14-bus main program is shown in figure 5.26. Results for fault classification and estimation of location were shown in Table 5.11 and Table 5.12 respectively.

Results of fault distance have been rounded off to one-decimal value. Results pertinent to transmission line between bus 6 and 13 are also being considered.

```

fault_distance_init = [0.8];
j = 1;
while j<(length(fault_distance_init)+1)
    fault_distance = fault_distance_init(j);
    fault_resistance = 5;
    Init %initial value of real time power system IEEE14 bus and line parameter. (look at init.m)
    sim('D:\kes study\system_15_bus_5.mdl')
    load bus_fault.mat %load data from *.mat and store in the name
    % rms_doing
    % S_inj = V_pre_bus_09_012(2,1)*conj(I_pre_line_09_14_012(2,1))+V_pre_bus_13_012(2,1)*conj(I_pre_line_13_14_012(2,1))
    %
    % %Prepare data
    % % V1 = abs(V_bus_13_012(2,1));
    % % del1 = angle(V_bus_13_012(2,1));
    % % V3 = abs(V_bus_09_012(2,1));
    % % del3 = angle(V_bus_09_012(2,1));
    % %
    % % p12 = real(V_pre_bus_13_012(2,1)*I_pre_line_13_14_012(2,1))
    % % q12 = imag(V_pre_bus_13_012(2,1)*I_pre_line_13_14_012(2,1))
    % % p32 = real(V_pre_bus_09_012(2,1)*I_pre_line_09_14_012(2,1))
    % % q32 = imag(V_pre_bus_09_012(2,1)*I_pre_line_09_14_012(2,1))
    %
    %
    % I_pre_32 = I_pre_line_09_14_012(2,1);
    % Z_line_32 = 0.12711+i*0.27038;
    % Y_line_32 = 1e-5;
    % V_pre_2 = (Z_line_32*Y_line_32+1)*V_pre_bus_09_012(2,1)+Z_line_32*I_pre_32;
    % I_pre_inj_2 = I_pre_line_09_14_012(2,1)+I_pre_line_13_14_012(2,1);

```

Figure 5. 25 Part of snapshot IEEE 14 bus system

Table 5. 11 Fault Classification

| Actual Fault type | Angle (δ°) | Fault resistance (Ω) | ANFIS-GK Fault Type |
|-------------------|--------------------------|-------------------------------|---------------------|
| A-G | 45 | 5 | A-G |
| A-G | 45 | 100 | A-G |
| B-G | 45 | 5 | B-G |
| B-G | 45 | 100 | B-G |
| C-G | 45 | 5 | C-G |
| C-G | 45 | 100 | C-G |
| ABG | 45 | 5 | ABG |
| ABG | 45 | 100 | ABG |
| BCG | 45 | 5 | BCG |
| BCG | 45 | 100 | BCG |
| ACG | 45 | 5 | ACG |
| ACG | 45 | 100 | ACG |

T

Table 5.11 shows that the type of fault was able to be justified correctly by using the proposed algorithm. Table 5.12 shows the fault distance estimation. Although the error is higher than training outcome, it is still acceptable for good estimation of

fault location. Reason for this observation might come from parameters in IEEE 14 bus system that has different condition compared to training. As a conclusion, the proposed ANFIS-GK has been tested with standard network to observe the performance.

Table 5. 12 Fault Location

| Fault type | Fault section | Fault location (km) | Fault resistance (Ω) | Estimated fault location (km) | Error |
|------------|---------------|---------------------|-------------------------------|-------------------------------|-------|
| A-G | 2 – 4 | 20km from Bus 2 | 5 | 20.37 | 0.37 |
| A-G | 2 – 4 | 80km from Bus 2 | 100 | 80.49 | 0.49 |
| B-G | 2 – 4 | 20km from Bus 2 | 5 | 20.56 | 0.56 |
| B-G | 2 – 4 | 80km from Bus 2 | 100 | 80.28 | 0.28 |
| C-G | 2 – 4 | 20km from Bus 2 | 5 | 20.25 | 0.25 |
| C-G | 2 – 4 | 80km from Bus 2 | 100 | 79.57 | 0.43 |
| AB-G | 2 – 4 | 20km from Bus 2 | 5 | 20.68 | 0.68 |
| AB-G | 2 – 4 | 80km from Bus 2 | 100 | 80.58 | 0.58 |
| AC-G | 2 – 4 | 20km from Bus 2 | 5 | 20.57 | 0.57 |
| AC-G | 2 – 4 | 80km from Bus 2 | 100 | 80.48 | 0.48 |
| BC-G | 2 – 4 | 20km from Bus 2 | 5 | 20.49 | 0.49 |
| BC-G | 2 – 4 | 80km from Bus 2 | 100 | 80.56 | 0.56 |
| A-G | 6 – 13 | 40km from Bus 6 | 5 | 40.67 | 0.67 |
| A-G | 6 – 13 | 60km from Bus 6 | 100 | 60.39 | 0.39 |
| B-G | 6 – 13 | 40km from Bus 6 | 5 | 40.38 | 0.38 |
| B-G | 6 – 13 | 60km from Bus 6 | 100 | 60.58 | 0.58 |
| C-G | 6 – 13 | 40km from Bus 6 | 5 | 40.52 | 0.52 |
| C-G | 6 – 13 | 60km from Bus 6 | 100 | 60.58 | 0.58 |
| AB-G | 6 – 13 | 40km from Bus 6 | 5 | 40.68 | 0.68 |
| AB-G | 6 – 13 | 60km from Bus 6 | 100 | 60.75 | 0.75 |
| AC-G | 6 – 13 | 40km from Bus 6 | 5 | 40.69 | 0.69 |
| AC-G | 6 – 13 | 60km from Bus 6 | 100 | 60.86 | 0.86 |
| BC-G | 6 – 13 | 40km from Bus 6 | 5 | 40.71 | 0.71 |
| BC-G | 6 – 13 | 60km from Bus 6 | 100 | 60.79 | 0.79 |

5.5.2 Fault Classification and Location of Real Data from Utility

22 real data are obtained which contain of; 12 cases of single line to ground, 5 cases of double line and 5 cases of double line to ground. The system voltage involved is 115kV, 230kV and 500kV. Whereas, the fault distance are varies from 0km to 271.8km. The raw data files in hand, are not possible to read directly. Thus, all data parameters need to be identified and read from that file. Since the expected input for proposed algorithm is voltage and current, specific procedures were needed to align with the requirement. The input data were in the form of detail coefficients of the respective fault types extracted from the voltages and currents. Twelve data were recorded in the table which expected to get the sum of 100%. On average, the algorithm should perform approximately 8.5% of each type of fault. Table 5.13 shows the classification of fault type with different system voltage and fault distance. The result shows that the algorithm able to classify all types of faults and obtain the total of 97.40%.

Table 5. 13 Percentage of real data classification

| Fault type | System Voltage | % of classified |
|------------|----------------|-----------------|
| Phase A-B | 115kV | 7.6 |
| Phase B-C | 115kV | 7.8 |
| Phase A-C | 115kV | 9.2 |
| Phase A-G | 115kV | 7.9 |
| Phase BC-G | 230kV | 8.5 |
| Phase B-C | 230kV | 7.5 |
| Phase A-B | 230kV | 9.1 |
| Phase B-G | 500kV | 8.1 |
| Phase C-G | 500kV | 9.1 |
| Phase BC-G | 500kV | 7.0 |
| Phase C-G | 115kV | 8.7 |
| Phase B-C | 230kV | 6.9 |
| | Total | 97.4 |

Table 5. 14 Results of Estimation Error for Utility Data

| Substation | Line length (km) | Fault type | Fault distance (km) | System Voltage (kV) | Error | Error (%) |
|------------|------------------|------------|---------------------|---------------------|-------|-----------|
| NPO1-UD1 | 98.5 | CG | 33 | 115 | 0.496 | 0.506 |
| NPO1-UD1 | 98.5 | AG | 60 | 115 | 0.435 | 0.442 |
| MM3-PY | 113.7 | BC | 22.8 | 115 | 0.461 | 0.405 |
| KK1-CPA | 86.6 | AC | 56.6 | 115 | 0.849 | 0.980 |
| NN-SO2 | 71.58 | AG | 40.1 | 115 | 0.533 | 0.745 |
| BKI-CT | 116.05 | BCG | 69.6 | 230 | 0.824 | 0.710 |
| NS-TTK | 48.5 | BC | 28.5 | 230 | 0.781 | 1.610 |
| AT1- TTK | 147.8 | AB | 73.9 | 230 | 0.665 | 0.449 |
| CBG-WN | 183.5 | CG | 128.5 | 500 | 0.443 | 0.241 |
| MM3-TTK | 325 | AG | 97.5 | 500 | 0.760 | 0.234 |
| MM3-TTK | 325 | BG | 162.5 | 500 | 0.697 | 0.214 |

Table 5.14 shows the results of estimation error in utility data. These results indicate that phase A to B (AB) has maximum estimation of error, 0.89. Although the error is higher than training outcome, it is still acceptable for good estimation of fault location. Reason for this observation might come from parameters and instrument being used in the power utility that has different condition compared to training. For a comparison pertinent to fault location, the calculation of real fault data used the standard method, one-ended impedance that being used in most numerical relays. Figure 5.27 shows the mentioned method.

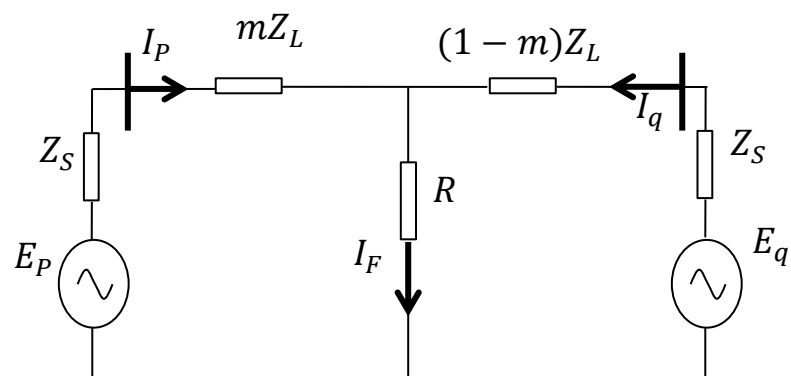


Figure 5. 26 Circuit representation of Line Fault

$$\text{From figure 5.27, } V_P = mI_P Z_L + I_F R_F \quad (5.2)$$

In equation 5.2, I_F need to be estimated to identify the fault location, m . The steps to calculate the fault location:

1. Choose a different set of vector based on phase selection algorithm to attain the vectors. Applied Equation 5.2 to identify either the phase to ground fault or a phase to phase fault.

Thus, for A to G fault;

$$I_P Z_L = I_a Z_L + I_n Z_E \quad (5.3)$$

$$\text{and } V_P = V_A$$

and for A to B fault:

$$I_P Z_L = (I_a - I_b) Z_L \quad (5.4)$$

$$\text{and } V_P = V_A - V_B$$

2. Identification of fault distance, m is done using the sine wave of I_F which get through zero, the instantaneous values of sine wave V_p and I_p . Calculated vectors of V_p and $I_p Z_L$ then has to be shifted by angle of fault current with 90° .

From equation 5.1;

$$m = \frac{V_P}{(I_P Z_L)} \text{ at } I_F = 0$$

$$= \frac{|V_P| * \sin(s-d)}{(|I_P Z_L| * \sin(e-d))} \quad (5.5)$$

Where, d = angle of fault current, I_F , s = angle of V_P , e = angle of $I_P Z_L$

For example, to calculate the fault location at *Station KK1* to *station NPO1*, circuit #1 using a fault locator which is implemented on numerical relay. The setting parameter for this line was:

Length line: 30.0km

Positive sequence impedance: $Z_L = 7.48 \angle 68^\circ$

Zero sequence compensation factors = $kZN = 0.63 \angle 11^\circ$

In basic practice, the current and voltage signals will be injected into the relay for assigning various faults; AG, BG, CG, AB, BC, and AC. The type of fault will define the respective parameters required to justify the fault distance. A protection engineer reads the distance to fault display on relay's Light Crystal Display (LCD) and calculate error of results as illustrated in Table 5.15. In the table, L_e is the estimated distance of fault location measured from the relay and L_t is the actual distance. L is total line length and the percentage of error is calculated using equation 5.1. According to the table, the range of error is about 0.23% to 2.4%.

Table 5. 15 Result testing on Relay

| Fault Type | Inject current and voltage values | L_t (km) | L_e (km) | Error | Error (%) |
|------------|--|------------|------------|-------|-----------|
| A-G | $V_a = 0.6476 \angle 0^\circ$, $I_a = 1 \angle -72.25^\circ$ | 1.63 | 1.5 | 0.13 | 0.433 |
| B-G | $V_b = 9.088 \angle -120^\circ$, $I_b = 1 \angle -192.25^\circ$ | 22.5 | 22.7 | 0.2 | 0.667 |
| C-G | $V_c = 4.263 \angle 120^\circ$, $I_c = 1 \angle -14.25^\circ$ | 7.94 | 8.6 | 0.66 | 2.200 |
| A-B | $V_a = 29.51 \angle -47.98^\circ$, $I_a = 1 \angle -38^\circ$ $V_b = 29.51 \angle -72.02^\circ$, $I_b = 1 \angle 142^\circ$ | 24.79 | 24.7 | 0.09 | 0.300 |
| B-C | $V_b = 28.91 \angle -176.83^\circ$, $I_b = 1 \angle -230^\circ$ $V_c = 28.91 \angle 176.83^\circ$, $I_c = 1 \angle -50^\circ$ | 4.48 | 4.4 | 0.08 | 0.266 |
| A-C | $V_a = 29.47 \angle 48.43^\circ$, $I_a = 1 \angle -60^\circ$ $V_c = 29.47 \angle 71.57^\circ$, $I_c = 1 \angle -240^\circ$ | 12.76 | 12.4 | 0.36 | 1.200 |

As a conclusion, the ANFIS-GK has been tested with real data with fix information, a few system voltages and variety of fault distance. No definite mathematical equations and line parameters were involved. Table 5.16 Shows the range of error in comparison between Table 5.14 and Table 5.15.

Table 5. 16 Comparison on range of error

| Item | Range of error (%) |
|---------------------------|--------------------|
| Calculated fault location | 0.23% to 2.2% |
| Proposed ANFIS-GK | 0.23% to 1.6% |

5.5.3 Comparison ANFIS-GK With ANN Approaches

In this case study, proposed ANFIS-GK method is compared with another scheme which implemented neural network approach. The simulation is set to justify the type and location of the fault using a number of fault data from the utility. The implemented ANN algorithm was illustrated as below;

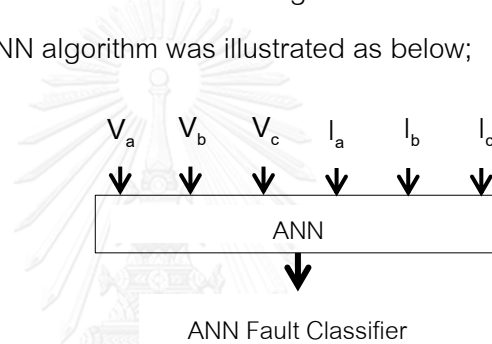


Figure 5. 27 Scheme for ANN Fault Classifier

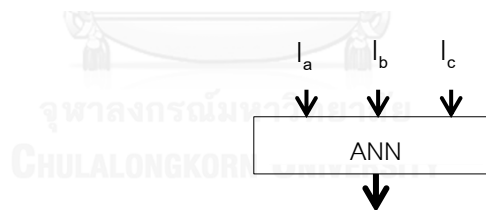


Figure 5. 28 Scheme for ANN Fault Location

Comparison between proposed scheme and ANN has shown that ANFIS-GK performed much better in obtaining the expected results. Basically, ANFIS-GK gave precision results in identification scheme when compared using the index error. Implementation of optimization has helped ANFIS-GK in learning process on the training data. The observation showed that ANFIS-GK is better than ANN scheme and best performance is obtained for single line to ground. The range of error for ANFIS-GK is within 0.2km to 0.8km. Whereas, the range of error for ANN is within 0.5km – 3.9km. GK has supported the result to be more generalized.

Table 5. 17 Comparison with ANFIS-GK and ANN

| ANN/ANFIS Fault type | Actual value in Km | ANN Fault Location | Error | Proposed ANFIS-GK | Error |
|----------------------|--------------------|--------------------|-------|-------------------|-------|
| BCG | 74.6 | 72 | 2.6 | 73.8 | 0.8 |
| AG1 | 71.6 | 70.3 | 1.3 | 71.1 | 0.5 |
| AG2 | 89.5 | 88.6 | 0.9 | 88.9 | 0.6 |
| BG | 115.8 | 115.3 | 0.5 | 115.5 | 0.3 |
| CG | 41.9 | 40.7 | 1.2 | 41.7 | 0.2 |
| BC | 28.5 | 32.4 | 3.9 | 28.98 | 0.48 |
| CG2 | 128.5 | 129 | 0.5 | 128.74 | 0.24 |
| ABG | 50.6 | 47.6 | 3.0 | 49.8 | 0.8 |

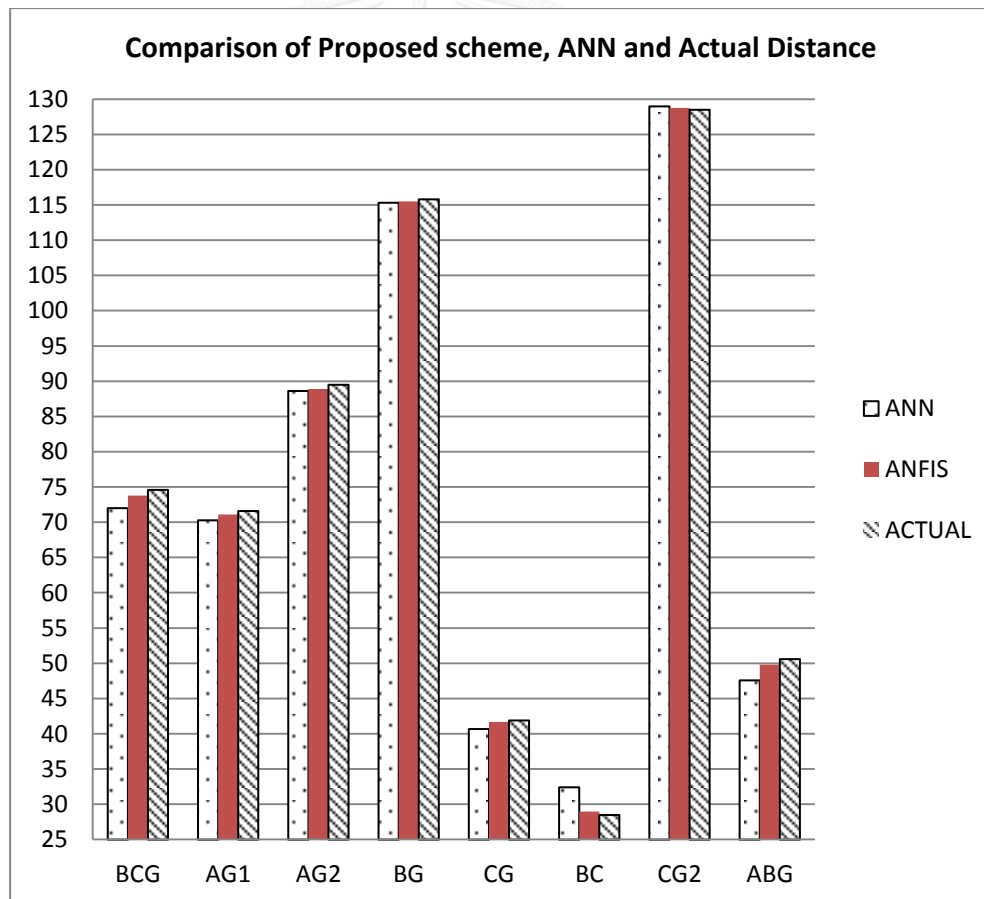


Figure 5. 29 Plotting Comparison of ANFIS-GK and ANN

5.5.4 Comparison and Performance of GK with FCM Algorithms

Generally, FCM algorithm is easy to be implemented. The steps are; firstly, Z, select the weighting exponent as $m > 1$, the number of clusters as $1 < c < N$, the norm-inducing matrix A and the termination tolerance $\mathcal{E} > 0$ in a respective dataset. The partition matrix randomly, then need to be initialized such that $U^{(0)} \in M_{fc}$. Secondly, when the termination tolerance has been attained, the membership values will be achieved. The only disadvantage is, FCM has been restricted by Euclidean distance.

GK followed the FCM algorithm by employing an adaptive distance norm. Each cluster has its own norm-inducing matrix A_i that used as an optimization variable in the c-means functional. This condition will allow every cluster to adjust the distance norm to the local topological structure of the data. The steps are; select the weighting exponent $m > 1$, the number of clusters as $1 < c < N$, and the termination tolerance $\mathcal{E} > 0$.

The difference between GK and FCM is pertinent to the computation of distance measure. The details have been explained in chapter 3 and 4. Table 5.18 shows the comparison of GK and FCM.

Table 5. 18 Comparison of GK and FCM

| Algorithm | Advantages | Disadvantages | Applicable |
|-----------|--|---|-----------------|
| FCM | A few iteration steps already provide a good approximation to the final solution | FCM tends to locate the centroid in the neighborhood of the larger cluster and misses the small, well-separated clusters. | Spherical shape |
| GK | In order to capture ellipsoidal properties of clusters, GK used the covariance matrix to adjust with different structures in the dataset | The clusters are narrower and the areas with higher membership are thinner | Line segments |

Set-up on experimental study:

300 simulated data pertinent to single line to ground fault, double line to ground, and double line were considered in this study. The aim is to observe the performance of each algorithm. The membership function of x and y are to be extracted using FCM and GK algorithms. The trial and error technique is used to amend the parameters. Table 5.19 shows the parameter used for simulation.

Table 5. 19 Parameter

| Parameter | FCM | GK |
|-----------------------------------|-------|-------|
| Number of clusters, c | 3 | 3 |
| Fuzziness of clustering, m | 2 | 2 |
| Termination tolerance, ϵ | 0.001 | 0.001 |

Figure 5.29 shows the performance on completion time compared to the number of clusters involved in the study. GK has performed higher completion compared to FCM. Similarly, figure 5.30 shows that GK able to complete the clustering task faster than FCM. The last characteristic is the performance of clustering capability as shown in figure 5.31.

i. Performance on completion time compared to the number of clusters

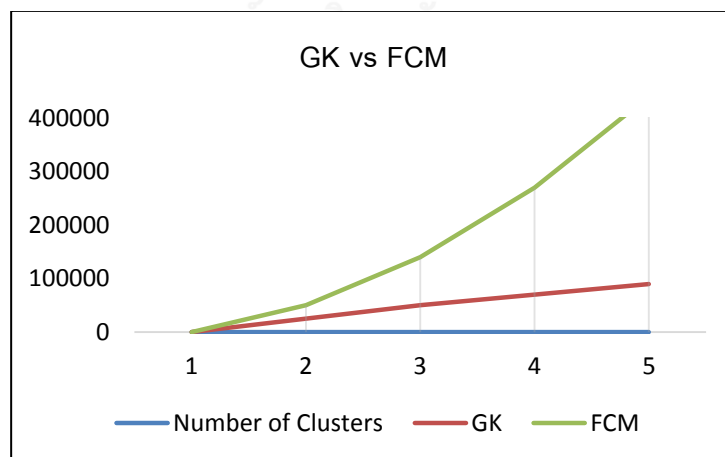


Figure 5. 30 GK vs FCM in terms of time completion with varying number of clusters

- i. Performance on completion time taken for clustering task

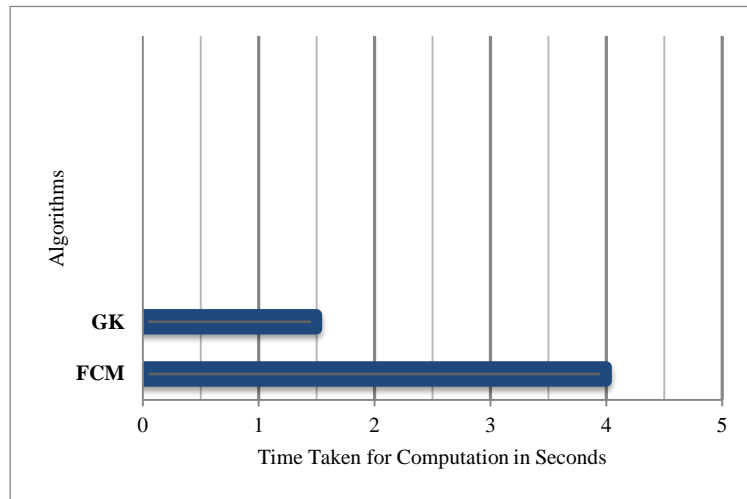


Figure 5. 31 Elapsed Time of FCM vs GK in completing clustering task

- ii. Performance of clustering

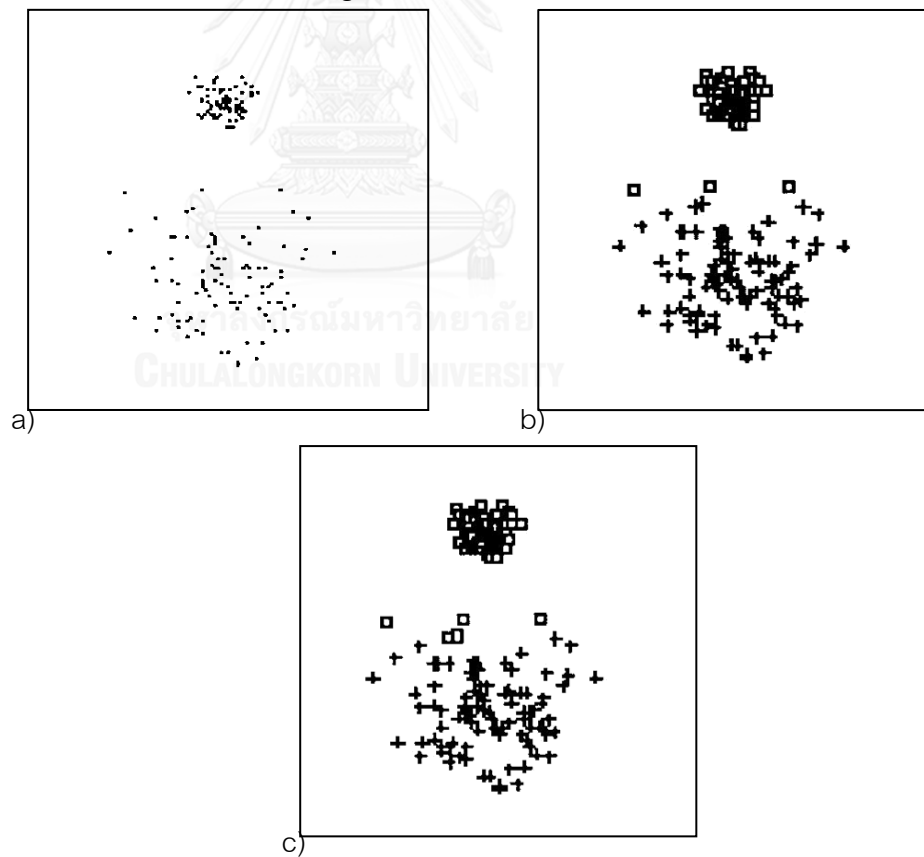


Figure 5. 32 a) the original data in scattered b) FCM clustering c) GK clustering

In the performance of clustering data, both FCM and

GK perform well. However, GK GK clustering has an advantage that smaller cluster has the capability to grab belongs to the large cluster. This is because, GK algorithm does not take size into account. It is observed that the GK clustering provide improved performance for a nonlinear function compared to FCM. As mentioned in the previous chapter, GK algorithm may applied to fault classification scheme. However, for fault location scheme, it requires the support from system identification method.

5.6 Graphic User Interface (GUI)

In the implementation part, a MATLAB GUI based simulation tool has been developed to provide an interactive and graphical medium that has ability to carry the tasks of proposed scheme more effective. This GUI is a convenient pictorial interface to a program. The toolbox developed may help in understanding the flow of scheme much easier. The presented results here are pertinent to single line to ground fault on the transmission line. Steps in the development of GUI are;

1. Open Matlab and type 'guide' in the command window
2. Select "Blank GUI (default) to create a new GUI dialogue box
3. Design every layer of code.
4. A new window will appear for further actions

When the program is run, the main window appears as in figure 5.32. It contains a few toggles, description and related instructions. In the 'main page' toggle, there are selections of 'manual', 'automatic' and 'help' which can help the user to choose the mode in executing the GUI. Figure 5.33 shows the description.

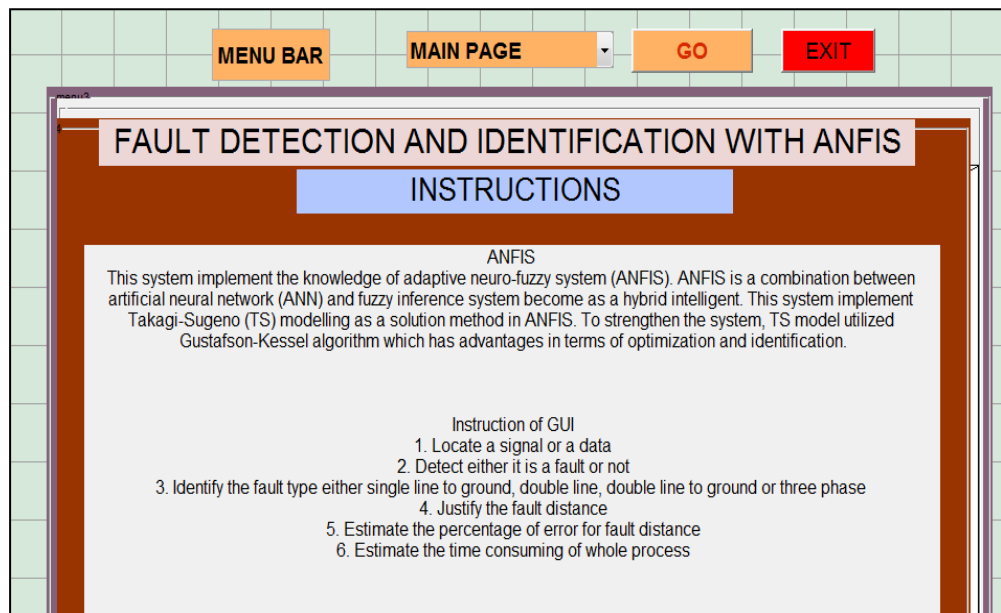


Figure 5. 33 Main window of ANFIS-GK GUI

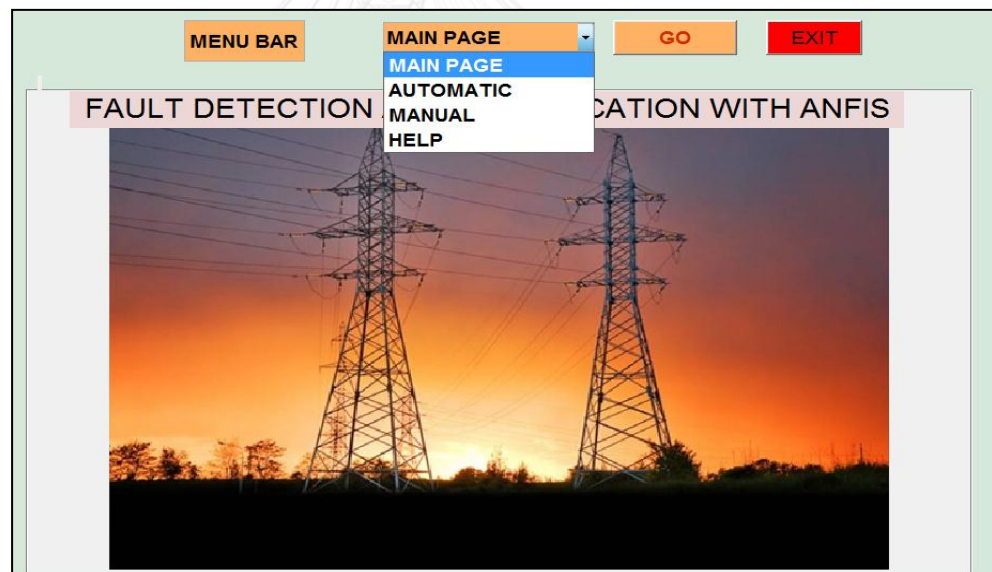


Figure 5. 34 Selection of mode

Figure 5.34 shows the window in automatic mode, whereas, figure 5.35 and 5.36 illustrate the windows in manual mode.

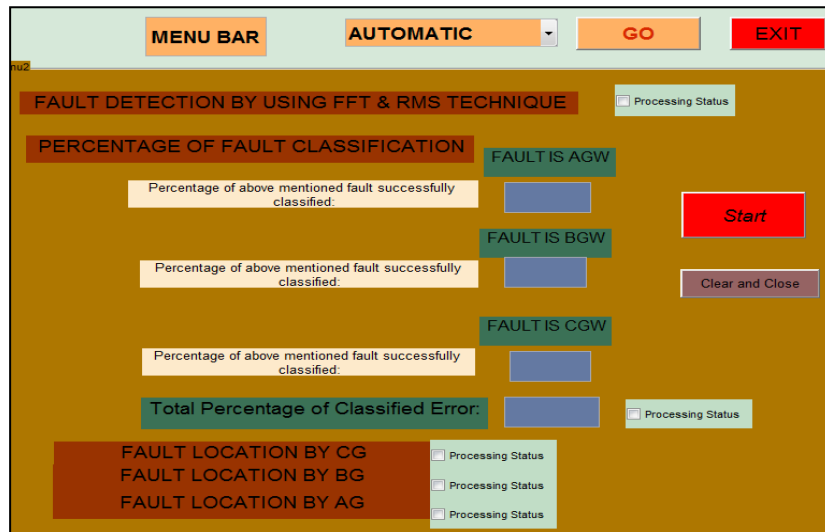


Figure 5. 35 Automatic mode

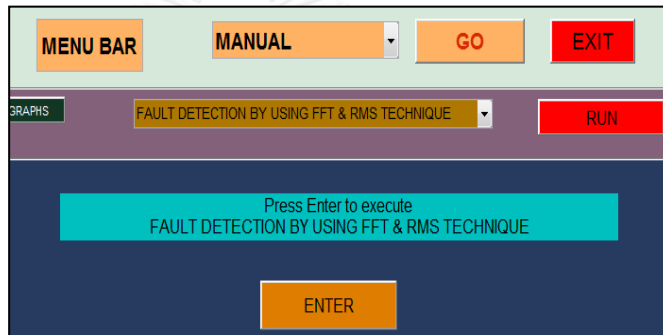


Figure 5. 36 Window in manual mode (1)

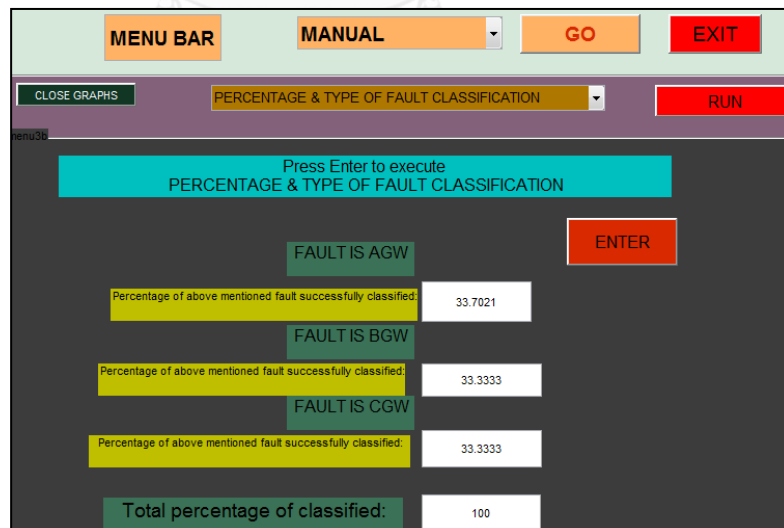


Figure 5. 37 Window in manual mode (2)

CHAPTER 6.0

CONCLUSION AND FUTURE WORKS

In order to improve traditional electromechanical relays, expertise in digital has a significant influence on the way relays operate and respond. Today, the intelligent computational techniques are ideal for economic as well as technical reasons. Economic factor was also important to be considered in improving the performance of accuracy in fault location.

6.1 Conclusion

In this research, we have proposed a novel scheme of automated fault detection and identification using ANFIS combined with wavelet transform which can be concluded as below;

1. The algorithm proposed in fault identification that aim for fault classification and fault location called ANFIS-GK algorithm.
2. Studies and analysis have shown a great performance and possible to execute as discussed in the previous chapter.
3. The requirement of algorithms is independent of line parameters since it manipulated the knowledge of artificial intelligence gained from ANFIS.
4. The proposed method also has very less involving of calculation and almost no affected by the fault resistance.

6.2 Contribution

Even though this thesis is concerned with the parallel transmission line, the contribution is likely to be applied in other types of transmission line as well. Upon completing this dissertation, the contributions can be enlightened as below:

1. Improves the previous ANFIS approach pertinent to requirement of huge training data by implementing the Takagi-Sugeno model and GK algorithm.
2. Improves the previous ANFIS approach pertinent to flow of the fault identification scheme that independence between fault classification and fault location. This matter will improve the reliability of the results.
3. Improve the robustness of the fault location approach since it has not considered the series impedance matrix per unit length.
4. Improve the reliability of the result by providing a precise error within a definite range.

6.3 Thesis Limitation

1. The modeling results are fairly accurate with respect to the choice of the critical training data set. The proper selection of the features is important as the ANFIS model is decided based upon the optimal choice. Rigorous experiments need to be performed to determine the best selection to fit into the optimal ANFIS model.
2. Although the concept of GK clustering algorithm has the ability in estimation with a small data set, but the values of definite data are still in undergo research.
3. Typically, only one ANFIS model for a transmission line. For other transmission line, new ANFIS model may require to be trained again.
4. The algorithm can work well if it has true actual line parameters, CT and VT error is small. The algorithm couldn't work well if extensive changes to the relaying system.

5. With the support of WAMS, SCADA, and Automation Substation in the future, the proposed model could have produced a better performance.

6.4 Future Works

There are a few possible potential avenues of further research that arise from the work carried out in this thesis as stated below:

- i. Further analysis of high impedance fault

In this research, the system voltage that being used in experimental studies is 115kV, thus fault resistance of 100Ω and 200Ω pertinent to single line to ground fault and double line to ground fault were considered as described in section 5.4. In the critical investigation on HIF should be doing for better improvement that should consider the respective sources and characteristics for more robustness of ANFIS-GK.

- ii. Initial membership function and rule extraction

Method of GK has been implemented in this research. Other methods could be tested against the model that can obtain small numbers of rules and maximize accuracy.

- ii. Learning algorithm

Effective search for the stable, suitable and optimal parameters tuning of ANFIS membership functions to speed up the learning process is considered necessary to obtain a more precise fuzzy model.

- iv. Further study on fault classifications

Prepare a fundamental study of fault classification using ANFIS. Further implementation is identifying the type of event either fault or non-fault interruption, transformer saturation and step change.

REFERENCES

- [1] El Sayed Mohamed Tag, "Fault Location for Series Compensated Transmission Line Based on Wavelet Transform and an ANFIS," in *Electric Power Quality and Supply Reliability Conference (PQ)*, Kuressaare 2010, pp. 229 - 236.
- [2] Jyh-Shing Roger Jang, "ANFIS: Adaptive-Network-Based Fuzzy Inference System," *IEEE Transactions on Systems, Man and Cybernetics*, vol. 23, pp. 665 - 685, May/Jun 1993 1993.
- [3] D. V. Coury and D. C. Jorge, "Artificial Neural Network Approach to Distance Protection of Transmission Lines," *IEEE Transactions on Power Delivery*, vol. 13, pp. 102 - 108, January 1998 1998.
- [4] Ramadoni Syahputra, "A Neuro-Fuzzy Approach For The Fault Location Estimation of Unsynchronized Two-Terminal Transmission Lines " *International Journal of Computer Science & Information Technology*, vol. 5, p. 23, February 2013.
- [5] M. Jayabharata Reddy and D. Mohanta, "A Wavelet-Fuzzy Combined Approach For Classification and Location of Transmission Line Faults," *International Journal of Electrical Power & Energy Systems*, vol. 29, pp. 669-678, 2007.
- [6] J. S. a. H. Afradi, "New and Accurate Fault Location Algorithm For Combined Transmission Lines Using Adaptive Network-Based Fuzzy Inference System," *Electric Power System Research, ELSEVIER* vol. 79, pp. 1538 - 1545, June.
- [7] W. Y. a. X. Y. Zeng Xiangjun, "Faults Detection for Power Systems," in *Faults Detection for Power Systems*, ed: INTECH Open Access Publisher, 2010.

- [8] S. R. Samantaray, Dash, P.K. and Panda, G., "Transmission Line Fault Detection Using Time-Frequency Analysis " in *2005 Annual IEEE INDICON*, Chennai, India, 2005, pp. 162 - 166
- [9] T. Adu, "An Accurate Fault Classification Technique For Power System Monitoring Devices," *IEEE Transactions on Power Delivery*, vol. 17, pp. 684-690, 2002.
- [10] E. Styvaktakis, M. H. Bollen, and I. Y. Gu, "Automatic Classification of Power System Events Using RMS Voltage Measurements," in *IEEE Power Engineering Society Summer Meeting, 2002* 2002, pp. 824-829.
- [11] T. Kawady and J. Stenzel, "A practical fault location approach for double circuit transmission lines using single end data," *Power Delivery, IEEE Transactions on*, vol. 18, pp. 1166-1173, 2003.
- [12] M. Kezunovic and Q. Chen, "A Novel Approach For Interactive Protection System Simulation," *IEEE Transactions on Power Delivery*, vol. 12, pp. 668-674, 1997.
- [13] D. Novosel, B. Bachmann, D. Hart, Y. Hu, and M. M. Saha, "Algorithms for locating faults on series compensated lines using neural network and deterministic methods," *Power Delivery, IEEE Transactions on*, vol. 11, pp. 1728-1736, 1996.
- [14] M. Sachdev and R. Agarwal, "A technique for estimating transmission line fault locations from digital impedance relay measurements," *Power Delivery, IEEE Transactions on*, vol. 3, pp. 121-129, 1988.
- [15] R. Aggarwal, D. Coury, A. Johns, and A. Kalam, "A practical approach to accurate fault location on extra high voltage teed feeders," *Power Delivery, IEEE Transactions on*, vol. 8, pp. 874-883, 1993.
- [16] J. Izykowski, R. Molag, E. Rosolowski, and M. M. Saha, "Accurate location of faults on power transmission lines with use of two-end unsynchronized measurements," *Power Delivery, IEEE Transactions on*, vol. 21, pp. 627-633, 2006.

- [17] J. Gracia, A. Mazon, and I. Zamora, "Best ANN Structures For Fault Location in Single and Double-Circuit Transmission Lines," *IEEE Transactions on Power Delivery* vol. 20, pp. 2389-2395, 2005.
- [18] "TRAVELING WAVE FAULT LOCATORS – APPLICATION AND RESULTS," Reason International 2008.
- [19] F. Han, X. H. Yu, M. Al-Dabbagh, and Y. Wang, "Fault Location in Power Distribution Networks Using Sinusoidal Steady State Analysis," in *Proceedings of the 7th Asia Pacific Complex Systems Conference*, 2004.
- [20] G. Gilcrest, G. Rockefeller, and E. Udren, "High-Speed Distance Relaying Using a Digital Computer I-System Description," *Power Apparatus and Systems, IEEE Transactions on*, pp. 1235-1243, 1972.
- [21] T. Adu, "A New Transmission Line Fault Locating System," *IEEE Trans. Power Delivery*, vol. 16, pp. 498 - 503, 2004.
- [22] T. Takagi, Y. Yamakoshi, M. Yamaura, R. Kondow, and T. Matsushima, "Development of a new type fault locator using the one-terminal voltage and current data," *power apparatus and systems, ieee transactions on*, pp. 2892-2898, 1982.
- [23] G. Song, J. Suonan, and Y. Ge, "An accurate fault location algorithm for parallel transmission lines using one-terminal data," *International Journal of Electrical Power & Energy Systems*, vol. 31, pp. 124-129, 2009.
- [24] X. Lin, H. Weng, and B. Wang, "A generalized method to improve the location accuracy of the single-ended sampled data and lumped parameter model based fault locators," *International Journal of Electrical Power & Energy Systems*, vol. 31, pp. 201-205, 2009.
- [25] A. A. Girgis, D. G. Hart, and W. L. Peterson, "A new fault location technique for two-and three-terminal lines," *Power Delivery, IEEE Transactions on*, vol. 7, pp. 98-107, 1992.

- [26] G. Ancell and N. Pahalawaththa, "Maximum likelihood estimation of fault location of transmission lines using travelling waves," *IEEE Transactions on Power Delivery*, vol. 9, pp. 680-689, 1994.
- [27] E. Vázquez-Martínez, "A travelling wave distance protection using principal component analysis," *International journal of electrical power & energy systems*, vol. 25, pp. 471-479, 2003.
- [28] X. Dong, W. Kong, and T. Cui, "Fault classification and faulted-phase selection based on the initial current traveling wave," *Power Delivery, IEEE Transactions on*, vol. 24, pp. 552-559, 2009.
- [29] Z. Q. Bo, G. Weller, T. Lomas, and M. A. Redfern, "Positional protection of transmission systems using global positioning system," *Power Delivery, IEEE Transactions on*, vol. 15, pp. 1163-1168, 2000.
- [30] P. Crossley and E. Southern, "The impact of the global positioning system (GPS) on protection and control," in *11th International Conference on Power System Protection, Bled, Slovenia*, 1998, pp. 1-5.
- [31] A. L. Dalcastagnê, S. Noceti Filho, H. Zurn, and R. Seara, "An iterative two-terminal fault-location method based on unsynchronized phasors," *Power Delivery, IEEE Transactions on*, vol. 23, pp. 2318-2329, 2008.
- [32] F. H. Magnago and A. Abur, "Fault location using wavelets," *Power Delivery, IEEE Transactions on*, vol. 13, pp. 1475-1480, 1998.
- [33] S. Ramaswamy, B. Kiran, K. Kashyap, and U. Shenoy, "Classification of power system transients using wavelet transforms and probabilistic neural networks," in *TENCON 2003. Conference on Convergent Technologies for the Asia-Pacific Region*, 2003, pp. 1272-1276.
- [34] L. A. Zadeh, "Fuzzy Sets," *Information and control*, vol. 8, pp. 338-353, 1965.
- [35] O. Castillo and P. Melin, *Soft Computing For Control of Non-Linear Dynamical Systems* vol. 63: Physica-Verlag Heidelberg, 2001.

- [36] T. Takagi and M. Sugeno, "Fuzzy Identification of Systems and Its Applications to Modeling and Control," *IEEE Transactions on Systems, Man and Cybernetics*, pp. 116-132, 1985.
- [37] S. A. S. A. Rahman, F. A. M. Yusof, M. Zailani, and A. Bakar, "The Method Review of Neuro-Fuzzy Applications in Fault Detection and Diagnosis System," *International Journal of Engineering & Technology*, vol. 10, 2010.
- [38] R. L. Cannon, J. V. Dave, and J. C. Bezdek, "Efficient implementation of the fuzzy c-means clustering algorithms," *Pattern Analysis and Machine Intelligence, IEEE Transactions on*, pp. 248-255, 1986.
- [39] R. N. Davé, "Use of the adaptive fuzzy clustering algorithm to detect lines in digital images," in *1989 Advances in Intelligent Robotics Systems Conference*, 1990, pp. 600-611.
- [40] A. Ferrero, S. Sangiovanni, and E. Zappitelli, "A Fuzzy-Set Approach to Fault-Type Identification in Digital Relaying," in *Proceedings IEEE Power Engineering Society Transmission and Distribution Conference, 1994*, 1994, pp. 269-275.
- [41] B. Das and J. V. Reddy, "Fuzzy-Logic-Based Fault Classification Scheme For Digital Distance Protection," *IEEE Transactions on Power Delivery*, vol. 20, pp. 609-616, 2005.
- [42] Z. Wang, V. Palade, and Y. Xu, "Neuro-Fuzzy Ensemble Approach For Microarray Cancer Gene Expression Data Analysis," in *International Symposium on Evolving Fuzzy Systems, 2006* 2006, pp. 241-246.
- [43] P. Panchariya, A. Palit, D. Popovic, and A. Sharrna, "Nonlinear System Identification Using Takagi-Sugeno Type Neuro-Fuzzy Model," in *Proceedings of 2nd International IEEE Conference Intelligent Systems, 2004.*, 2004, pp. 76-81.
- [44] P. K. Dash, Pradhan A.K., and Panda G., "A Novel Fuzzy Neural Network Based Distance Relaying Scheme," *IEEE Transactions on Power Delivery*, vol. 15, pp. 902 - 907, July 2000 2000.

- [45] R. Babuka, P. Van der Veen, and U. Kaymak, "Improved Covariance Estimation For Gustafson-Kessel Clustering," in *Proceedings of the IEEE International Conference on Fuzzy Systems, 2002.*, 2002, pp. 1081-1085.
- [46] F. Chen and T. Ou, "Sales Forecasting System Based on Gray Extreme Learning Machine With Taguchi Method in Retail Industry," *Expert Systems with Applications*, vol. 38, pp. 1336-1345, 2011.
- [47] Karthikeyan Kasinathan, "Power System Fault Detection and Classification By Wavelet Transforms and Adaptive Resonance Theory Neural Networks," Master, The Graduate School, University of Kentucky, 2007.
- [48] A. K. Ghosh and D. L. Lubkeman, "The classification of power system disturbance waveforms using a neural network approach," *Power Delivery, IEEE Transactions on*, vol. 10, pp. 109-115, 1995.
- [49] R. M. de Castro Fernández and H. N. D. Rojas, "An overview of wavelet transforms application in power systems," in *14th Power Syst. Comput. Conf*, 2002.
- [50] A. T. A. Jain, and R. N. Patel,, "Fault Classification of Double Circuit Transmission Line Using Artificial Neural Network," *World Academy of Science, Engineering and Technology*, vol. 2, pp. 789 - 794, 2008.
- [51] F. Magnago and A. Abur, "Fault Location Using Wavelets," *IEEE Transactions on Power Delivery*, vol. 13, pp. 1475 - 1480 October 1998.
- [52] K. Gayathri, "Comparative Study of Fault Identification and Classification on EHV Lines Using Discrete Wavelet Transform and Fourier Transform Based," 2008.
- [53] J. Upendar, C. Gupta, and G. Singh, "ART2 and Wavelet Transform based Approach for Power System Fault Classification," *Proceedings of World Academy of Science: Engineering & Technology*, vol. 51, 2009.
- [54] R. Rajeswari, N. Kamaraj, and K. Swarup, "Fault Diagnosis of Parallel Transmission Lines Using Wavelet Based ANFIS," *International Journal of Electrical and Power Engineering*, vol. 1, pp. 410-415, 2007.

- [55] V. Malathi and N. Marimuthu, "Multi-Class Support Vector Machine Approach For Fault Classification in Power Transmission Line," in *IEEE International Conference on Sustainable Energy Technologies, ICSET 2008.*, 2008, pp. 67-71.
- [56] J. Upendar, C. Gupta, and G. Singh, "Discrete Wavelet Transform and Genetic Algorithm Based Fault Classification of Transmission Systems," in *Proceeding of 15th National Power Systems Conference(NPSC)*, 2008, p. 328.
- [57] K. Razi, M. T. Hagh, and G. Ahrabian, "High Accurate Fault Classification of Power Transmission Lines Using Fuzzy Logic," in *International Power Engineering Conference, 2007.*, 2007, pp. 42-46.
- [58] P. Chen, B. Xu, J. Li, and Y. Ge, "Modern Travelling Wave Based Fault Location Techniques for HVDC Transmission Lines," *Transactions of Tianjin University*, vol. 14, pp. 139-143, 2008.
- [59] N. Zhang and M. Kexunovic, "Coordinating Fuzzy ART Neural Networks to Improve Transmission Line Fault Detection and Classification," in *IEEE Power Engineering Society General Meeting, 2005.*, 2005, pp. 734-740.
- [60] M. Korkali, H. Lev-Ari, and A. Abur, "Traveling-wave-based fault-location technique for transmission grids via wide-area synchronized voltage measurements," *Power Systems, IEEE Transactions on*, vol. 27, pp. 1003-1011, 2012.
- [61] Sachin R. Yerekar, "Fault Location System for Transmission Lines in One-terminal By using Impedance-Traveling Wave Assembled Algorithm," in *8th EEEIC International Conference on Environment and Electrical Engineering*, Karpacz, Poland, 2009.
- [62] M. Gilany, D. K. Ibrahim, and E. T. Eldin, "Traveling-Wave-Based Fault-Location Scheme For Multiend-Aged Underground Cable System," *IEEE Transactions on Power Delivery*, vol. 22, pp. 82-89, 2007.

- [63] F. S. Carvalho and S. Carneiro Jr, "Detection of Fault Induced Transients in EHV Transmission Lines for the Development of a Fault Locator System," in *International Conference on Power Systems Transients-IPST, USA*, 2003.
- [64] A. Borghetti, M. Bosetti, M. Di Silvestro, C. A. Nucci, and M. Paolone, "Continuous-Wavelet Transform For Fault Location In Distribution Power Networks: Definition Of Mother Wavelets Inferred From Fault Originated Transients," *IEEE Transactions on Power Systems*, vol. 23, pp. 380-388, 2008.
- [65] R. Lovassy, L. T. Kóczy, I. J. Rudas, and L. Gál, "Fuzzy Neural Networks as "Good" Function Approximators."
- [66] S.-M. Yeo, C.-H. Kim, K. Hong, Y. Lim, R. Aggarwal, A. Johns, *et al.*, "A Novel Algorithm For Fault Classification in Transmission Lines Using a Combined Adaptive Network and Fuzzy Inference System," *International Journal Of Electrical Power & Energy Systems*, vol. 25, pp. 747-758, 2003.
- [67] H. Wang, C. Huang, L. Yao, Y. Qian, and X. Jiang, "Application of Gustafson-Kessel Clustering Algorithm in The Pattern Recognition for GIS," *PRZEGLĄD ELEKTROTECHNICZNY (Electrical Review)*, vol. 87, pp. 215-219, 2011.
- [68] S. Dourlens, N. Chatry, V. Perdereau, and M. Drouin, "Lateral Position Control of a Vehicle on Highway by Memory Neuron Networks," in *NC*, 1998, pp. 768-771.

APPENDIX

A.1. IEEE-14 Bus System Data

| Bus No. | P Generated (p.u) | Q Generated (p.u) | P Load (p.u) | Q Load (P.u) | Q Generated max (p.u) | Q Generated min (p.u) |
|---------|-------------------|-------------------|--------------|--------------|-----------------------|-----------------------|
| 1 | 2.32 | 0.00 | 0.00 | 0.00 | 10.0 | -10.0 |
| 2 | 0.4 | -0.424 | 0.2170 | 0.1270 | 0.5 | -0.4 |
| 3 | 0.00 | 0.00 | 0.9420 | 0.1900 | 0.4 | 0.00 |
| 4 | 0.00 | 0.00 | 0.4780 | 0.00 | 0.00 | 0.00 |
| 5 | 0.00 | 0.00 | 0.0760 | 0.0160 | 0.00 | 0.00 |
| 6 | 0.00 | 0.00 | 0.1120 | 0.0750 | 0.24 | -0.06 |
| 7 | 0.00 | 0.00 | 0.00 | 0.00 | 0.00 | 0.00 |
| 8 | 0.00 | 0.00 | 0.00 | 0.00 | 0.24 | -0.06 |
| 9 | 0.00 | 0.00 | 0.2950 | 0.1660 | 0.00 | 0.00 |
| 10 | 0.00 | 0.00 | 0.0900 | 0.0580 | 0.00 | 0.00 |
| 11 | 0.00 | 0.00 | 0.0350 | 0.0180 | 0.00 | 0.00 |
| 12 | 0.00 | 0.00 | 0.0610 | 0.0160 | 0.00 | 0.00 |
| 13 | 0.00 | 0.00 | 0.1350 | 0.0580 | 0.00 | 0.00 |
| 14 | 0.00 | 0.00 | 0.1490 | 0.0500 | 0.00 | 0.00 |

A.2 IEEE 14-Bus System Line Data

| From Bus | To Bus | Resistance (p.u) | Reactance (p.u) | Line Charging (p.u) |
|----------|--------|------------------|-----------------|---------------------|
| 1 | 2 | 0.01938 | 0.05917 | 0.0528 |
| 1 | 5 | 0.05403 | 0.22304 | 0.0492 |
| 2 | 3 | 0.04699 | 0.19797 | 0.0438 |
| 2 | 4 | 0.05811 | 0.17632 | 0.0374 |
| 2 | 5 | 0.05695 | 0.17388 | 0.034 |
| 3 | 4 | 0.06701 | 0.17103 | 0.0346 |
| 4 | 5 | 0.01335 | 0.04211 | 0.0128 |
| 4 | 7 | 0.00 | 0.20912 | 0.00 |
| 4 | 9 | 0.00 | 0.55618 | 0.00 |
| 5 | 6 | 0.00 | 0.25202 | 0.00 |
| 6 | 11 | 0.09498 | 0.1989 | 0.00 |
| 6 | 12 | 0.12291 | 0.25581 | 0.00 |
| 6 | 13 | 0.06615 | 0.13027 | 0.00 |
| 7 | 8 | 0.00 | 0.17615 | 0.00 |
| 7 | 9 | 0.00 | 0.11001 | 0.00 |
| 9 | 10 | 0.03181 | 0.08450 | 0.00 |
| 9 | 14 | 0.12711 | 0.27038 | 0.00 |
| 10 | 11 | 0.08205 | 0.19207 | 0.00 |
| 12 | 13 | 0.22092 | 0.19988 | 0.00 |
| 13 | 14 | 0.17093 | 0.34802 | 0.00 |

VITA

Noramalina Abdullah was born in Perak, Malaysia, on December 15 1979. She received B.Tech. degree in Quality Control and Instrumentation from University Science of Malaysia and M.Eng. in Electrical Engineering from University Technology of Malaysia. She conducted the graduate studies at Power System Research Laboratory, Department of Electrical Engineering, Faculty of Engineering, Chulalongkorn University, Thailand. Her research interests include power system and artificial intelligence.

